

INFORMATION TO USERS

This material was produced from a microfilm copy of the original document. While the most advanced technological means to photograph and reproduce this document have been used, the quality is heavily dependent upon the quality of the original submitted.

The following explanation of techniques is provided to help you understand markings or patterns which may appear on this reproduction.

1. The sign or "target" for pages apparently lacking from the document photographed is "Missing Page(s)". If it was possible to obtain the missing page(s) or section, they are spliced into the film along with adjacent pages. This may have necessitated cutting thru an image and duplicating adjacent pages to insure you complete continuity.
2. When an image on the film is obliterated with a large round black mark, it is an indication that the photographer suspected that the copy may have moved during exposure and thus cause a blurred image. You will find a good image of the page in the adjacent frame.
3. When a map, drawing or chart, etc., was part of the material being photographed the photographer followed a definite method in "sectioning" the material. It is customary to begin photoing at the upper left hand corner of a large sheet and to continue photoing from left to right in equal sections with a small overlap. If necessary, sectioning is continued again — beginning below the first row and continuing on until complete.
4. The majority of users indicate that the textual content is of greatest value, however, a somewhat higher quality reproduction could be made from "photographs" if essential to the understanding of the dissertation. Silver prints of "photographs" may be ordered at additional charge by writing the Order Department, giving the catalog number, title, author and specific pages you wish reproduced.
5. PLEASE NOTE: Some pages may have indistinct print. Filmed as received.

Xerox University Microfilms

300 North Zeeb Road
Ann Arbor, Michigan 48106

76-21,183

RAPHAN, Theodore, 1947-
A PARAMETER ADAPTIVE APPROACH TO
OCULOMOTOR SYSTEM MODELING.

City University of New York, Ph.D., 1976
Engineering, biomedical

Xerox University Microfilms, Ann Arbor, Michigan 48106

A PARAMETER ADAPTIVE APPROACH
TO
OCULOMOTOR SYSTEM MODELING

by

Theodore Raphan

A dissertation submitted to the Graduate
Faculty in Engineering in partial fulfillment of
the requirements for the degree of Doctor of Philosophy
The City University of New York

1976

This manuscript has been read and accepted for the Graduate Faculty in Engineering in satisfaction of the dissertation requirement for the degree of Doctor of Philosophy.

5/18/76

date

Ralph Mekele

Chairman of Examining Committee

5/18/76

date

Jacques E. Benveniste

Executive Officer

Professor Egon Brenner

Professor Bernard Cohen

Professor George Kranc

Professor Ralph Mekele (Chairman)

Professor Se Jung Oh

Supervisory Committee

Abstract

A PARAMETER ADAPTIVE APPROACH
TO OCULOMOTOR SYSTEM MODELING

by

Theodore Raphan

Advisor: Professor Ralph Mckel

This dissertation investigates the utilization of a parameter adaptive technique in modeling the oculomotor subsystem responsible for generating saccades or quick eye movements. The mathematical technique is based upon a model reference system configuration and the design of a parameter controller whose control signals are used to update and identify the saccadic generator's mathematical model. In the model-reference configuration, the reference system represents the actual physiological system by the stimulus response data which are available from experimentation. The postulated model system is constructed initially as an approximate mathematical representation of the reference system and is derived from considerations of lesion, stimulation, intracellular, and extracellular studies of the oculomotor system. The controller's equations used to update the model's parameters are derived using Liapunov's direct method in order to insure the convergence of the derived algorithms.

Several artificial modeling examples are presented in order to

illustrate the design of the parameter controller and its adaptive capabilities. It is shown that by utilizing a modified model-reference adaptive approach, a "confidence criterion" could be defined which monitors the adaptation and gives a measure of the amount of adaptation which has taken place. For each of the examples, some or all of the initial values assumed for the model parameters are purposely chosen different from the corresponding reference system parameters. Using the model-reference configuration and the parameter controller, the model's parameters are updated and are shown to approach the corresponding values of the reference system parameters.

In applying this technique to modeling the saccadic generator, the reference system is assumed to be the neural signals recorded in a region of the brain known as the Paramedian zone of the Pontine Reticular Formation (PPRF). Only the neural activity present in the PPRF associated with quick eye movements was considered and not the overall closed loop behavior of the saccadic system. There is electrophysiological evidence to suggest that the PPRF contains the neuron classes responsible for driving the eyes to make saccades and quick phases of nystagmus. In formulating an initial model to simulate the neural activity, the firing frequencies of particular unit types are considered to be the state variables of the saccadic generator. Accepting the hypothesis that the saccadic generator is a state determined system, realization theory is utilized to gain insight into the organizational structure of the PPRF. This leads to a system matrix which can be used to explain various aspects of oculomotor function. In the model, the subsystem generating the state

variables within the PPRF (long and medium lead burst units) is the mechanism that controls the neurons which are driving the motor nucleus directly (short lead burst units). These neurons also stimulate a neural integrator providing the pulse-step necessary to produce saccades and quick phases. The pause units act as a switch to enable or disable the saccadic generator.

The controlling part of the model behaves essentially as a "relaxation oscillator". When a pulse is applied to the saccadic generator, there is a slow buildup of activity in the state variables. When a critical threshold level is reached, the dynamic characteristics of the model change. This forces the saccadic generator back to its equilibrium position. In terms of the physiology, the saccadic generator is outputting to the motor nucleus during this interval. When a step is applied, a stable condition can never be achieved, since as soon as the feedback drives the generator below some threshold, a slow buildup of activity resumes. This leads to the periodic quick phases which are similar to those observed during induced nystagmus.

The model has focused on the dynamic response of neuron classes to various stimuli and how they are organized centrally to drive the eyes in the saccadic mode. In describing oculomotor behavior, there is evidence to suggest that the nervous system is capable of performing addition, multiplication, integration, threshold sensing, and switching. Therefore, in the model realization such functional relationships are used. The PPRF is thus conceived as a multiloop system with positive and negative feedback. The order of the system which has been chosen

to be two and the nonlinearities that have been introduced in the model realization account for the biphasic character of the neuronal behavior. The various identified parameters determine the dynamic response of the state variables corresponding to the different neuron types. It is shown that if particular feedback elements are altered and if appropriate slow phase information is introduced into the neural integrator, the model becomes unstable and spontaneous oscillations may result. This may be analagous to spontaneous nystagmus which occurs after lesions in the Pontine Reticular Formation. Thus a mathematical basis has been established to understand the neuronal organization of the PPRF and how it might produce rapid eye movements.

Acknowledgements

I wish to express my extreme gratitude to my mentor, Professor Ralph Mekel, for his guidance and encouragement throughout the course of this research. The many hours of technical discussions and his many valuable criticisms and suggestions are most appreciated.

I would like to thank all the members of my Doctoral guidance and examining committee, Professors Egon Brenner, William Blesser (Polytechnic Institute of New York), Bernard Cohen (Mount Sinai School of Medicine/CUNY), George Kranc, and Se Jung Oh for the time and effort each has taken to read and constructively criticize this dissertation.

I would especially like to express my thanks to Professor Egon Brenner, Provost of the City College of New York, for his continuous interest, encouragement and helpful suggestions throughout the preparation of this dissertation.

I wish to particularly express my gratitude and sincerest thanks to Professor Bernard Cohen of the Mount Sinai School of Medicine for his invaluable assistance throughout the course of this research. The many hours of informative discussions about physiological systems and eye movement mechanisms are greatly appreciated. I am also indebted to him and Dr. Voelker Henn for allowing me the use of their data which was utilized in this work.

Thanks are also due to Professor William Blesser of the Polytechnic Institute of New York for his suggested corrections of this manuscript.

I would like to also thank Mr. Charles Lasner for helping me learn the use of the PDP 8 computer and allowing me the use of the PQS Monitor System to run my programs.

The help of Ms. Valerie Josephson in drawing some of the figures which have been used in the dissertation is greatly appreciated.

The efforts of my wife, Dr. Deborah Raphan, and my sister, Ms. Barbara Mintz, in typing this manuscript are deeply appreciated.

Finally, I would like to acknowledge the partial support given to me by The City University of New York Research Foundation under FRAP Award No. 11058, The National Institutes for Neurological and Communicable Diseases (NINCDS) under Grant No. NS-00294, The National Science Foundation (NSF) under Grant No. 74-00938, and The National Aeronautics and Space Administration (NASA) under Grant No. NGR-33-013-053.

TABLE OF CONTENTS

Chapter		Page
1	INTRODUCTION	1
	1.1 Rationales and Motivation	1
	1.2 Organization of Dissertation	5
2	THE EYE MOVEMENT CONTROL SYSTEM	8
	2.1 Introduction	8
	2.2 Historical Background	10
	2.3 The Saccadic System	13
	2.3.1 The Saccadic System Properties	13
	2.3.2 Neurophysiology of the Saccadic System	16
	2.3.3 Saccadic System Models	20
	2.4 Slow Eye Movements	27
	2.4.1 Smooth Pursuit System Properties	27
	2.4.2 Vestibular System Properties (Vestibular Nystagmus)	30
	2.4.3 The Properties of the Optokinetic System (Optokinetic Nystagmus)	36
	2.5 Visual-Vestibular Interaction	42
3	MATHEMATICAL TECHNIQUE FOR ADJUSTING PARAMETER VALUES OF THE MODEL	44
	3.1 Introduction	44
	3.2 Historical Background	45
	3.3 Mathematical Theory of Adaptation	49
	3.3.1 Statement of Problem	49
	3.3.2 Phase Variable Form Realization (Controllable Form)	53
	3.3.3 Observable Form Realization	62

3.4	Digital Computer Simulation Examples	69
3.4.1	Example 1 - Second Order System with 2 Unknown Parameters (Phase Variable Form)	69
3.4.2	Example 2 - Second Order System with 2 Unknown Parameters (Observable Form)	77
3.5	Confidence Criterion for Modeling Approach	84
3.6	Modified Model-Reference Adaptive Controller Design	87
3.7	Examples Showing the Modified Model Reference Adaptation	93
3.7.1	Example 1 - Two Parameter Adaptation for an Observable Form Realization	94
3.7.2	Example 2 - Three Parameter Adaptation for a Controllable Form Realization	97
3.7.3	Example 3 - Four Parameter Adaptation for an Observable Form Realization	104
4	STATE THEORETIC MODELING OF THE OCULOMOTOR SYSTEM	113
4.1	Introduction	113
4.2	Realization of Saccadic Generator Model	116
4.3	Testing of Model to Establish Conceptual Viability	125
4.4	Slow Phase Generator Model	131
4.4.1	Introduction	131
4.4.2	Realization of a Slow Phase Generator Model	133
5	APPLICATION OF PARAMETER ADAPTIVE APPROACH TO THE OCULOMOTOR SYSTEM MODEL (QUICK PHASE GENERATION)	140
5.1	Introduction	140
5.2	Experimental Procedure for Data Acquisition and Reference System Formulation	141
5.3	Controller Design for Adaptation of Parameters of the Quick Phase Generator Model	150

5.4	Identification of Parameters	155
5.5	Discussion of Results	175
6	SUMMARY AND CONCLUSIONS	180
6.1	Summary	180
6.2	Recommendations for Future Research	185
APPENDIX A:	THEORY OF STABILITY IN THE SENSE OF LIAPUNOV	186
APPENDIX B:	WEIGHTED MINIMUM MEAN SQUARE ERROR POLYNOMIAL APPROXIMATION TO DATA	188
APPENDIX C:	COMPUTER PROGRAMS USED TO GENERATE THE CORRECTIVE DYNAMICS FOR THE EXAMPLES IN SECTION 3.4	192
APPENDIX D:	COMPUTER PROGRAMS USED TO GENERATE THE CORRECTIVE DYNAMICS FOR THE EXAMPLES IN SECTION 3.7	193
BIBLIOGRAPHY		195

LIST OF ILLUSTRATIONS

Figure		Page
2.1	Oculomotor pathways as suggested by the experimental primate model	17
2.2	PRF burst units(a-d), PRF pause units (e-f)	21
2.3	Model of Young and Stark for saccadic and pursuit eye movements in response to an unpredictable target	22
2.4 A	Saccadic portion of the Young and Stark model	23
2.4 B	Saccadic model for target steps above threshold with the eye dynamics neglected	23
2.5	Three typical eye movement patterns in response to a 10 /sec. ramp input	29
2.6	Typical vestibular nystagmus	32
2.7	Diagrammatic representation of a single semicircular canal indicating essential features only	33
2.8	Typical optokinetic record for square wave velocity input	37
2.9	Graphs of parameters of OKN of one monkey	39
2.10	Data of Fig. 2.9 replotted for individual parameters	40
3.1	Model reference configuration for adaptation of a model in state form	50
3.2	Phase variable form realization for a second order model	71
3.3	Adaptation of parameters h_1 and h_0 (Example 1)	74
3.4	Model reference system errors e_1 and e_2 vs. time during adaptation (Example 1)	75
3.5	Adaptation of parameters h_1 and h_0 in parameter space (Example 1)	76
3.6	Observable form realization for a second order model (two parameter adaptation)	78
3.7	Adaptation of parameters h_1 and h_0 (Example 2)	82

3.8	Model reference system errors e_1 and e_2 vs. time during adaptation (Example 2)	82
3.9	Adaptation of parameters h_1 and h_0 in parameter space and the behavior of the errors e_1 and e_2 in error space (Example 2)	83
3.10 A	Modified model-reference configuration for adaptation of a model in state form	88
3.10 B	Second order realization of a modified model	89
3.11	Parameters h_1 and h_0 adaptation for modified model-reference system	95
3.12	Portion of Liapunov function used in evaluating confidence criterion	96
3.13	Parameter h_1 adaptation for modified model-reference system (Example 2)	99
3.14	Parameter h_0 adaptation for modified model-reference system (Example 2)	100
3.15	Parameter g_0 adaptation for modified model-reference system (Example 2)	101
3.16	Portion of Liapunov function ($V_1 = e^t \underline{M} e$) used in evaluating confidence criterion (Example 2)	102
3.17	Parameter h_1 and h_0 adaptation for modified model-reference system (Example 3)	105
3.18	Parameters h_1 and h_0 adaptation for modified model-reference system (Example 3) (cont.)	106
3.19	Parameters h_1 and h_0 adaptation for modified model reference system (Example 3) (cont.)	107
3.20	Parameters g_1 and g_0 adaptation for modified model reference system (Example 3)	108
3.21	Parameters g_1 and g_0 adaptation for modified model-reference system (Example 3) (cont.)	109
3.22	Parameters g_1 and g_0 adaptation for modified model-reference system (Example 3) (cont.)	110
3.23	Portion of Liapunov function ($V = e^t \underline{M} e$) used in evaluating confidence criterion ¹ (Example 3)	111

4.1 A	Conceptual model for the generation of saccadic eye movements	114
4.1 B	Instantaneous frequency vs. time behavior of burst units recorded in PPRF.	117
4.2 A	State realization of saccadic generator with ideal integrators	120
4.2 B	State realization of the saccadic generator model with nonideal integrators	121
4.3	Response of saccadic generator model to a pulse input	126
4.4	Response of saccadic generator model to a step input	127
4.5	Response of saccadic generator model to a sinusoidal input	128
4.6	Model variables and associated neurons	130
4.7	A state realization for a slow phase generator	132
5.1	Frequency (impulses per sec.) vs. time for A)One type of long lead burst unit B)different type of long lead burst unit	144
5.2	Frequency (impulses per sec.) vs. time for short lead burst unit (medium lead burst unit)	145
5.3	Polynomial fits to frequency (impulses per sec.) vs. time plots for different neuron types	146
5.4	Flow graph of reference system formulation	149
5.5	Program for saccadic generator model parameter identification	158
5.6	Model parameter values at end of each adaptation sub-interval for $f_1 = 0$	162
5.7	Adaptation of parameter h_1 of saccadic generator model for $f_1 = 0$.	163
5.8	Adaptation of parameter h_0 of saccadic generator model for $f_1 = 0$.	164
5.9	Adaptation of parameter h_2 of saccadic generator model for $f_1 = 0$	165

5.10	Adaptation of parameter h_3 of saccadic generator model for $f_1 = 0$	166
5.11	Adaptation of parameter g_0 of saccadic generator model for $f_1 = 0$	167
5.12	Adaptation of parameter g_1 of saccadic generator model for $f_1 = 0$	168
5.13	Model parameter values at end of each adaptation subinterval for $f_1 \neq 0$	169
5.14	Adaptation of parameter h_1 of saccadic generator model for $f_1 \neq 0$	170
5.15	Adaptation of parameter h_0 of saccadic generator model for $f_1 \neq 0$	171
5.16	Model generated state variables for a quick phase movement	172
5.17	Model nystagmus generation	173
5.18	Comparison of physiological variables (frequency of firing of units) with state variables and variable f_2 of the model	174
5.19	Location of neuron type z_1 in saccadic generator model	177
5.20	Location of neuron type z_2 in saccadic generator model	178
5.21	Location of neuron type f_2 in saccadic generator model	179
B-1	Computer program for obtaining polynomial approximation to data	191

CHAPTER 1

INTRODUCTION

1.1 Rationales and Motivation

The oculomotor system is an important subject for biomedical research because of the close relationship of looking to seeing, i.e., of eye movements to vision, and because it is prominently involved in many patients with disease of the brain and muscles. An elucidation of the functional aspects of oculomotor control as well as the physiological organization should prove useful in diagnosing and treating patients whose eye movements have been impaired. The purpose of this research is to contribute towards the understanding of the organization of the oculomotor system.

The system engineering approach to biological modeling has made important contributions to understanding of brain mechanisms in recent years. In particular a large amount of work has been done in modeling the oculomotor system and a number of workers have produced models which account for many of the observed oculomotor responses to various inputs. This work will be summarized in Chapter 2. In general these models have been limited to descriptions of the input-output behavior of the overall oculomotor response to various stimuli. They have not dealt specifically with how individual neuron classes within the brain are coordinated to produce eye movements. Recent advances in physiology have made it possible to record from neurons which are responsible for producing eye movements in the central oculomotor system of alert monkeys. Therefore, there is a need to formulate models which explain

oculomotor system unit behavior and relate it to the oculomotor response. This is particularly important since there are currently no anatomical or physiological techniques for determining the sequence of activity or structural relations existing among the various neuron classes in the portions of the brain where eye movements are produced. Insight into this problem could come from models which explain the oculomotor system response in terms of variables which can be related to unit behavior.

Lesion, stimulation, intracellular and extracellular studies have shown the Pontine Reticular Formation (PRF) to be an important area for quick phase generation (13). The lesion studies (4, 9, 38) indicate the necessity of this region of the brain for producing rapid eye movements. The stimulation and intracellular studies (4, 10, 12, 41, 49, 50) show connectivity of regions and cells involved in eye movement. The extracellular studies (14, 57, 62) demonstrate that the individual firing of the PRF cells is associated with eye movements. Although much insight has been gained into brainstem organization using these standard neurophysiological techniques, it is unlikely that their usage alone will determine how neuron classes in the PRF are coordinated to produce a rapid eye movement. A method utilizing a combined neurophysiological and system theoretic approach seems more suited for this purpose. This thesis, therefore, attempts to provide a theoretical basis for understanding how neurons recorded in this region of the brain can be combined to create a sufficient pulse generator for producing a quick eye movement.

The mathematical model and overall modeling technique may have future practical value by relating parameter variations in the model to pathological conditions in man and monkeys. It is therefore important to have a technique whereby the parameters of a system may be determined by measurements made on its state variables. Such techniques have been studied in the past and the general problem of determining a system's parameter has come to be known as the system identification problem.

The purpose of all the identification schemes which have been developed is to determine the dynamics of the process under investigation or identify parameters which govern its behavior. One simple and flexible method which has been studied over the last decade is the model-reference adaptive approach. This technique consists of applying a known input to a model system and an unknown reference system, measuring the state error and designing an adaptive controller to adjust the parameters of the model so that reference system and model are approximately equivalent.

In this dissertation a parameter adaptive approach is used to identify the parameters of the quick phase generator as a subsystem of the oculomotor system. Liapunov's second method is utilized in designing the controller adaptive algorithms used for identification. Such adaptive algorithms have the advantage that they result in globally asymptotically stable systems and convergence is always guaranteed. Other designs based on gradient approaches may exhibit instability in some cases (73). The technique may also be extended to time varying systems (69, 70) and classes of nonlinear systems as is done in this

dissertation. In addition the use of Liapunov's second method provides useful performance criteria which examine the quality of adaptation.

The next section describes the organization of the dissertation and how the above mentioned goal is achieved.

1.2 Organization of Dissertation

This dissertation is organized into three parts. The first part (Chapter 2) gives a description of the prominent aspects of the oculomotor system and a review of the research which has been done to understand its function. In Section 2.3 the function and neurophysiology is examined. Some of the more important models which have been developed using an engineering system theoretic approach* are reviewed in Section 2.3.3. All of these models generally treat the system from an input-output point of view without regard to relating model variables or parameters to centrally recorded neural behavior.

The second part of the thesis (Chapter 3) develops the mathematical technique which is used in this dissertation to identify the parameters of the model for quick phase generation. The method is a parameter adaptive approach to system identification, using a Liapunov function to design the adaptive algorithms. In Section 3.3 the controller is designed for both a controllable and observable form realization for a system. The derived algorithms are implemented for an example which had been proposed as a model for a human operator in a tracking task (67). Different realizations are adapted to show the dynamic characteristics of the controller for different conditions. In Section 3.5 a "Confidence Criterion" is developed as an aid in determining how much adaptation has taken place over the identification

* The use and application of control systems theory and techniques

interval. This criterion may also be used as an aid in choosing the parameters of the controller to obtain different convergence rates. However, in order to use the criterion a modified model-reference configuration had to be utilized. This is developed in Section 3.6. In Section 3.7 examples are shown which demonstrate the convergence of the derived algorithms and show the behavior of the "confidence criterion."

The third part of the thesis, (Chapters 4 and 5), deals with the application of the parameter adaptive approach to identify the parameters of a proposed quick phase generator.

In Chapter 4 conceptual models for saccadic generation and slow phase generation are developed from a state theoretic point of view. The state variables of the oculomotor system are assumed to be representative of the frequency of firing of various unit types in the oculomotor system. The conceptualization of the saccadic generator is based on relaxation oscillator theory to explain the biphasic behavior for the recorded units which are being modeled.

The conceptual viability of such a configuration is demonstrated by showing that such a generator could give the known oculomotor responses by appropriately coupling position and velocity information. By assuming that the slow phase velocity signal is the predominant signal driving the quick phase generator during nystagmus, the various aspects of nystagmus can be predicted and the state variables of the quick phase generator model are similar to the observed unit activity.

In Chapter 5 the parameter adaptive approach developed in Chapter 3 is applied to the saccadic generator model. The parameters associated with the quick phase generator for nystagmus generation are then identified. It is assumed that the slow phase velocity signal is driving the quick phase generator. Therefore, in the model reference configuration the input into the model is a step equal to the slow phase velocity of the induced nystagmus. The adaptation is done for a typical quick phase movement of approximately 12 degrees using 45 degrees/second as a stimulus.

The conclusions and results obtained from this research are described in Chapter 6. It is suggested that the PPRF is a multiloop system with positive and negative feedback and contains sufficient neuron classes to time and generate quick eye movements. The manner in which the neurons are coupled to each other determine their dynamic response. In the quick phase generator model this is represented by the parameters h_1 and g_1 . The variation in these parameters may be related to various disorders in the PPRF region. The order of the system which has been chosen to be two and the nonlinearities that have been introduced in the model realization account for the biphasic character of the neuronal behavior. Thus a mathematical basis has been established to understand the neuronal organization of the PPRF and how it might produce rapid eye movements.

CHAPTER 2

THE EYE MOVEMENT CONTROL SYSTEM

2.1 Introduction

The function of the eye movement control system is to move the eyes to subserve vision. There are two primary inputs into this system; the visual system and the vestibular system. The goal of the visual system is to maintain visual acuity or fixate objects of interest. The vestibular system provides a compensatory mechanism to stabilize the environment during head movements (11, 16, 84, 92, 117). In response to visual and vestibular stimuli all animals make combinations of two types of movements; quick or saccadic movements and slow or smooth pursuit movements. Saccades shift the gaze of the eye from one point to another and have peak velocities ranging to 600 degrees/sec. in man and 1000 degrees/sec. in monkey (34, 82). These rapid movements bring an image from the periphery of the retina to the high resolution region of the retina, the fovea, which covers an angle of approximately $\frac{1}{2}^{\circ}$ in the center of the visual field (113). Smooth pursuit movements on the other hand are continuous movements of the eye and can be elicited only when the image of a target moves smoothly over the retina. Their velocities are generally slower than those of saccadic movements, usually being less than $40^{\circ}/\text{sec.}$ (83, 113, 119).

Nystagmus is an interaction of both types of movements. It is composed of smooth following movements called slow phases interspersed with rapid movements in the opposite direction called quick phases. Nystagmus can be induced by stimulation of either the visual or vest-

ibular system. The visual system is stimulated by moving a textured visual field before an observer and the resultant response is known as Optokinetic Nystagmus (OKN). Perception of visual information occurs during the slow phases whereas the quick phases are primarily for resetting the eye so that tracking may be resumed. The vestibular system is stimulated with linear or angular acceleration. This induces a slow compensatory deviation of the eyes followed by a quick phase; this is called vestibular nystagmus.

Other types of movements which the eye can perform are vergence movements which are used for viewing near targets. They have the characteristics of slow movements (106, 121).

In the next section a brief historical background of oculomotor research is given and the remainder of the chapter describes those aspects of the oculomotor system which are necessary for the theoretical formulation of the mathematical model.

2.2 Historical Background

It is the characteristic dual mode operation* (29, 107, 108) of the oculomotor system which motivated Rashbass (79) to study whether quick and slow phase movements were different modes of action of the same neurological apparatus or were separate subsystems utilizing different pathways. His studies and those of others (82, 83, 114, 115, 116) support the contention that the quick and slow movements are under separate control in the Central Nervous System (CNS). These modes are coordinated to maintain a moving target within the foveal region, thereby providing the best visual acuity. The saccadic system achieves its goal by quick corrective movements. The pursuit system responds to velocity information and controls the eye movements so as to match target velocity.

Viewed in this way, the Oculomotor system lends itself to a system theoretic engineering approach which mathematically models the observed responses to stimuli. These models should ultimately be representations of how the system works and be formulated in explicit terms.

Fender and Nye (31) were the first to view the oculomotor system from a system theoretic point of view. The method of analysis was a sinusoidal steady state approach and demonstrated the approximate frequency response of the system. It showed the upper cutoff frequency for sinusoidal tracking and indicated that there was some velocity feedback from proprioceptors in addition to the retinal image feedback. The sinusoidal approach does not bring into evidence the separate

* Fast and slow aspects of eye movement

saccadic and smooth pursuit subsystems. Young and Stark (114, 115) introduced a model which does describe separate parallel control branches. Because of its importance and usefulness in devising experiments to study the Oculomotor system, this model will be described in more detail in Section 2.3.3. Briefly, the Young and Stark model of visual tracking is a sampled data system which is divided into two distinct subsystems: a saccadic subsystem and a smooth pursuit subsystem. The saccadic subsystem is a position servomechanism to direct the eyes toward the target. The pursuit subsystem is a velocity servomechanism to rotate the eyes at the same angular velocity as the target.

To describe Vestibular Nystagmus, Sugie and Jones (101, 102) incorporated the "sampled data" idea of Young and Stark into a model of vestibular nystagmus. In the Sugie and Jones Model the output signal of the semicircular canals drives an integrator for the slow phases of nystagmus. The input-output transfer function of the semicircular canals is given by a second order linear system.* A fixed interval sampling mechanism samples the output signal of the semicircular canals and is used as a negative input to the integrator for generating the quick phases of nystagmus. Barnes and Benson(2) point out that the fixed interval sampling mechanism of the Sugie and Jones model cannot account for the variation in the duration of the slow phase components and the increased frequency of saccades associated with increasing magnitude of eye velocity (58). Barnes and

*Discussed in Section 2.5.3.

Benson (2) incorporated a threshold element in the saccadic generator rather than a fixed sampler, to compensate for this deficiency. With the addition of this element, nystagmus was produced by various types of inputs which approximated the nystagmic response of humans.

Recently there has been considerable effort in the utilization of the "single cell approach" in trying to understand the neuronal makeup of the control of eye movements (14, 35, 47, 55, 56, 57, 85, 87). However, in view of the complexity of the neural apparatus for eye movements shown in extracellular studies, it seems unlikely that the functional role of the various types of neurons will be easily unraveled in conventional electrophysiological studies. A more promising line of approach would appear to be to match unit activity recorded in the brainstem of alert animals to that which is predicted from models of the oculomotor system. These models should be valuable because they may give new insights into understanding the organization of the oculomotor system and suggest new experiments.

In this thesis, state-theoretic models for saccadic and smooth pursuit behavior will be presented and analyzed. For a particular realization of a model for quick phase generation, it will be shown that certain unit activity in the brain can be related to state variable behavior.

Before formulating these models, the basic characteristics of the eye movement control system will be reviewed and the basis for the models established.

2.3 The Saccadic System

Saccades and quick phases of nystagmus are interspersed in almost every type of eye movement. Consequently, the saccadic system has a central role in any overall model of the oculomotor system. A description of its functional properties is given in this section as a theoretical basis for the model developed in Chapters 4 and 5.

2.3.1 The Saccadic System Properties

Saccades are the most rapid movements the eyes make, and they can be elicited by a variety of stimuli. Saccades can be made voluntarily without concomitant slow movements. Therefore, their time domain behavior and properties have been extensively studied. The response of the oculomotor system to a random step of a target off the fovea is a saccade after a delay of approximately 200-250 msec. (reaction time). The reaction time increases with the magnitude of the saccade. In humans, a 5 degree saccade has a latency of approximately 200 msec. (36, 82, 113). If, however, the target motion is periodic so that it can be predicted, the tracking performance can be improved, so that no latencies are apparent (97). The duration of saccades is approximately a linear function of the size of the movements (34, 82).

One of the more interesting aspects of the saccadic system is the observation made by Westheimer (107, 108). In his experiment a target was made to jump to one side and then back again in less than 200 msec. The eyes responded by jumping to one side after a saccadic reaction time and then back again after another reaction time. Wheelles et al (109) reinvestigated this result by applying

a step in target displacement of 6 degrees to one side followed by a step in target displacement of 6 degrees to the other side after waiting T msec. They found that if T was much smaller than 200 msec. (≈ 50 msec.) then the eyes were more likely to ignore the first target step. Becker and Fuchs (3) examined the response of the saccadic system to double steps of target displacement with and without visual fixation points. They found that the duration of saccades in the dark is longer than in light and also that large movements are packaged as two sub-movements with approximately a 70 msec. latency between the first and second part of the movement.

Some other interesting properties of the saccadic system are brought out when a saccade is made in conjunction with a smooth pursuit movement. Rashbass (79) showed that if a target steps to one side and then moves with constant velocity in the opposite direction and recrosses its original position within approximately one saccadic latency (200 msec.), no saccadic response occurs. Robinson (83, 88) has also studied saccades made in conjunction with smooth pursuit movements and has concluded that rate of change of retinal error as well as the error itself is utilized by the Central Nervous System (CNS) in determining the size of saccades.

The quick phase movements which occur during optokinetic and vestibular nystagmus have the same dynamic properties as saccades and are presumably generated by the same mechanism (90). Quick phases of nystagmus have been generally assumed to be refixations of the eyes after the limit of travel from the center position in the orbit was reached. Horridge (52) showed that quick phases of nystagmus are not

merely resetting mechanisms but are more closely tied to signal processing in the Central Nervous System (CNS). Hood (51), Dix and Hood (28), and Yasui (112) showed that during nystagmus the eyes tended to beat toward the quick phase side. Sugie and Jones (102) in formulating their model for vestibular nystagmus also implicitly assume that the quick phases are not merely resetting mechanisms. They imply that slow phase information is used to innervate the quick phase generator. The contention that the quick phases of nystagmus are generated by slow phase information is also expressed by Barnes and Benson (2) in their model for vestibular nystagmus and is a fundamental postulate in this thesis.

To understand the central functions performed in producing a saccade, Young and Stark (114, 115) modeled the eye movement control system using sampled data control system theory.* However, attempts to explain all of the properties of the saccadic system have led to radical revisions of the Young model. The updated models have become so complex that their value in helping understand the oculomotor system is questionable (36). Models of vestibular nystagmus (101, 102) utilizing the "sampled data" concept also are lacking in their ability to explain all the properties of quick phase eye movements. It would appear that a more viable approach is to examine the oculomotor system from within and construct models related to unit activity in light of the more recent neurophysiological developments. To this end the next section describes the saccadic system from a neurophysiological point of view.

* See section 2.3.3

2.3.2 Neurophysiology of the Saccadic System

Lesion and stimulation studies (4, 74) have suggested that the Oculomotor control signals which are initiated by a visual input follow certain pathways. These are summarized by Pasik and Pasik (76) and are shown in Fig. 2.1 taken from their paper. Conjugate eye movements to one side which are elicited by visual stimuli presumably arise in the cortex of the contralateral cerebral hemisphere. The functional pathways descend in a converging fashion toward the brainstem tegmentum or reticular formation. The pathways approach the midline in the midbrain tegmentum, cross over at the level of the oculomotor nuclear complex and descend to the paramedian zone of the pontine reticular formation between the levels of the fourth and sixth nerve nuclei. From there the oculomotor signals eventually reach the nuclear groups innervating the individual eye muscles (11).

It is known that the reticular formation of the pons and mesencephalon are critical structures for the generation of slow and rapid eye movements and positions of fixation in the horizontal plane from lesion and stimulation studies (4). However how the reticular formation is organized to produce these movements is unclear. One of the contributions of this research is to develop a model from a system theoretic point of view which gives greater insight into the nature of reticular control of eye movements. Early clinical evidence to suggest that the pontine reticular formation plays an important role in Oculomotor function was summarized by Freeman (33). Lorente de No (60) was the first to demonstrate that nystagmus was affected by pontine reticular formation lesions and postulated that quick phases of

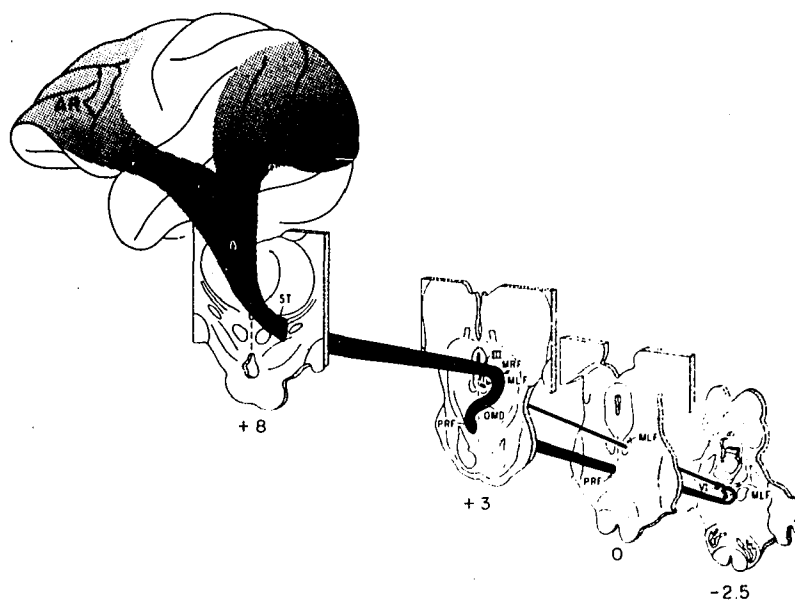


Fig. 2.1 Oculomotor pathways as suggested by the experimental primate model. The cerebral surface and the brain sections are drawn to different scales. AR, arcuate sulcus of frontal lobe. LU, lunate sulcus separating from parietal and temporal lobes. ST, subthalamic region. MRF, mesencephalic reticular formation. III, oculomotor nerve nucleus. OMD, oculomotor decussation. PRF, pontine reticular formation. VI, abducens nerve nucleus. MLF, medial longitudinal fasciculus. Numbers below sections represent anteroposterior stereotaxic coordinates. The graded stippling indicates the location of physiologic pathways for conjugate gaze to the right; they are widely represented at the left cerebral hemisphere and become progressively more concentrated toward the left MRF, decussate at the level of and ventral to the oculomotor nuclear complex, and descend in the right paramedian zone of the PRF to the level of the sixth (VI) nerve nucleus. Some of the pathways activate this nucleus, innervating the right lateral rectus muscle; and some cross the midline to ascend in the left MLF and activate the left third (III) nerve nucleus, innervating the left medial rectus muscle. Contralateral conjugate gaze defects are produced by large lesions above the decussation of the physiologic pathways (OMD); ipsilateral deficits are caused by small lesions below the decussation. Lesions of the MLF result in disconjugate eye movements. Taken from Pasik and Pasik (76).

nystagmus are produced in this region. Bender and Shanzer (4) and Cohen et al (9) have done experiments confirming that the pontine reticular formation contains the neural activity necessary for the generation of saccades. Bender and Shanzer (4) proved that lesions of the Pontine Tegmentum in monkeys cause paralysis of ipsilateral (same side) conjugate gaze and Cohen et al (9) found that all ipsilateral rapid eye movements and positions of fixation in the ipsilateral hemifield of movement were lost after pontine reticular formation lesions.

In stimulation studies by Cohen and Komatsuzaki (12) positions of fixation and all types of horizontal eye movements were induced by stimulation of a functionally specific area of the pontine reticular formation known as the paramedian zone of the pontine reticular formation (PPRF). When the PPRF was electrically stimulated, the eyes moved in the horizontal plane to the ipsilateral side. The movements were conjugate and similar in amplitude and velocity in both eyes. Eye movements induced by PPRF stimulation were of constant velocity and continuous eye movements were induced by unilateral or bilateral stimulation of the PPRF. Eye movements with velocities in the saccadic range were also induced by PPRF stimulation. This lends support to the contention that the PPRF is the site of generation of rapid eye movements in the horizontal plane. The stimulation studies suggest that there is a neural integrator which must mediate the activity between the PPRF and motor nucleus (12). Skavenskii and Robinson (92) also suggest that such an integrator exists from sinusoidal studies on the vestibulo-ocular reflex. Robinson (89) has also shown that the cerebellum is important for maintaining the integrative properties

of the integrator.

Extracellular studies of unit activity and gross potential changes in the PPRF substantiate the hypothesis that rapid eye movements, i.e. saccades and quick phases of nystagmus, are generated in the PPRF. Cohen and Henn (14), Luschei and Fuchs (62) and Keller (57) have found that neurons in the pontine reticular formation change their activity in association with rapid eye movements. The units were classified into essentially two classes:

1. Burst Units
2. Pause Units

The burst units fire with a burst of spikes before and during quick eye movements. Their activity is similar during all rapid eye movements, i.e. saccades or quick phases of optokinetic or vestibular nystagmus. In most units the latency before the onset of a movement is between 12-20 msec. In others the latencies are as high as 150 msec. There are burst units which fire maximally or exclusively during eye movements in a particular direction, the timing of these units being positively related to the size of the movement. Cohen and Henn (14) and Luschei and Fuchs (62) also found an almost linear relationship between duration of burst and duration of eye movement of some units. It has recently been found (17) that there are certain neurons whose activity is related to direction as well as duration or amplitude of movement. It has also been found that timing is solely represented in some PPRF units and direction of eye movement in others. The direction sensitive units have very specific direction of action and many are horizontal. The pause units are those units which are inhibited and pause their activity during rapid eye movements. The onset of

a pause is abrupt and precedes the initiation of the rapid movement by an interval which is approximately 15 msec.

The various units are shown in Fig. 2.2. Fig. 2.2a shows a short lead burst unit which precedes a quick eye movement by approximately 15 msec. Figures 2.2 b,c and d show various types of long lead burst units and Figures 2.2 e and f show the pause units. The observations on the unit behavior which has been described will be used in Chapter 4 in developing a model for quick phase generation by assuming that certain units recorded in the PPRF may be viewed as state variables of the quick phase generator.

With all this information about the neural activity in the PPRF region, a need exists to establish a mathematical model to add an organizational framework to help understand how these unit types are coordinated to move the eyes in the saccadic mode. In the next section a review of saccadic system models will be presented and in Chapter 4 the state model based on the above mentioned neuronal unit activity will be formulated and analyzed.

2.3.3 Saccadic System Models

The first viable model for saccadic eye movements was presented by Young and Stark (114, 115). Their original model which described both saccadic and pursuit eye movements in response to an unpredictable target is shown in Figure 2.3. The saccadic portion of the model is shown in Fig. 2.4 A and B. Essentially the model behaves in the following fashion.

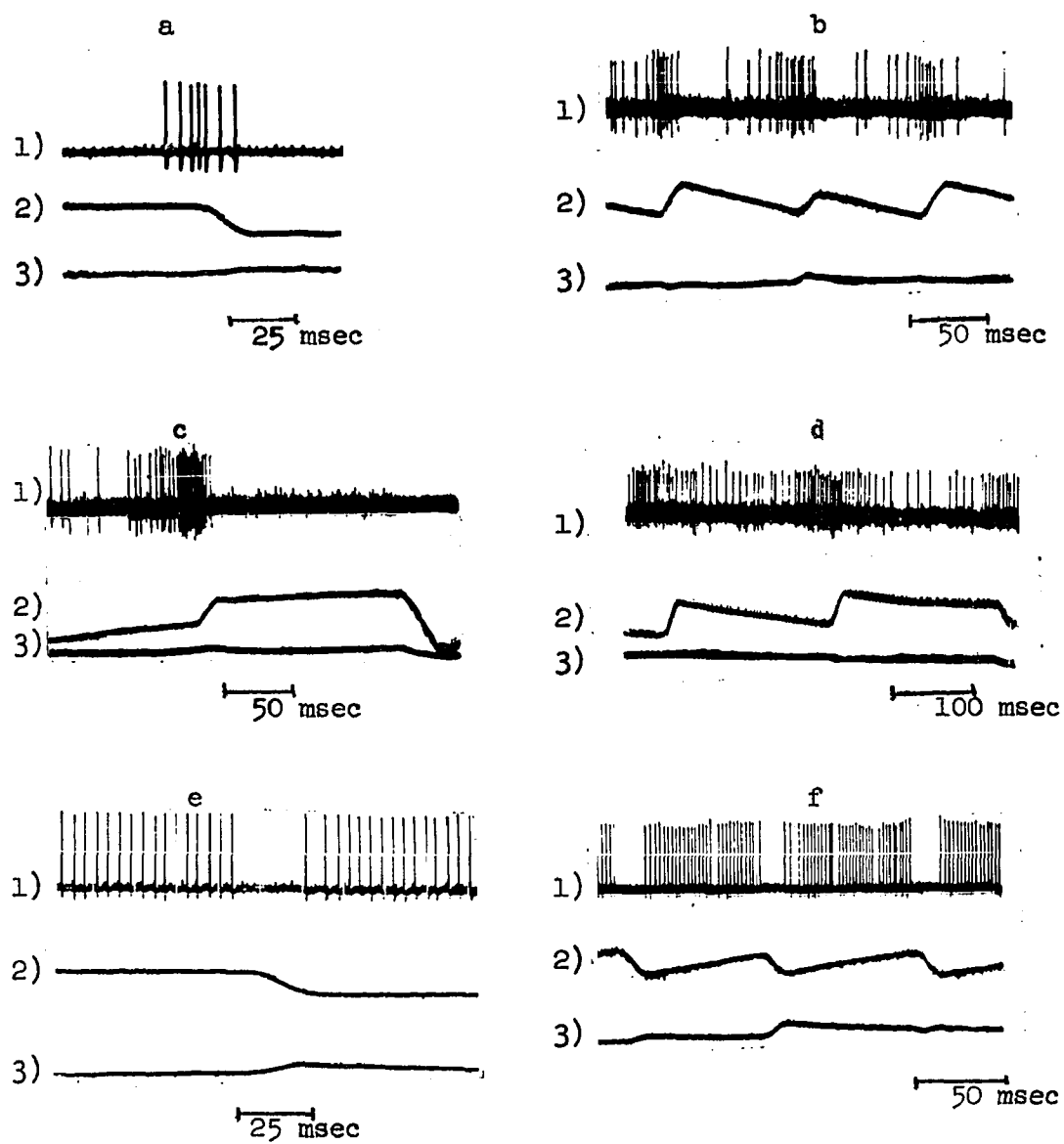


Fig. 2.2 PRF Burst Units (a-d) PRF Pause Units (e-f)

1- Unit Activity
 2- Horizontal EOG
 3- Vertical EOG

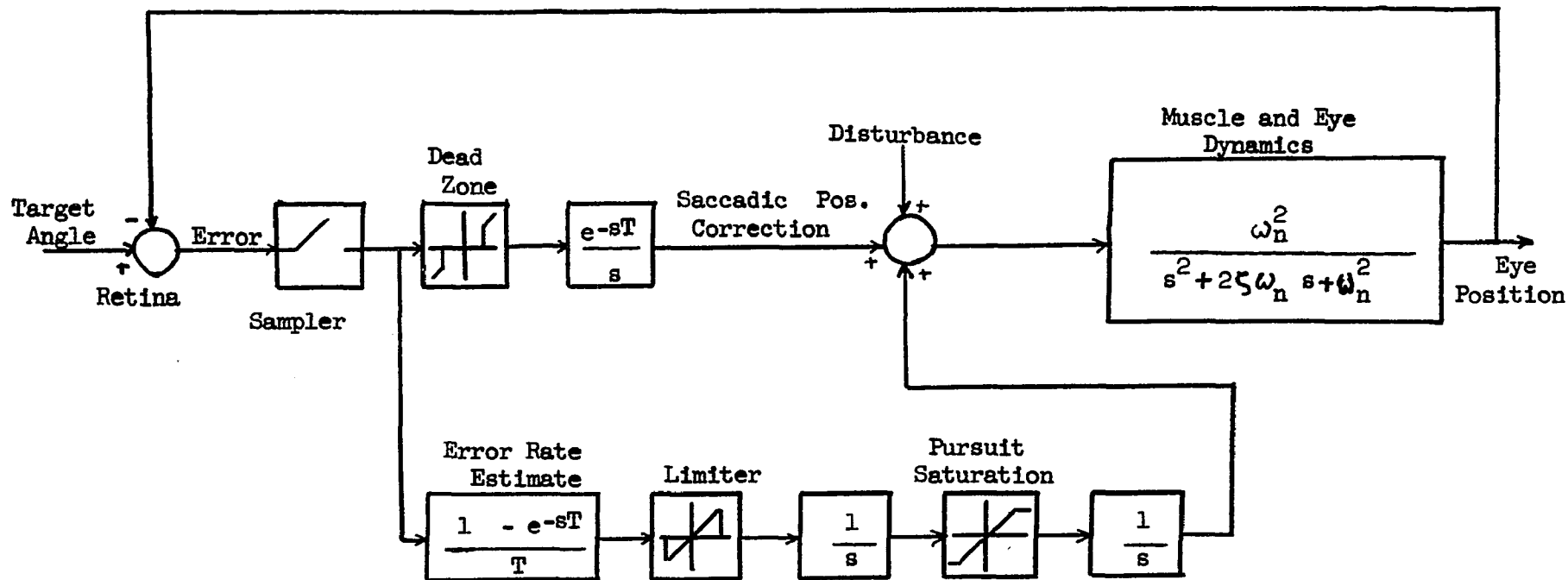


Fig. 2.3 Model of Young and Stark for saccadic and pursuit eye Movements in Response to an unpredictable target (Taken from Young and Stark (114))

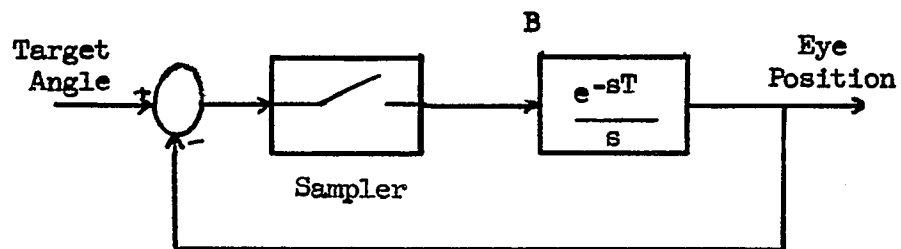
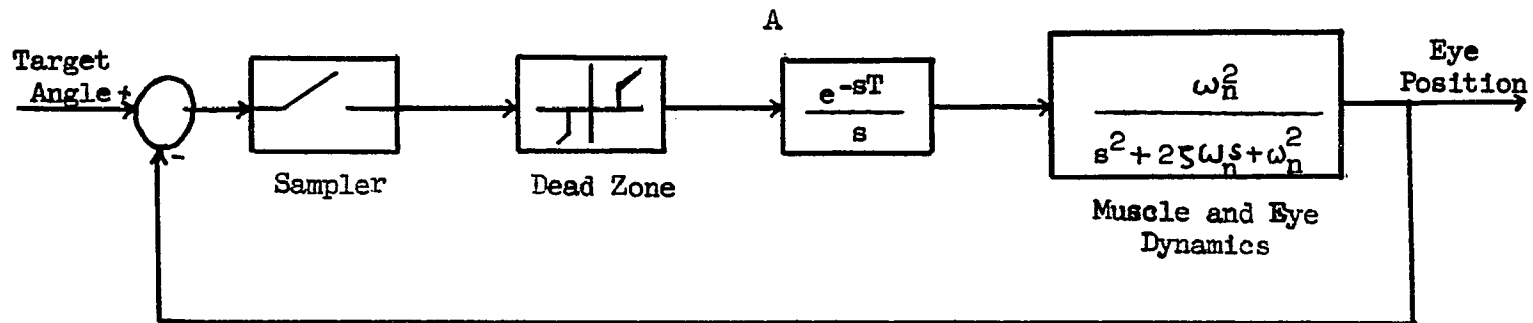


Fig. 2.4 A- Saccadic portion of Young and Stark model
 B- Saccadic model for target steps above threshold
 with the eye dynamics neglected

The error between the desired angle of gaze and the actual eye position is sensed at the retina. The error is sampled by an impulse modulator at intervals equal to the refractory period of a saccadic movement (≈ 200 msec.). The sampler is also synchronized to begin its operation with the onset of the target motion, provided the eye had not made a saccadic movement within the previous refractory period. The nonlinear dead zone element accounts for the lack of saccadic response to extremely small target displacements (113). The error impulse is delayed by one refractory period and integrated to give the step command which when applied to Westheimer's model of the mechanical plant of the oculomotor system (107, 108), yields the appropriate saccadic response.

This model was important since it was the first time an attempt was made to model the overall input-output behavior of the oculomotor system. It brought into evidence the intermittency property of the saccadic system as demonstrated by Westheimer (107, 108), provided a quantitative analysis of eye movement control, and provided a theoretical framework for experimentation.

The Young model predicts eye movements correctly when only saccades are required. However, it does not adequately predict correct saccadic behavior when these movements are made in conjunction with a smooth pursuit movement. Robinson (84) explains this by suggesting that the rate of change of retinal error as well as retinal error is utilized by the Central Nervous System (CNS) in determining the size of the saccades. Other experiments which the Young model fails to explain are the Wheelless and Rashbass experiments. Wheelless et al (109) showed that in response to a double step in

target displacement (first to one side and then to the other), the eye frequently makes a single saccade to the final position of the target when the second target step is within 50-100 msec. of the first. Young's model predicts that the eye should make two saccades under all circumstances. The Rashbass experiment (79) showed that if a target steps to one side and then moves with constant velocity in the opposite direction crossing its original position within 150-200 msec., no saccadic response occurs. The model predicts saccades would occur. An attempt to explain these experiments by the Young model has led to postulating a finite sampling interval and a nonsynchronous sampler (116).

Other studies of the saccadic system led to models of the plant dynamics in order to infer the nature of the control signals which must be generated centrally to move the eye. Robinson (82) pointed out the overdamped nature of the plant as opposed to the underdamped nature assumed by Westheimer (107, 108) which was incorporated in the Young model. Cook and Stark (23) also analyzed the plant and found a "homeomorphic" model such that a direct correspondence could be established between model parameters and physiological elements. Sobotkin (93) showed how Robinson's model can be made to behave as Cook's model for a saccadic response by using an adaptive approach similar to that developed in this thesis. These studies were important because they demonstrated that the internal processing in the Young model had to be modified. Rather than generating a step to drive an underdamped plant as is done in the Young model for saccadic generation, a pulse step was needed to drive the overdamped plant. Modified models, as presented by Fuchs (38) and Robinson (86, 89)

were further attempts to correct the failings of the original Young and Stark model. However, as the patching continues these models become more and more complex and it becomes exceedingly difficult to attach any neurophysiological basis to the model.

With the recent advances in electrophysiology it is clear that models of the neural organization of the saccadic generator are required in order to bring into evidence the nature of the central saccadic controller. This is one of the goals of this thesis and will be discussed in detail in Chapters 4 and 5.

In the next section the smooth pursuit system is described. A review of its properties and those of the slow phase generators of vestibular nystagmus and OKN will aid in the formulation of a slow-phase generator model developed in Section 4.4.

2.4 Slow Eye Movements

The eye generally makes three types of slow versional eye movements; Smooth pursuit movements when tracking a smoothly moving target; slow phases of vestibular nystagmus; and slow phases of Optokinetic nystagmus. Much is known about the neurophysiology of the vestibular system and how slow phase information reaches the eye muscle motoneurons. The visual pathways responsible for producing smooth pursuit and slow phases of Optokinetic nystagmus are largely unknown. Because of the similarities between all these types of slow eye movements, a similar central mechanism is indicated. Therefore the models which have been established for the vestibulo-ocular reflex arc could give clues as to how visual information is processed to generate slow phase eye movements. In section 2.4.3 models of the vestibulo-ocular reflex arc are reviewed and in Chapter 4 a general model for slow phase generation for both Optokinetic nystagmus and vestibular nystagmus is formulated. First, however, the properties of the smooth pursuit system are reviewed.

2.4.1 Smooth Pursuit System Properties

The smooth pursuit system controls slow continuous movements of the eye when tracking a moving target. The function of the system is to stabilize retinal images by matching the angular velocity of the eyes to that of the target. It differs from the saccadic system by responding essentially to velocity inputs rather than position inputs and by being continuous in nature as opposed to being discrete.

One of the basic experiments which suggest that the pursuit system responds primarily to velocity of the target was performed by Rashbass (79). The stimulus was a step followed by a ramp in the opposite direction. This elicited a smooth pursuit movement after a certain latency which was followed by a saccade after another latency. At the start of the eye movement, the eye was actually moving in a direction away from the position of the target apparently responding to velocity and not to the position of the target. It should be noted that target velocity is presumably reconstructed by the brain by adding retinal slip velocity and eye velocity. The latter is presumably obtained from a corollary discharge through the oculomotor centers from outflow information (46, 112).

Since the saccadic system displays a refractory period in its response, the question whether a similar refractory period exists for the smooth pursuit system has also been studied. Robinson (83) showed that the smooth pursuit system can be made to respond to two separate stimuli spaced only 75 milliseconds apart. This substantiates that during pursuit the eye behaves very nearly in a continuous fashion. Also, Stark (98) demonstrated the absence of a refractory period for successive changes in smooth pursuit eye movements.

Although primarily responding to target velocity, the smooth pursuit system also seems to have some sensitivity to position information. Robinson (83) found that the eyes make three types of movement in response to ramps of position. These responses are shown in Fig. 2.5 together with the percent observation of each type of response. For all three, there is a latency of approximately 125-150 msec. In the most common response (Type 1) there is an overshoot in

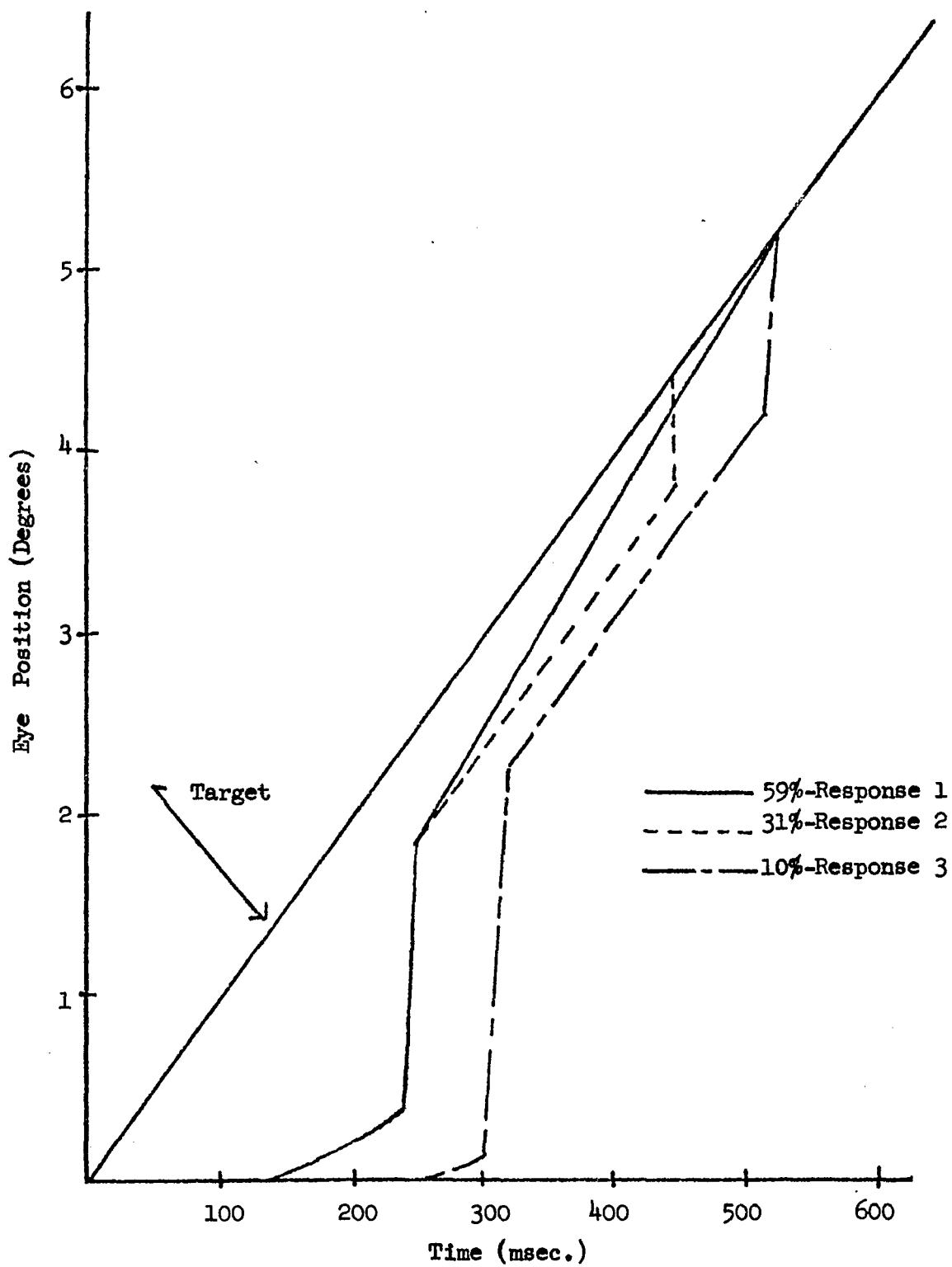


Fig. 2.5 Three typical eye movement patterns in response to a 10 deg/sec ramp input. Taken from Robinson(83)

velocity after the saccade. This indicates that some positional information is being used by the smooth pursuit system for tracking purposes. This view has also been expressed by Young (119).

The smooth pursuit system also exhibits nonlinear characteristics such as saturation and threshold. Rashbass (79) found that target velocity of at least .8 deg./sec. are required to produce any pursuit movements and that saturation occurred at approximately 40 deg./sec. in humans (113).

The neurophysiological aspects of the smooth pursuit system are largely unknown. Crosby and Henderson (24) described cortical connections from the occipital lobe to the tegmentum and superior colliculi and refer to them as being concerned with automatic eye movements. However, no one as yet has been able to induce smooth pursuit movements by stimulation of the occipital cortex and therefore to attribute smooth responsibility to this part of the brain is speculative. Recently Cohen et al (10) have been able to produce slow eye movements by stimulation of the region around the PPRF. Sparks and Sides (95) have also recorded neurons in the PPRF associated with horizontal eye movements ~~during tracking~~.

2.4.2 Vestibular System Properties (Vestibular Nystagmus)

One of the functions of the vestibular organ is to stabilize the visual axis in space. In this regard it is similar to the smooth pursuit system and optokinetic system which stabilize targets and visual surround respectively on the retina. Stimulation of the vestibular apparatus by linear and angular acceleration induces reflex

compensatory movements of the eyes in the orbit approximately equal and opposite to the movement of the head in space (92). The processing of the signal emanating from the vestibular organ has been studied using both electrophysiological techniques and an engineering systems approach. These studies have traced some of the pathways involved in the vestibulo-ocular reflex and led to the formulation of models to describe its function. For a complete review see Cohen (16) and Young (117).

When the vestibular system is subjected to a constant angular velocity, the eyes perform a jerky rhythmical to and fro motion known as nystagmus. A typical vestibular nystagmus record is shown in Fig. 2.6. The to and fro motion is characterized by a slow deviation of the eyes opposite to the direction of rotation and a quick movement of the eyes back. The characteristics of the quick phases or saccadic eye movements have already been discussed in sec. 2.3.3. The sense organs responsible for the oculomotor reflex to head rotation described above are the three semicircular canals. They are arranged approximately orthogonally in the inner ear. Each canal is filled with a fluid, the endolymph, which flows within the canal whenever an angular acceleration in the plane of the canal is experienced by the head. As the endolymph moves, it displaces a gelatinous structure, the cupula, which is in an enlarged portion of the canal known as the ampulla. Cupula movement is detected by small hair-like cells which code the displacement into neural activity in the nerve endings synapsing on them (61). A diagram of a semicircular canal is shown in Fig. 2.7.

When an individual semicircular canal or its nerve is stimulated, eye movements are induced which lie in planes parallel to the plane of

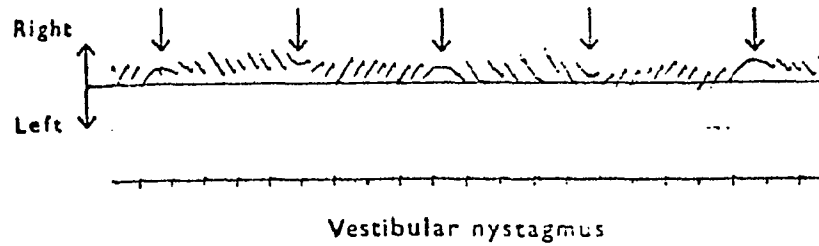


Fig. 2.6 Typical vestibular nystagmus record. (Top trace shows eye position as a function of time. Arrows indicate change in direction of angular velocity. Bottom trace indicates time trace. Each mark Represents 1 Sec.) Taken from Hood(51).

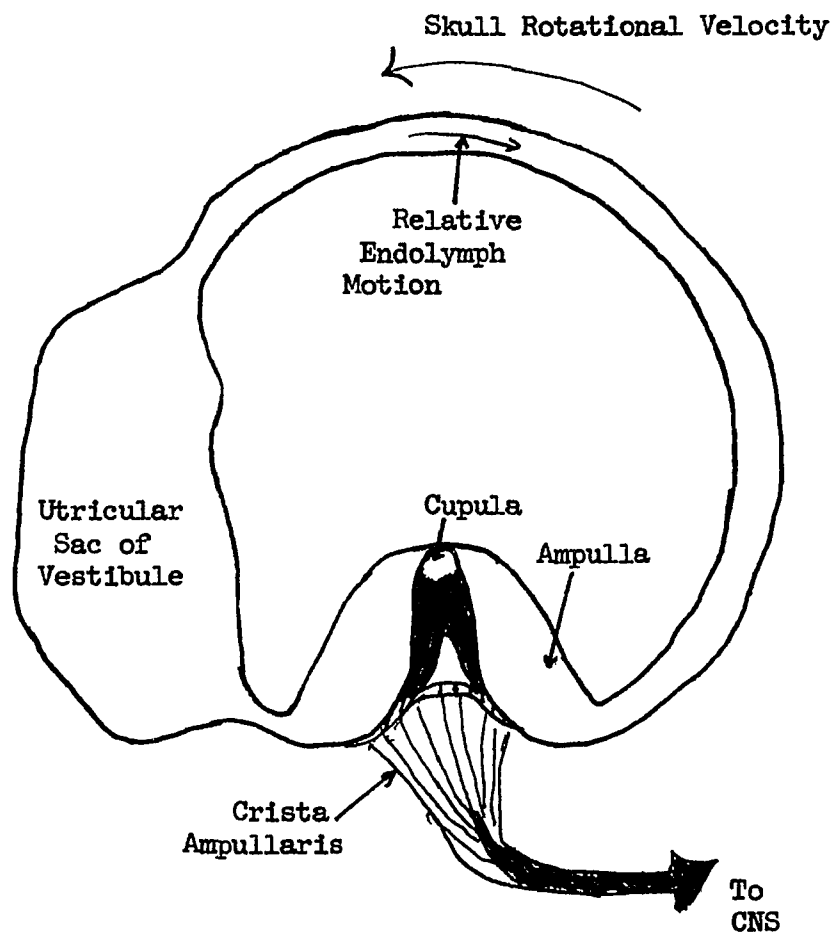


Fig. 2.7 Diagrammatic representation of a single semicircular canal indicating essential features only. Redrawn from Sugie and Jones (101,102)

that canal (7, 8, 30, 103). The neurons from the semicircular canals synapse primarily in the rostral, medial, and superior vestibular nuclei (78). Axons from cells in the vestibular nucleus on the side ipsilateral to the stimulus project across the brain stem to the contralateral abducens nucleus causing the opposite lateral rectus muscle to contract (77). Direct projections from the vestibular nucleus to the ipsilateral medial rectus motoneurons probably lie in the median longitudinal fasciculus (MLF) and it is these projections which could be responsible for generating the slow phases of nystagmus. This is supported by evidence from lesion studies which show that the MLF not only participates in eye movements induced by the vestibular apparatus but is important for ipsilateral adduction during all types of rapid horizontal eye movements (11). This would imply that the MLF is a final integrating step before projecting onto the motoneurons which move the eyes. It is also postulated that the slow phase signal innervates the PPRF where the signals for quick phase generation are produced.

One of the first models attempted to explain the response of the vestibular system to stimuli was formulated by Steinhausen (99). He used a torsion pendulum model for the semicircular canal which was then described by the differential equation:

$$\frac{d^2\zeta}{dt^2} + a_1 \frac{d\zeta}{dt} + a_0\zeta = b_1 \frac{dr}{dt} \quad 2.1$$

where ζ is the cupula deflection and r is the angular velocity and a_1 and a_0 are parameters which determine the systems dynamic response. Goldberg and Fernandez (32,39,40) measured the time constant of

the neuronal behavior of peripheral neurons innervating the labyrinth and compared it with the torsion pendulum model. They found the system to be highly overdamped with a large time constant of approximately 5 sec. and a small time constant of about .005 sec. The value of the large time constant is smaller than that obtained from measurements made on the nystagmus which follows stimulation and is approximately 15-20 sec. in monkey and man (117). In either case, the vestibular system responds very rapidly to steps in angular velocity and operates over a wide frequency band for sinusoidal inputs (92).

The transfer function relating cupula displacement to velocity input is given by:

$$\frac{\zeta(s)}{R(s)} = \frac{b_1 s}{s^2 + a_1 s + a_0} \quad 2.2$$

Where $\zeta(s)$ and $R(s)$ are the Laplace transform of the cupula deflection and angular velocity respectively. This equation has been used by many researchers in modeling vestibular nystagmus (2, 102, 112). The transfer function given by Eq. 2.2 is used to transfer the head velocity signal to generate the slow phase velocity signal. This signal is then used to drive a saccadic generator for the quick phases of nystagmus and is also integrated to generate the slow phases of nystagmus.

Robinson (86) suggested the idea that the saccadic generator behaves as a "one shot" multivibrator, with some threshold sensing neuronal network. Barnes and Benson (2) incorporated this idea into their model of vestibular nystagmus and introduced

a lead network to compensate for the lag introduced into the quick phase generator by the threshold sensing network. In terms of the state theory used in this dissertation this would imply that the slow phase generator is a third order subsystem of the oculomotor system: two states to account for the canal dynamics and one to account for the lead which is introduced before driving the saccadic system. This is explored in greater detail in Section 4.4.2 where a state theoretic slow phase generator is formulated. Young (117) has noted that the vestibular system has some adaptation associated with it and has modeled it by introducing an adaptation operator. Goldberg and Fernandez (39) have also found this adaptation in some peripheral neurons in the eighth nerve.

The remaining portion of this chapter gives a description of optokinetic nystagmus and visual vestibular interaction.

2.4.3 The Properties of the Optokinetic System (Optokinetic Nystagmus)

Optokinetic Nystagmus (OKN) is a dual mode operation of the eye movement control system induced by a moving visual surround. The response to this visual stimulus is a to and fro movement of the globe. The most effective way to elicit OKN is to stimulate the peripheral retina as well as the fovea with full field rotation (5). Although the response can be suppressed under some circumstances, it is generally reflexive and involuntary in nature. A typical OKN response is shown in Fig. 2.8.

The quick phases of OKN have characteristics not significantly different from those of vestibular nystagmus quick phases and saccades

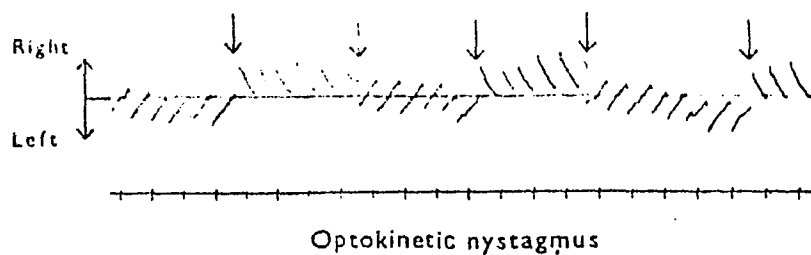


Fig. 2.8 Typical optokinetic record for square wave velocity input. (Arrows indicate change in direction of velocity). Top trace is eye position vs. time. Bottom trace is the time code (1 mark represents 1 second). Taken from Hood (51).

(90) and are presumably generated by the same central mechanism (See Sec. 2.3). The slow phases of OKN are generated by a system which essentially responds to velocity information. This is similar to the system which generates the slow phases of vestibular nystagmus and smooth pursuit. Collewijn (18, 19, 20, 21) examined the optokinetic slow phase response in rabbits for step and sinusoidal inputs. He found that the system was not responsive to steps in position input (Amplitude .5 - 4 deg/sec) and was a velocity servomechanism. Velocities up to 1 deg/sec are followed well with a gain of .7 - .9. The maximal eye velocity is reached soon after the start of the stimulation for step inputs and has a latency of approximately 100 - 200 msec. For velocities above 1 deg./sec the following is poor and approaches stimulus velocities only after long periods of time. In sinusoidal movements increases in stimulus amplitude and/or frequency results in a decreased gain but only a small phase lag of the eye movement. An analog computer model has been formulated which displays these characteristics to explain the type of function which might be performed centrally (21).

A thorough quantitative analysis of the slow phase velocity characteristics of OKN in the monkey has not been carried out. Komatsuzaki et al (58) did measure various parameters of OKN such as maximum quick phase velocity, slow phase velocity, frequency (beats/sec.), and total eye deviation and related these to stimulus velocity. They found a generally increasing function, although nonlinear, of stimulus velocity. The results of their studies are shown in Figs. 2.9 and 2.10. Cheng and Outerbridge (6) have recently shown that as the stimulus speed increases, the frequency of the

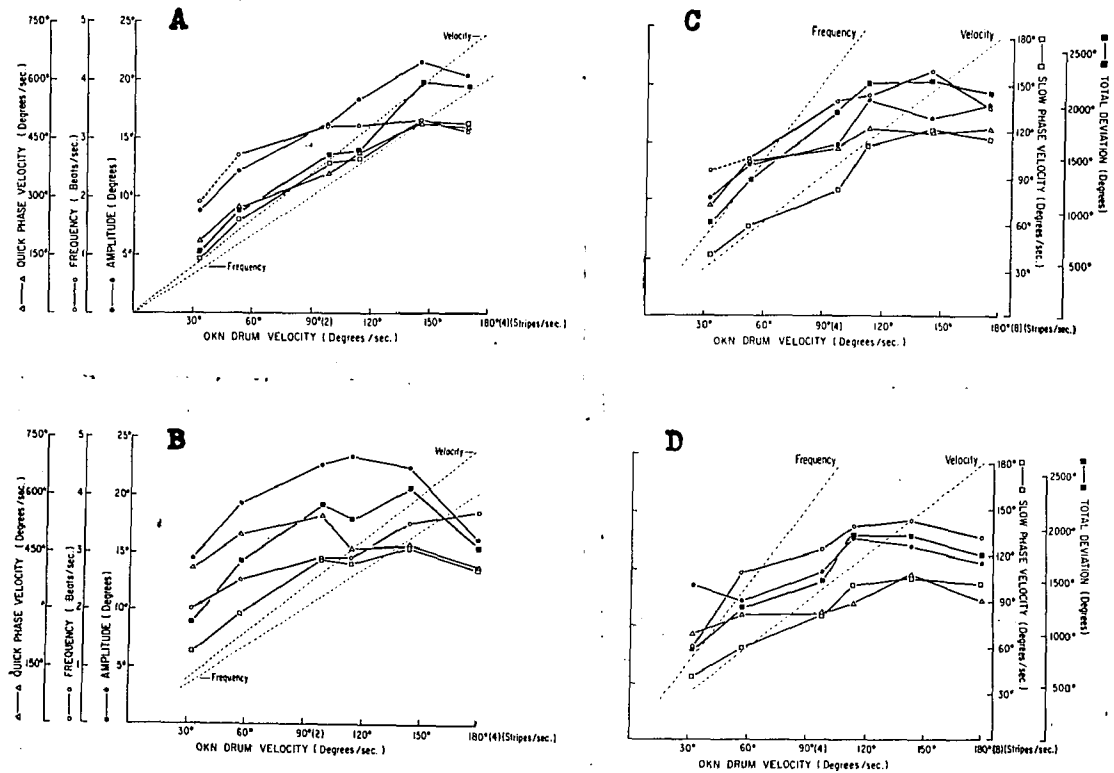


Fig. 2.9 Graphs of parameters of OKN of one monkey. Graphs A and C were obtained from data recorded on the same date and B and D from data taken 5 days later. A and B are the standard test situation with eight stripes on the OKN drum. In C and D the number of stripes was doubled. Each point is the mean value of a single parameter over a 30-second period. The velocity and frequency of the OKN stimulus are shown on the abscissa in degrees/sec and stripes/sec. Perfect following for slow phase velocity in degrees/sec or for frequency in beats/sec would follow the dotted lines marked "Velocity" and "Frequency". The closed boxes are symbols for total deviation in degrees, the open boxes for maximum slow phase velocity in degrees sec. the open triangles for maximum quick phase velocity in degrees sec. the closed circles for amplitude of beats in degrees and the open circles for frequency in beats sec. Taken from Komatsuzaki et al (58)

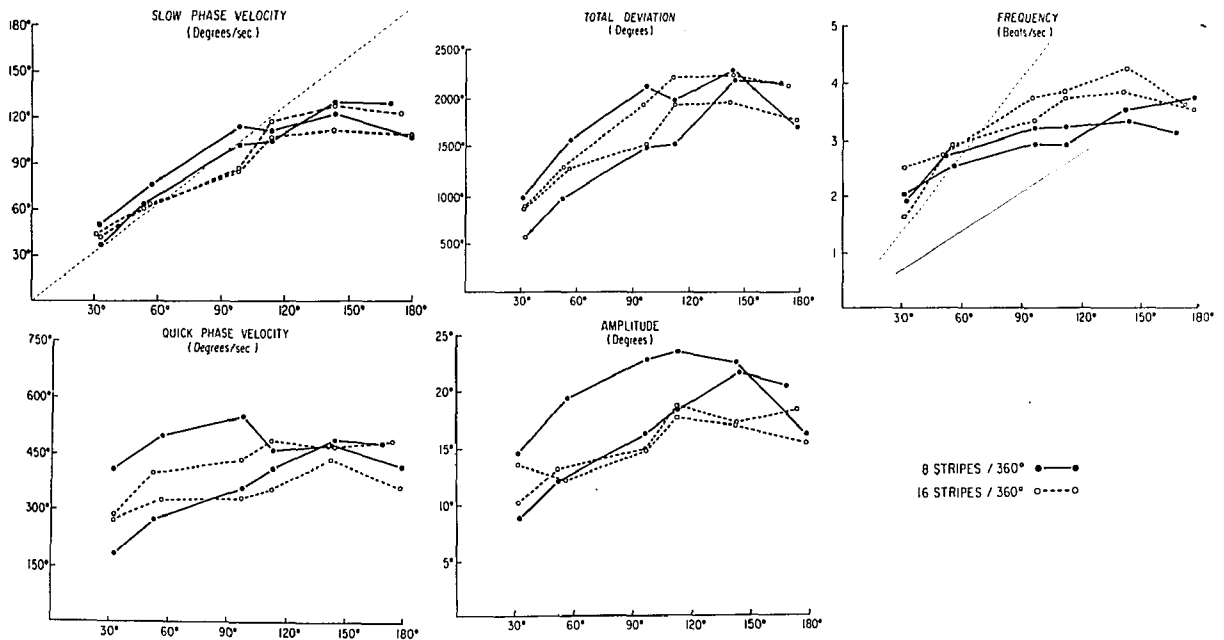


Fig. 2.10 Data of Fig. 2.9 replotted for individual parameters. The solid lines in each graph show the response to the normal test situation (8 lines 360°). The dotted lines show the response to doubling the number of stripes in the OKN drum. The underlying dotted line in the graph of slow phase eye velocity shows perfect following for each velocity of drum rotation. In the graph of frequency the underlying solid line shows frequency changes which would occur if one beat of nystagmus corresponded to the passage of one stripe when there were 8 stripes/ 360° . The dotted line shows 1 : 1 following for 16 stripes/ 360° . Taken from Komatsuzaki et al (58).

nystagmus beats approaches a bimodal distribution where the second frequency is a harmonic of the previous one. All of these studies indicate that environmental velocity is the important signal in driving the optokinetic system and probably is responsible for driving the saccadic generator to initiate the quick phases of nystagmus. This idea will be used in Chapter Five when a parameter adaptive scheme is used to identify the parameters of a quick phase generator using neuronal activity as the reference system states.

Because of the seemingly common nature of saccadic generation for vestibular and optokinetic nystagmus, the question arises as to whether there is coupling between the slow phase generators of vestibular nystagmus and OKN. This is indeed the case and is briefly described in the next section.

2.5 Visual-Vestibular Interaction

There is an intimate relationship between the visual and vestibular system and recently there has been established evidence that there is an interaction (5, 15, 16, 26, 27, 48, 75). One example is "Flash nystagmus" which is induced by flickering a light in one eye (75). Because the direction of this nystagmus is dependent on the position of the head in space, it indicates that the vestibular system has a role in producing it. The interaction is also shown by the sensation of self-movement (circularvection) caused by whole field rotation in man (5, 26). This shows that the central mechanism responsible for sensing self-rotation from the labyrinth is also coupled into by the visual system. The exact coupling mechanism is not clear but the peripheral retina is important in inducing circularvection (5).

From a neurophysiological point of view Cohen et al (15), have demonstrated that monkeys are unable to maintain slow phase velocities of more than 45 - 60/sec. during OKN after unilateral or bilateral labyrinthectomy. This indicates that the optokinetic system utilizes the vestibular system for higher velocity following. Moreover, the nystagmus which follows OKN when the animal is put in darkness (Optokinetic after nystagmus) is abolished after bilateral labyrinthectomy (15, 104, 105). Dichgans et al (27) and Henn et al (48) demonstrated that activity of neurons in the vestibular nucleus was either enhanced or decreased by inducing OKN in one direction or another. For a more complete review of the vestibular-visual interaction see Cohen (16).

From the above it is clear that the vestibular system is

affected by visual input. Using a state theoretic approach a complete slow phase generator can be formulated which takes this effect into account by introducing coupling coefficients in the system matrix between vestibular and visual state variables. In Section 4.4 such a generator is formulated.

This concludes Part One of the dissertation which describes the essential properties of the Oculomotor Control System. The next chapter which is the second part of the dissertation develops the mathematical theory which is utilized for adapting the parameters of the model for quick phase generation.

CHAPTER 3

MATHEMATICAL TECHNIQUE FOR ADJUSTING PARAMETER VALUES OF THE MODEL

3.1 Introduction

The mathematical approach used to establish a correspondence between states in a model and unit firing in the oculomotor system is called a parameter adaptive technique. This technique uses a model-reference system configuration (66, 73) in conjunction with a Liapunov function formulated for the purpose of identifying the model parameters. The initial model in the configuration is formulated based on physiological arguments and the reference system is considered to represent the actual eye movement control subsystem. A Liapunov function is formulated based on the response error equation obtained from a comparison of the reference and model systems when both are subjected to the same stimulus. The Liapunov function together with its first time derivative in accordance with Liapunov's stability criteria provide the dynamics needed to identify the model's parameters. The adaptive identification of the model is implemented by utilizing the stimulus response data, the unit activity data, and the constraints imposed upon the time derivative of the Liapunov function. The mathematical development of the parameter adaptive technique is presented in the chapter for two realizations of the model. Artificial examples are shown to demonstrate the convergence properties of the model-reference system.

The next section reviews the literature related to system modeling and identification using a model-reference adaptive approach.

3.2 Historical Background

The model-reference adaptive approach is a popular technique used in the design of adaptive control systems. It is particularly useful in applications which require rapid adaptation i.e. auto-pilots (37). The conventional model-reference adaptive design forced a given reference system to respond in approximately the same way as a specified mathematical model for a given stimulus. This objective was realized by designing a controller which compared the output of the reference system with that of the model and adapted or changed the parameters of the reference system so that the response to the given stimulus for both systems would be approximately equal according to some performance index. If the controller's role is modified so that it updates the model's parameters to match the input-output characteristics of the reference system, the model-reference configuration may be used to identify the reference system.

Whitaker et al (110) were one of the first to apply a parameter adjustment technique in their application to controlling the behavior of an aircraft. They used a model reference configuration with three adjustable system parameters and three indices of performance, one for each parameters. They derived the adaptive algorithms based on the gradient of an even function of the error between model and reference system outputs. The error function chosen was very critical and convergence was not guaranteed.

Osborn et al (72) modified the above mentioned method by choosing the adjusting mechanism to minimize the integral square error by a gradient technique. This method became very popular and has been

known as the "MIT rule."

At about the same as these studies were being carried on, Margolis (63) and Staffenson (96) were applying the parameter adaptive technique to the study of the identification problem. They called this technique the learning model approach. They minimized the sensitivity function using a gradient technique and in this way the adaptive algorithm were similar to the "MIT rule" mentioned earlier.

With the popularization of Liapunov's direct method (44, 54, 59) many researchers started applying this technique to model-reference adaptive control systems (42, 43, 65, 66, 69, 70, 73, 80).

Rang (80) was one of the first to design a corrective dynamics controller based on a Liapunov function. The basis for his design was to force a system to behave according to a given model by designing a controller to make the error between the output of the model and the system be asymptotically stable. However, his design was not a parameter adjustment scheme and he found that the adaptive properties were relatively slow and large transients occurred if the process coefficients and tracking parameters differed widely. Grayson (42, 43) implemented the controller in a slightly different way and was able to obtain more rapid convergence times. However, this manner of design had the shortcoming that although the error goes asymptotically to zero, there is no parameter adjustment. Therefore it cannot be used in an identification scheme.

Parks (73) extended the Liapunov technique by alleviating somewhat the shortcomings of the "MIT rule" and the methods of Rang (80) and Grayson (42, 43). He designed a controller to adapt the parameters of a given reference system to that of a specified model

using Liapunov's direct method. He points out the analytical difficulties associated with the "MIT rule" and gives an example of a second order system such that a controller designed using this "MIT rule" leads to instability. He therefore redesigned the adaptive algorithms for problems considered by other researchers (53, 111) using Liapunov's direct method. However, he chooses the derivative of the Liapunov function negative semi-definite so that if the error goes to zero, the parameters stop changing and consequently makes the tracking equations input dependent.

In a paper by Shahein et al (94) these shortcomings are emphasized and an attempt is made to choose the derivative of the Liapunov function negative definite in error and parameter misalignment. However, the obtained parameter adjusting equations are dependent on the derivatives of the input and unknown parameters.

Mekel (65, 66) utilized a Liapunov function to identify the parameters of a human operator in a control task. It was in this study that different realizations of a system were first explored as a possible means of uncovering the mechanisms by which a system is controlled.

Narendra and Kudva (69, 70) extended some of the ideas of modeling via a Liapunov function to modeling where not all state variables are measurable. The algorithms developed have very long adaptation time and in many cases appear not to work.

In all studies done so far no criterion has been defined which assesses the adaptation properties of the controller or has any attempt been made to identify models whose exact structure is not that of the reference system (inexact identification).

In the next section the mathematical theory of adaptation will be derived and shown how it may be used in the modeling of the saccadic generator of the oculomotor system.

3.3 Mathematical Theory of Adaptation

In this section the mathematical derivation of the adaptive control algorithms used for identification is presented. It is shown how different realizations of a system lead to adaptive algorithms which have different convergence properties. The derivations have been carried out for two such realizations of a system: The "phase variable form" realization which is closely related to the "controllable form" realization; and the "observable form" realization. Both of these are important in the theoretical development of the model for saccadic generation considered in this dissertation.

3.3.1 Statement of Problem

Before considering the derivation of the various adaptive algorithms, a statement of the basic problem is given. Consider the model-reference system configuration depicted in Figure 3.1. The reference system may represent any part of the oculomotor system which is to be modeled and is referred to as the oculomotor subsystem. The stimulus response data and the state vector for the subsystem are assumed to be available from experimentation. It is further assumed that the oculomotor subsystem is a state determined proper differential system* and may be described by the differential equation:

$$\frac{d^n z}{dt^n} + a_{n-1} \frac{d^{n-1} z}{dt^{n-1}} + \dots + a_0 z = b_m \frac{d^m r}{dt^m} + b_{m-1} \frac{d^{m-1} r}{dt^{m-1}} + \dots + b_0 r \quad 3.3.1$$

* A proper differential system is one where $n > m$ in Equation 3.3.1

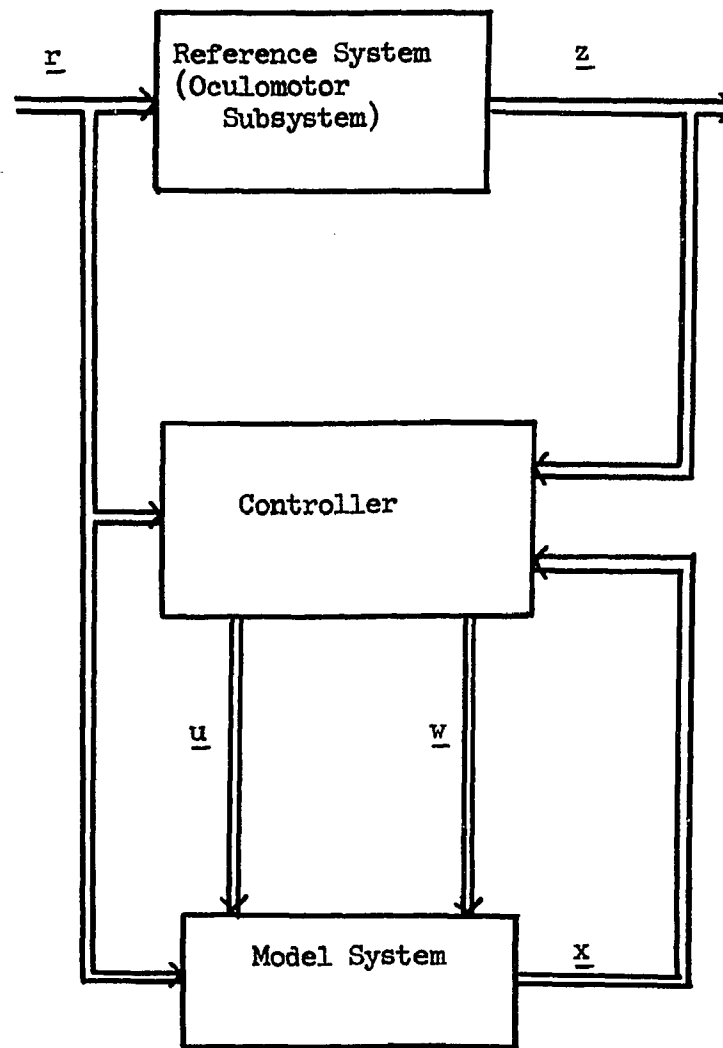


Fig. 3.1 Model-Reference configuration for adaptation of a model in state form. Controller design based on Liapunov function. \underline{r} is the stimulus vector, \underline{z} and \underline{x} are the reference system and model system state vectors respectively, and \underline{u} and \underline{w} are the controller adaptation vectors.

This n th order differential equation is equivalent to a system of n first order differential equations and in vector notation it takes the form:

$$\dot{\underline{z}} = A \underline{z} + B \underline{r} \quad 3.3.2$$

where \underline{z} denotes the state vector, \underline{r} represents the stimulus vector and $\dot{\underline{z}} = \frac{dz}{dt}$. The elements of matrices A and B , which are related to the coefficients of the differential equation (Equation 3.3.1) are unknown and are to be identified based on the measurements made on its state vector \underline{z} and the input \underline{r} . Matrices A and B will be said to have been identified when Equation 3.3.2 has a response which is approximately equal to that of the physical system (oculomotor subsystem) under consideration when both are subjected to the same stimulus.

As a starting point for the modeling approach, a tentative mathematical model system of the same form as Equation 3.3.2 is chosen. Let the model system represent the reference system and be described by the following vector differential equation:

$$\dot{\underline{x}} = H \underline{x} + G \underline{r} \quad 3.3.3$$

where \underline{r} is the same stimulus vector as for Equation 3.3.2, and \underline{x} and $\dot{\underline{x}}$ are the model's state vector and the derivative of the state vector respectively. The aim is then to adapt the elements of matrices H and G so that eventually $H \rightarrow A$ and $G \rightarrow B$. The final values of the elements of matrices H and G are unknown but they may be assigned a set of initial values which are updated to match the reference system response. To insure convergent adaptation, Liapunov's direct method is used to derive the adaptive algorithms and the initial matrices H_0 and G_0 are chosen so that their elements lie in the stability region of the Liapunov function (66, 67, 68).

For linear single input differential systems which are proper of order n , there are several ways of realizing relationships as given by Equations 3.3.2 and 3.3.3. The realization depends on the choice made for the state variables and different choices will lead to different realizations (120). The realization problem could give clues as to the actual structure of a physiological system where the structure is virtually indeterminable by anatomical means.

In the next sections identification algorithms for Controllable and Observable form realizations will be derived using Liapunov's direct method.

3.3.2 Phase Variable Form Realization (Controllable Form)

In this subsection a phase variable form realization of the model is discussed. The state variables chosen are referred to as phase variables, a name that stems from the coordinates of the phase space. This choice of state variables is practical since it has the ready physical interpretation as one variable being the rate of change of the other or vice versa, as one being the integral of the other. In considering the neurophysiological makeup of the brainstem this would be interpreted as one class of neurons integrating the activity of another class of neurons. This type of behavior is quite plausible when one considers neurons on a cellular level (71, 91).

In order to derive the identification dynamics for a controllable form realization of the oculomotor subsystem's mathematical model, one must first formulate the error vector differential equation for the model-reference system in terms of those phase variables.

It should be noted that initially the response of the reference system will not be the same as the response of the tentative mathematical model, when both are subjected to the same stimulus. This is because the tentative model's parameters are assumed initially different from those of the reference system.

For an n th order system, n state variables are necessary and sufficient to represent the dynamic behavior of the system and the phase variable form realization matrices of Eqs. 3.3.2 and 3.3.3.

A, B, H, and G assume the following form (120)

$$A = \begin{bmatrix} 0 & 1 & 0 & \dots & 0 \\ 0 & 0 & 1 & \dots & 0 \\ \dots & \dots & \dots & \dots & \dots \\ 0 & 0 & 0 & \dots & 1 \\ -a_0 & -a_1 & -a_2 & \dots & -a_{n-1} \end{bmatrix} \quad 3.3.4 \quad B = \begin{bmatrix} 0 & 0 & 0 & \dots & 0 \\ 0 & 0 & 0 & \dots & 0 \\ \dots & \dots & \dots & \dots & \dots \\ 0 & 0 & 0 & \dots & 0 \\ b_0 & b_1 & b_2 & \dots & b_m \end{bmatrix} \quad 3.3.5$$

$$H = \begin{bmatrix} 0 & 1 & 0 & \dots & 0 \\ 0 & 0 & 1 & \dots & 0 \\ \dots & \dots & \dots & \dots & \dots \\ 0 & 0 & 0 & \dots & 1 \\ -h_0 & -h_1 & -h_2 & \dots & -h_{n-1} \end{bmatrix} \quad 3.3.6 \quad G = \begin{bmatrix} 0 & 0 & 0 & \dots & 0 \\ 0 & 0 & 0 & \dots & 0 \\ \dots & \dots & \dots & \dots & \dots \\ 0 & 0 & 0 & \dots & 0 \\ g_0 & g_1 & g_2 & \dots & g_m \end{bmatrix} \quad 3.3.7$$

Note also that

$$\underline{r} = \begin{bmatrix} r_1 \\ r_2 \\ \cdot \\ \cdot \\ r_m \end{bmatrix} \quad 3.3.8 \quad \text{where} \quad r_k = \frac{d^{k-1} r}{dt^{k-1}}$$

The difference between the model's response and the reference system response is the model-reference system error. Let this error be denoted by vector \underline{e} and defined as

$$\underline{e} = \underline{z} - \underline{x} \quad 3.3.9$$

Note that \underline{e} , \underline{x} , and \underline{z} are time varying vectors given by

$$\underline{z} = \begin{bmatrix} z_1 \\ z_2 \\ \cdot \\ \cdot \\ z_n \end{bmatrix} \quad 3.3.10$$

$$\underline{x} = \begin{bmatrix} x_1 \\ x_2 \\ \cdot \\ \cdot \\ x_n \end{bmatrix} \quad 3.3.11$$

$$\underline{e} = \begin{bmatrix} e_1 \\ e_2 \\ \cdot \\ \cdot \\ e_n \end{bmatrix} \quad 3.3.12$$

Differentiating Eq. 3.3.9 with respect to time yields

$$\dot{\underline{e}} = \dot{\underline{z}} - \dot{\underline{x}} \quad 3.3.13$$

where the dot denotes the time derivative and the vectors $\dot{\underline{z}}$, $\dot{\underline{x}}$, and $\dot{\underline{e}}$ are given by

$$\dot{\underline{z}} = \begin{bmatrix} \dot{z}_1 \\ \dot{z}_2 \\ \cdot \\ \cdot \\ \dot{z}_n \end{bmatrix} \quad 3.3.14$$

$$\dot{\underline{x}} = \begin{bmatrix} \dot{x}_1 \\ \dot{x}_2 \\ \cdot \\ \cdot \\ \dot{x}_n \end{bmatrix} \quad 3.3.15$$

$$\dot{\underline{e}} = \begin{bmatrix} \dot{e}_1 \\ \dot{e}_2 \\ \cdot \\ \cdot \\ \dot{e}_n \end{bmatrix} \quad 3.3.16$$

Substituting Equations 3.3.2 and 3.3.3 into Equation 3.3.13 yields, after some algebraic manipulations, the vector error differential equation for the model reference system:

$$\dot{\underline{e}} = \underline{H} \underline{e} + \underline{b} \underline{u}^t \underline{z} + \underline{d} \underline{w}^t \underline{r} \quad 3.3.17$$

or

$$\dot{\underline{e}} = \underline{A} \underline{e} + \underline{b} \underline{u}^t \underline{x} + \underline{d} \underline{w}^t \underline{r} \quad 3.3.17'$$

where the superscript t denotes the matrix or vector transpose.

The vectors \underline{u} and \underline{w} are the parameter misalignment vectors and may be related to the reference system and model system matrices expressed in Equations 3.3.2 and 3.3.3 by the following relationships:

$$\underline{A} - \underline{H} = \underline{b} \underline{u}^t \quad 3.3.18$$

$$\underline{B} - \underline{G} = \underline{d} \underline{w}^t \quad 3.3.19$$

where vectors \underline{b} , \underline{u} , \underline{d} , and \underline{w} are given by:

$$\underline{b} = \begin{bmatrix} 0 \\ 0 \\ \vdots \\ \vdots \\ 1 \end{bmatrix} \quad 3.3.20$$

$$\underline{u} = \begin{bmatrix} -a_0 + h_0 \\ -a_1 + h_1 \\ \vdots \\ \vdots \\ -a_{n-1} + h_{n-1} \end{bmatrix} \quad 3.3.21$$

$$\underline{d} = \begin{bmatrix} 0 \\ 0 \\ \vdots \\ \vdots \\ 1 \end{bmatrix} \quad 3.3.22$$

$$\underline{w} = \begin{bmatrix} b_0 - g_0 \\ b_1 - g_1 \\ \vdots \\ \vdots \\ b_{n-1} - g_{n-1} \end{bmatrix} \quad 3.3.23$$

The adaptive algorithms are derived based on either equation 3.3.17 or 3.3.17'. The equation one chooses to work with determines the type of adaptation which must be implemented on the digital computer. If Equation 3.3.17 is used then Liapunov's criterion has to be satisfied based on a time varying matrix \underline{H} . This leads to complicated control algorithms since the stability of the system must be checked each time

H changes. However, if it is assumed that the reference system, represented by the matrix A, is a stable system, then the existence of a Liapunov function is assured (59) and a stable controller can be determined. Therefore Equation 3.3.17' is used in deriving the adaptive algorithms.

Equation 3.3.17' may be viewed as consisting of three perturbational vectors \underline{e} , \underline{u} , and \underline{w} , denoting the model-reference system error and parameter misalignment vectors respectively, in terms of which a Liapunov function may be formulated. An appropriate Liapunov function should be positive definite in the error as well as in parameter misalignments. Therefore, one may choose a Liapunov function of the form

$$V = \underline{e}^t M \underline{e} + \underline{u}^t N \underline{u} + \underline{w}^t Q \underline{w} \quad 3.3.24$$

where matrices M, N, and Q are symmetric square matrices and given by:

$$M = \begin{bmatrix} m_{11} & m_{12} & \dots & m_{1n} \\ m_{12} & m_{22} & \dots & m_{2n} \\ \vdots & \vdots & \ddots & \vdots \\ m_{1n} & m_{2n} & \dots & m_{nn} \end{bmatrix} \quad 3.3.25$$

$$N = \begin{bmatrix} n_{11} & n_{12} & \dots & n_{1n} \\ n_{12} & n_{22} & \dots & n_{2n} \\ \vdots & \vdots & \ddots & \vdots \\ n_{1n} & n_{2n} & \dots & n_{nn} \end{bmatrix} \quad 3.3.26$$

$$Q = \begin{bmatrix} q_{11} & q_{12} & \dots & q_{1n} \\ q_{12} & q_{22} & \dots & q_{2n} \\ \vdots & \vdots & \ddots & \vdots \\ q_{1n} & q_{2n} & \dots & q_{nn} \end{bmatrix} \quad 3.3.27$$

The elements of the preceding matrices may be constants or functions of the state variables.

When considering linear or piecewise linear constant reference systems*, matrices M, N, and Q may be restricted to be constant matrices chosen in accordance with Liapunov's stability criterion.

Differentiating equation 3.3.24 with respect to time and then substituting Equation 3.3.17' and its transpose given by

$$\dot{\underline{e}}^t = \underline{e}^t A^t + \underline{z}^t \underline{u} \underline{b}^t + \underline{r}^t \underline{w} \underline{d}^t \quad 3.3.28$$

the time derivative of the Liapunov function is obtained in the following form:

$$\dot{V} = -\underline{e}^t D \underline{e} + 2 \left[\dot{\underline{u}}^t N + \underline{z}^t (\underline{b}^t M \underline{e}) \right] \underline{u} + 2 \left[\dot{\underline{w}}^t Q + \underline{r}^t (\underline{d}^t M \underline{e}) \right] \underline{w} \quad 3.3.29$$

where

$$D = A^t M + M A \quad 3.3.30$$

In matrix form

$$D = \begin{bmatrix} d_{11} & d_{12} & \dots & d_{1n} \\ d_{12} & d_{22} & \dots & d_{2n} \\ \vdots & \vdots & & \vdots \\ \vdots & \vdots & & \vdots \\ d_{1n} & d_{2n} & \dots & d_{nn} \end{bmatrix} \quad 3.3.31$$

* This will be the case when the oculomotor subsystem being identified behaves in a linear or piecewise linear time invariant fashion during the identification interval.

Liapunov's criterion for stability calls for $V > 0$ and $\dot{V} \leq 0$.

One way to comply with Liapunov's criterion for stability is to constrain the elements of the matrix D to satisfy the following conditions:

$$\begin{aligned} d_{ii} &> 0 \\ d_{ij} &= d_{ji} = 0 \end{aligned} \quad 3.3.32$$

where i and j denote row and column respectively. However, since an unknown system matrix A is involved in solving Equation 3.3.30, a trial and error procedure must be used to obtain the elements of the M and D matrices until convergent algorithms are obtained. This however is less objectionable than finding a Liapunov function for a time varying system.

If the derivative of the Liapunov function is further constrained by letting

$$\dot{\underline{u}}^t N + \underline{z}^t (\underline{b}^t M \underline{e}) = 0 \quad 3.3.33$$

$$\dot{\underline{w}}^t Q + \underline{r}^t (\underline{d}^t M \underline{e}) = 0 \quad 3.3.34$$

then the controller dynamics for updating the parameters of the model are determined by these equations.

These equations can be summarized as follows:

Equation 3.3.32 insures that matrix D is positive definite ($D > 0$).

Equation 3.3.30 can then be solved for a positive definite matrix M^* .

Matrices N and Q must also be chosen positive definite ($N > 0$, $Q > 0$)

in order to insure convergent adaptive algorithms. The elements of

* There always exists such a matrix if the matrix A represents a stable system (59, 64)

matrices M , N , and Q are not unique and are used as controller design parameters to vary the convergence properties of the identification dynamics.

It should be noted that because of the constraints imposed by Equations 3.3.33 and 3.3.34, the derivative of the Liapunov function (\dot{V}) is negative semidefinite as opposed to negative definite. This is because \dot{V} is only a function of the model reference system error and does not depend on the parameter misalignment vectors \underline{u} and \underline{w} . This implies that the error equation is only stable and the possibility of oscillations in parameter misalignment space may exist without having exact identification.

By solving equations 3.3.33 and 3.3.34 for the control vectors \underline{u} and \underline{w} , explicit expressions for the identification controller dynamics may be realized. Since $\underline{b}^t M \underline{e}$ is a scalar quantity, one may obtain from Equations 3.3.33 and 3.3.34 the following relationships:

$$\dot{\underline{u}}^t = -\underline{z}^t N^{-1} (\underline{b}^t M \underline{e}) \quad 3.3.35$$

$$\dot{\underline{w}}^t = -\underline{r}^t N^{-1} (\underline{d}^t M \underline{e}) \quad 3.3.36$$

The transpose of Equations 3.3.35 and 3.3.36 yields

$$\dot{\underline{u}} = - (N^t)^{-1} \underline{z} (\underline{b}^t M \underline{e}) \quad 3.3.37$$

$$\dot{\underline{w}} = - (Q^t)^{-1} \underline{r} (\underline{d}^t M \underline{e}) \quad 3.3.38$$

In order to formulate the mathematical adaptive algorithms in terms of the model parameters (elements of H and G matrices), a relationship among Equations 3.3.28, 3.3.19, 3.3.35, and 3.3.36 must

be obtained. This may be done by assuming that the changes in the reference system (oculomotor subsystem) parameters are much slower than the variation of the model parameters. Matrices A and B may then be considered as being time invariant over the identification interval. Therefore, differentiating equation 3.3.18 and 3.3.19 respectively with respect to time yields

$$-\dot{\underline{H}} = \underline{b} \dot{\underline{u}}^t \quad 3.3.39$$

$$-\dot{\underline{G}} = \underline{d} \dot{\underline{w}}^t \quad 3.3.40$$

since \underline{b} and \underline{d} are constant vectors. Substituting Equations 3.3.35 and 3.3.36 into Equations 3.3.39 and 3.3.40 one obtains

$$\dot{\underline{H}} = \underline{b} \underline{z}^t N^{-1} (\underline{b}^t M \underline{e}) \quad 3.3.41$$

$$\dot{\underline{G}} = \underline{d} \underline{r}^t Q^{-1} (\underline{d}^t M \underline{e}) \quad 3.3.42$$

Integration of Equations 3.3.41 and 3.3.42 over the identification time interval yields

$$\underline{H} = \underline{H}_0 + \int_0^T \underline{b} \underline{z}^t N^{-1} (\underline{b}^t M \underline{e}) dt \quad 3.3.43$$

$$\underline{G} = \underline{G}_0 + \int_0^T \underline{d} \underline{r}^t Q^{-1} (\underline{d}^t M \underline{e}) dt \quad 3.3.44$$

where \underline{H}_0 and \underline{G}_0 are the initially chosen matrices for the mathematical model and T is the identification interval.

The mathematical model will be considered to have been identified when both model and oculomotor system produce approximately the same response when subjected to identical stimuli. A "confidence criterion"

that checks the model convergence to the reference system will be discussed in Section 3.5 where its purpose and usefulness will be demonstrated. In terms of Equation 3.3.2 this means that one has identified matrices A and B. Experimentation has also indicated that by varying the matrices N and Q the convergence rate for identification changes. It is conjectured that optimal values for N and Q exist so that identification time is reduced to a minimum. A study of the nature of the convergence for different parameter values and finding the optimal matrices is a topic for future research.

3.3.3 Observable Form Realization

In this subsection state variables are defined which lead to a state realization different from the phase variable realization presented in section 3.3.2 and is known as the observable form representation. This form is shown to be particularly important in deriving the adaptive algorithms used to identify the saccadic generator model*.

Let it be assumed that the reference system may be expressed by the differential equation

$$\dot{\underline{z}} = A \underline{z} + \underline{b} r \quad 3.3.45$$

where

$$A = \begin{bmatrix} -a_{n-1} & 1 & 0 & \dots & 0 \\ -a_{n-2} & 0 & 1 & \dots & 0 \\ \dots & \dots & \dots & \dots & \dots \\ -a_1 & 0 & 0 & \dots & 1 \\ -a_0 & 0 & 0 & \dots & 0 \end{bmatrix} \quad 3.3.46$$

$$\underline{b} = \begin{bmatrix} b_{n-1} \\ b_{n-2} \\ \dots \\ \dots \\ b_0 \end{bmatrix} \quad 3.3.47$$

*See Section 5.3

The a's and b's are unknown and are to be identified. A model system may now be considered of the same form and given by the following state equations:

$$\dot{\underline{x}} = H \underline{x} + \underline{g} r \quad 3.3.48$$

where

$$H = \begin{bmatrix} -h_{n-1} & 1 & 0 & \dots & 0 \\ -h_{n-2} & 0 & 1 & \dots & 0 \\ \cdot & \cdot & \cdot & \cdot & \cdot \\ -h_1 & 0 & 0 & \dots & 1 \\ -h_0 & 0 & 0 & \dots & 0 \end{bmatrix} \quad 3.3.49$$

$$\underline{g} = \begin{bmatrix} g_{n-1} \\ g_{n-2} \\ \cdot \\ \cdot \\ g_0 \end{bmatrix} \quad 3.3.50$$

The form of these matrices may be obtained by examining the nth order differential equation which may be expressed as follows:

$$\frac{d^n z}{dt^n} + \frac{d^{n-1}(a_{n-1} z)}{dt^{n-1}} + \dots + a_0 z = \frac{d^{n-1}(b_{n-1} r)}{dt^{n-1}} + \dots + b_0 r \quad 3.3.51$$

where r denotes the stimulus for the system and z denotes its response. If the state variables are chosen as follows:

$$\begin{aligned} z_1 &= z \\ z_2 &= \dot{z}_1 + a_{n-1} z - b_{n-1} r \\ \cdot \\ z_n &= \dot{z}_{n-1} + a_1 z - b_1 r \end{aligned} \quad 3.3.52$$

the differential equation given by 3.3.51 is equivalent to a system of n first order differential equations which are represented by Equation 3.3.45 with the matrices as shown by Equations 3.3.46 and 3.3.47.

In order to identify matrix A and vector \underline{b} , the same procedure as used for the controllable form realization in Section 3.3.2 is

followed. First the error differential equation for the composite model-reference system as shown in Figure 3.1 is formulated. An identification controller is then designed, based on Liapunov's criterion, which updates matrix H and vector \underline{g} so that eventually the response of the model system approximates that of the Oculomotor system to a given stimulus. The reference system is considered identified when $H \rightarrow A$ and $\underline{g} \rightarrow \underline{b}$.

The state error vector expressing the difference between the reference system response and the tentative model system response when both are subjected to the same stimulus can again be expressed as

$$\underline{e} = \underline{z} - \underline{x} \quad 3.3.53$$

Differentiating Eq. 3.3.53 with respect to time yields

$$\dot{\underline{e}} = \dot{\underline{z}} - \dot{\underline{x}} \quad 3.3.54$$

Substituting Eqs. 3.3.45 and 3.3.48 into 3.3.54 gives after some manipulations the error differential equation

$$\dot{\underline{e}} = H \underline{e} + (A - H) \underline{z} + (\underline{b} - \underline{g}) r \quad 3.3.55$$

or

$$\dot{\underline{e}} = A \underline{e} + (A - H) \underline{x} + (\underline{b} - \underline{g}) r \quad 3.3.55'$$

The equation one chooses to work with determines the type of adaptation which must be implemented on the digital computer. If Eq. 3.3.55 is used then Liapunov's criterion will have to be satisfied based on a time varying matrix H . This leads to complicated control algorithms since the stability equations have to be checked each time matrix H is updated. However if it is assumed that the reference system is a

stable system then the existence of a Liapunov function is assured (59) and a stable controller can be determined. Therefore Eq.3.3.55' is used in deriving the adaptive algorithms.

Let the parameter misalignments be given as:

$$\underline{A} - \underline{H} = \underline{u} \underline{c}^t \quad 3.3.56$$

$$\underline{b} - \underline{g} = \underline{w} \quad 3.3.57$$

where the superscript, t , denotes the vector transpose and vectors \underline{u} , \underline{w} , and \underline{c} are given by

$$\underline{u} = \begin{bmatrix} u_1 \\ u_2 \\ \cdot \\ \cdot \\ u_n \end{bmatrix} = \begin{bmatrix} -a_{n-1} + h_{n-1} \\ -a_{n-2} + h_{n-2} \\ \cdot \\ \cdot \\ -a_0 + h_0 \end{bmatrix} \quad 3.3.58$$

$$\underline{w} = \begin{bmatrix} w_1 \\ w_2 \\ \cdot \\ \cdot \\ w_n \end{bmatrix} = \begin{bmatrix} b_{n-1} - \varepsilon_{n-1} \\ b_{n-2} - \varepsilon_{n-2} \\ \cdot \\ \cdot \\ b_0 - \varepsilon_0 \end{bmatrix} \quad 3.3.59$$

$$\underline{c} = \begin{bmatrix} 1 \\ 0 \\ \cdot \\ \cdot \\ 0 \end{bmatrix} \quad 3.3.60$$

Since $\underline{c}^t \underline{x} = x_1$, Equation 3.3.55' may be written in the following form

$$\dot{\underline{e}} = \underline{A} \underline{e} + \underline{u} x_1 + \underline{w} r \quad 3.3.61$$

where x_1 and r are scalars and denote the response and stimulus respectively.

Equation 3.3.61 may be looked upon as containing three perturbational quantities. These are the model reference error \underline{e} , and the parameter misalignment vectors \underline{u} and \underline{w} .

In order to design the identification controller, a Liapunov function for Equation 3.3.61 is chosen such that it is both positive definite in model reference system error as well as in parameter misalignment vector error vector. Therefore, an appropriate Liapunov function is chosen in the same way as for the controllable form realization. Let the Liapunov function be given by:

$$V = \underline{e}^t M \underline{e} + \underline{u}^t N \underline{u} + \underline{w}^t Q \underline{w} \quad 3.3.62$$

where matrices M, N, and Q are symmetric positive definite matrices whose elements are constants. Differentiating Eq.3.3.61 and its transpose, the time derivative of the Liapunov function is obtained as follows:

$$\dot{V} = -\underline{e}^t D \underline{e} + 2 \underline{u}^t (N \dot{\underline{u}} + M \underline{e} x_1) + 2 \underline{w}^t (Q \dot{\underline{w}} + M \underline{e} r) \quad 3.3.63$$

where

$$-D = A^t M + M A \quad 3.3.64$$

To satisfy Liapunov's criterion $V > 0$, $\dot{V} \leq 0$, Eq.3.3.64 may be solved in the same manner as described for the controllable form realization (See Section 3.3.2)

Letting

$$N \dot{\underline{u}} + M \underline{e} x_1 = 0 \quad 3.3.65$$

$$Q \dot{\underline{w}} + M \underline{e} r = 0 \quad 3.3.66$$

Equations 3.3.65 and 3.3.66 constitute the basic relations from which the adaptive controller and the identification dynamics may be realized. Rearranging Equations 3.3.65 and 3.3.66 one obtains the relationship

$$\dot{\underline{u}} = -N^{-1} M \underline{e} \underline{x}_1 \quad 3.3.67$$

$$\dot{\underline{w}} = -Q^{-1} M \underline{e} r \quad 3.3.68$$

Equations 3.3.67 and 3.3.68 represent the identification dynamics and the realization of these equations produces the adaptive controller dynamics. Matrices M, N, and Q are obtained in the same manner as in Section 3.3.2.

In order to formulate the mathematical adaptive algorithms in terms of the model parameters (elements of H and G matrices), a relationship among Equations 3.3.56, 3.3.57, 3.3.67, and 3.3.68 must be obtained. This may be done by assuming that the changes in the reference system (Oculomotor subsystem) parameters are much slower than the variations of the model parameters. Matrices A and B may then be considered as being time invariant over the identification interval. Therefore, differentiating Equations 3.3.56 and 3.3.57 with respect to time yields

$$\dot{\underline{H}} = -\dot{\underline{u}} \underline{c}^t \quad 3.3.69$$

$$\dot{\underline{g}} = -\dot{\underline{w}} \quad 3.3.70$$

Substituting Equations 3.3.67 and 3.3.68 into Equations 3.3.69 and 3.3.70 gives

$$\dot{\underline{H}} = N^{-1} M \underline{e} \underline{x}_1 \underline{c}^t \quad 3.3.71$$

$$\dot{\underline{g}} = Q^{-1} M \underline{e} r \quad 3.3.72$$

Integration of Equations 3.3.71 and 3.3.72 yields the following relationships:

$$H = H_0 + \int_0^T (N^{-1} M \underline{e} x_1 \underline{e}^t) dt \quad 3.3.73$$

$$\underline{g} = \underline{g}_0 + \int_0^T (Q^{-1} M \underline{e} r) dt \quad 3.3.74$$

where H_0 and \underline{g}_0 are the initially assumed values for the matrix H and vector \underline{g} and T denotes the identification interval.

The next section demonstrates the controller adaptive algorithms with various digital computer simulations.

3.4 Digital Computer Simulation Examples *

In this section the design and implementation of the parameter adaptive control algorithms are demonstrated by two examples. They show the adaptation of phase variable and observable form realizations of a second order model system. The parameters of the model system are intentionally chosen different from that of the reference system and then adapted using the algorithms derived in Section 3.3. It is shown how the model-reference error vector approaches zero and the model parameters approach those of the reference system over the identification interval.

Because these examples are chosen merely to demonstrate the convergence of the adaptive algorithms, the reference system parameters are assumed known. However when the reference system is not known exactly some measure will be needed in order to monitor the adaptation. Therefore in Section 3.7 these examples are studied again in terms of a "Confidence Criterion" for model adaptation using a modified model-reference adaptive approach. This is discussed in Sections 3.5 and 3.6.

3.4.1 Example 1 - Second order system with 2 unknown parameters (Phase Variable Form)

This example examines the performance of the adaptive controller when used with a second order model. The system matrix for the model which contains two unknown parameters, is to be identified for a phase variable form realization. The reference system under consideration is assumed to be described by the differential equation:

*These examples identify different realizations of a differential system proposed as a model for a human operator in a control task (65,67)

$$\ddot{z} + 22 \dot{z} + 121 z = 102 \dot{r} + 187 r \quad 3.4.1$$

where r is the input and z is the response. A tentative mathematical model for the reference system is chosen of the form:

$$\ddot{x} + h_1 \dot{x} + h_0 x = 102 \dot{r} + 187 r \quad 3.4.2$$

where x is the response and r is the same input as for Eq.3.4.1.

The problem at hand is to identify h_1 and h_0 so that the reference system and model have the same response to a given input. It is assumed that h_1 and h_0 are completely arbitrary, except that one may assign initial values to h_1 and h_0 which lie within the stability region of the Liapunov function chosen for identification. The initial values are denoted by h_{10} and h_{00} . A controller or an adaptive algorithm is now realized which updates the initially chosen values of h_1 and h_0 so that the final mathematical model represents the reference system.

For a phase variable representation of Eq.3.4.2 the H matrix for the model system has the form

$$\begin{bmatrix} 0 & 1 \\ -h_0 & -h_1 \end{bmatrix} \quad 3.4.3$$

and the realization is shown in Figure 3.2. Equations 3.3.37, 3.3.38 and 3.3.39 and 3.3.40 may now be used to find the controller dynamics and they are given by the following relationships:

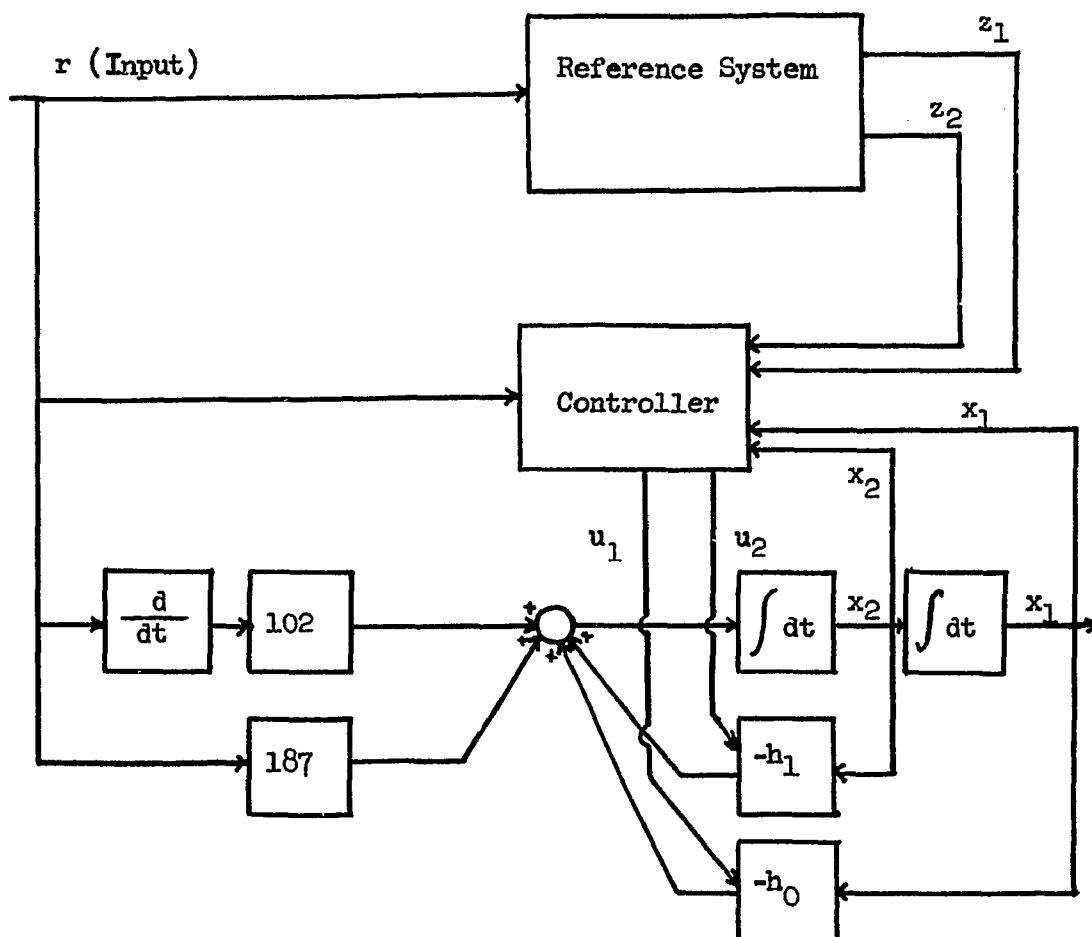


Fig. 3.2 Phase variable form realization for a second order model (Two parameter adaptation)

$$\begin{bmatrix} \dot{u}_1 \\ \dot{u}_2 \end{bmatrix} = \begin{bmatrix} \dot{h}_0 \\ \dot{h}_1 \end{bmatrix} = \begin{bmatrix} \frac{m_{12} e_1 + m_{22} e_2}{n_{11} n_{22} - n_{12}^2} (- x_1 n_{22} + x_2 n_{12}) \\ \frac{m_{12} e_1 + m_{22} e_2}{n_{11} n_{22} - n_{12}^2} (x_1 n_{12} - x_2 n_{11}) \end{bmatrix} \quad 3.4.4$$

Note that \dot{w}_1 and \dot{w}_2 are equal to zero for this example.

In order to satisfy Liapunov's stability criterion i.e. $V > 0$, $\dot{V} < 0$, the following conditions are imposed:

$$n_{11} > 0$$

$$n_{22} > 0 \quad 3.4.5$$

$$n_{11} n_{22} - n_{12}^2 > 0$$

$$m_{11} > 0$$

$$m_{22} > 0 \quad 3.4.6$$

$$m_{11} m_{22} - m_{12}^2 > 0$$

and from Equation 3.3.30

$$D = \begin{bmatrix} 2 a_0 m_{12} & a_0 m_{22} + a_1 m_{12} - m_{11} \\ a_0 m_{22} + h_1 m_{12} m_{11} & 2 (a_1 m_{22} - m_{12}) \end{bmatrix} \quad 3.4.7$$

Equation 3.4.7 contain the unknown parameters and consequently choosing the elements of the matrix M to obtain a convergent controller becomes a trial and error procedure. In many cases some range of values are

known for the parameters of the unknown system and this eases the problem of finding appropriate elements of the matrix M to obtain convergent algorithms. Because Liapunov's criterion is only a sufficient condition to obtain a convergent controller, parameters which do not satisfy these equations will also sometimes lead to converging algorithms.

In Figures 3.3 and 3.4, are shown the time behaviour of the parameter adaptation and the state errors. The behaviour in parameter space is shown in Figure 3.5. The controller design matrices were chosen as:

$$M = \begin{bmatrix} 4268 & 29 \\ 29 & 30 \end{bmatrix} \quad 3.4.8$$

$$D = \begin{bmatrix} 7018 & 0 \\ 0 & 1262 \end{bmatrix} \quad 3.4.9$$

$$N = \begin{bmatrix} 1 & .5 \\ .5 & 1 \end{bmatrix} \quad 3.4.10$$

The starting values of the parameters are

$$h_{10} = 100 \quad h_{00} = 50 \quad 3.4.11$$

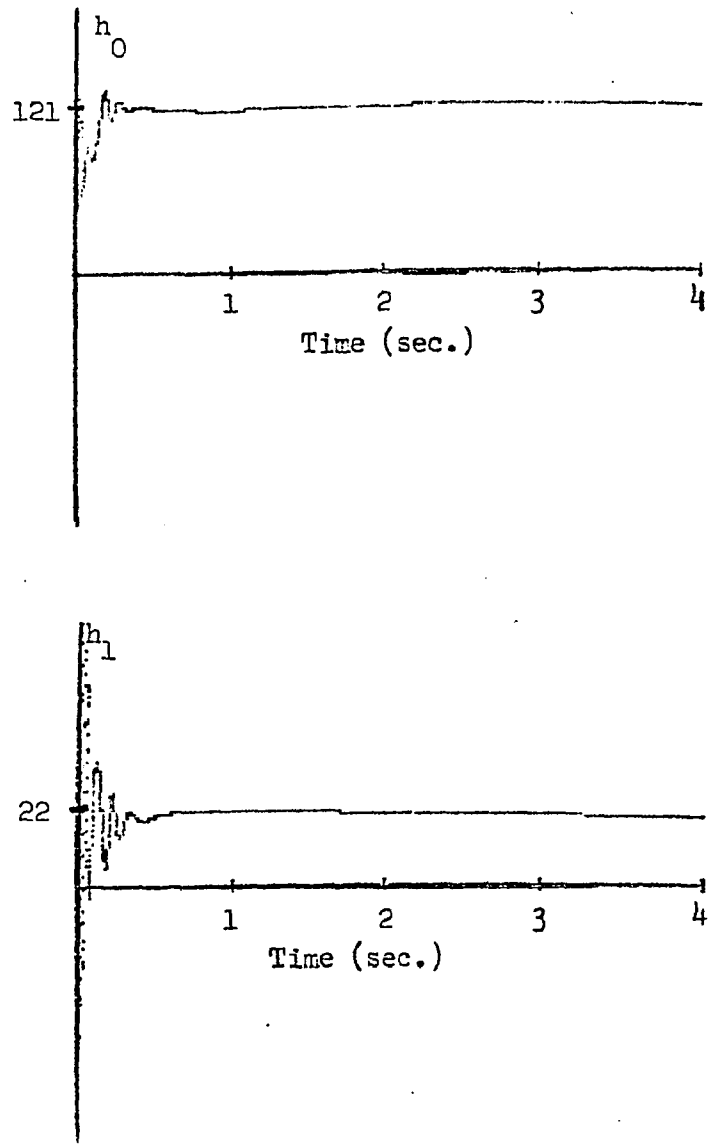


Fig. 3.3 Adaptation of parameters h_1 and h_0 (Example 1)

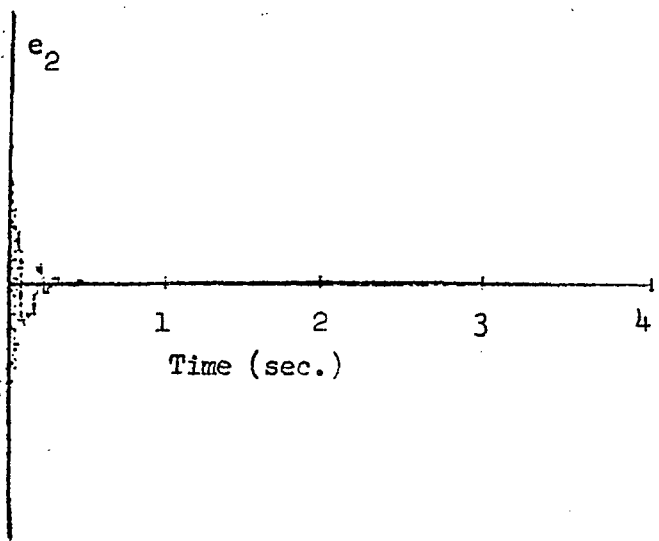
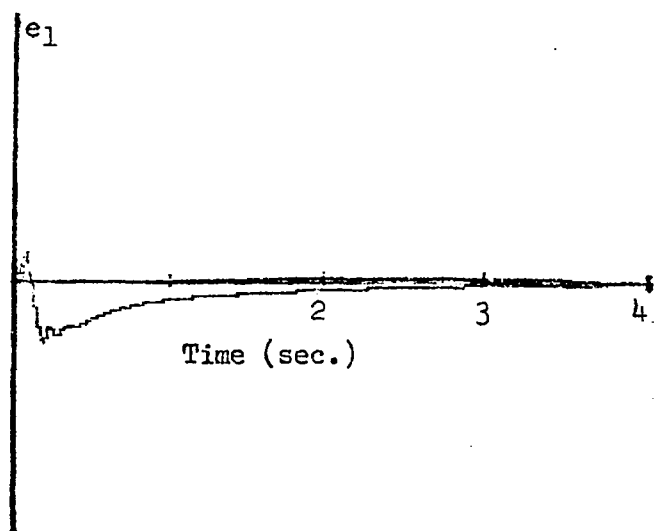


Fig. 3.4 Model-Reference system errors e_1 and e_2 vs. time during adaptation (Example 1)

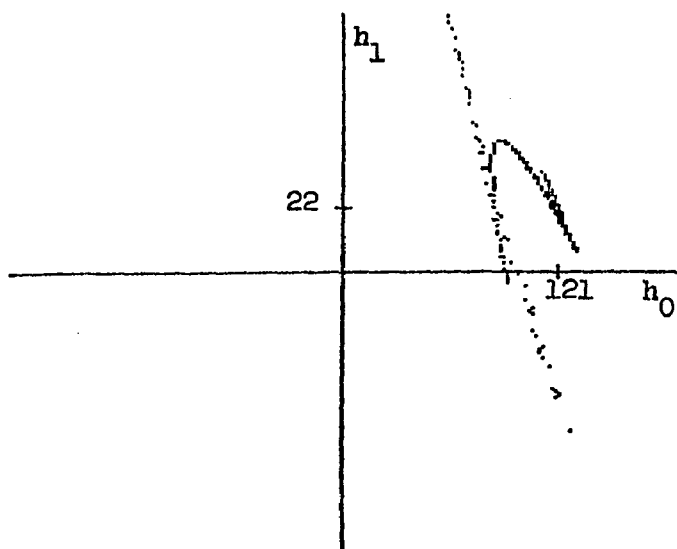


Fig. 3.5 Adaptation of parameters h_1 and h_0 in parameter space (Example 1). Starting values of parameters $h_1 = 100$, $h_0 = 50$ Final values of Parameters $h_1 = 22^{10}$, $h_0 = 121$.

3.4.2. Example 2 - Second Order System with 2 Unknown Parameters
(Observable Form)

This example examines the performance of the adaptive controller when applied to a second order model system. The system matrix, which contains two unknown parameters, is to be identified for an Observable Form realization.

The reference system is again assumed to be described by the differential equation

$$\ddot{z} + 22 \dot{z} + 121 z = 102 \dot{r} + 187 r \quad 3.4.12$$

where r is the input and z is the response.

A tentative mathematical model for the reference system is again chosen of the form

$$\ddot{x} + h_1 \dot{x} + h_0 x = 102 \dot{r} + 187 r \quad 3.4.13$$

where h_1 and h_0 should adapt to the values 22 and 121 respectively. Therefore a controller must be designed to update the initially chosen values of h_1 and h_0 . For an Observable Form realization of Equation 3.4.13, the H matrix for the model has the form

$$H = \begin{bmatrix} -h_1 & 1 \\ -h_0 & 0 \end{bmatrix} \quad 3.4.14$$

and the realization is shown in Figure 3.6.

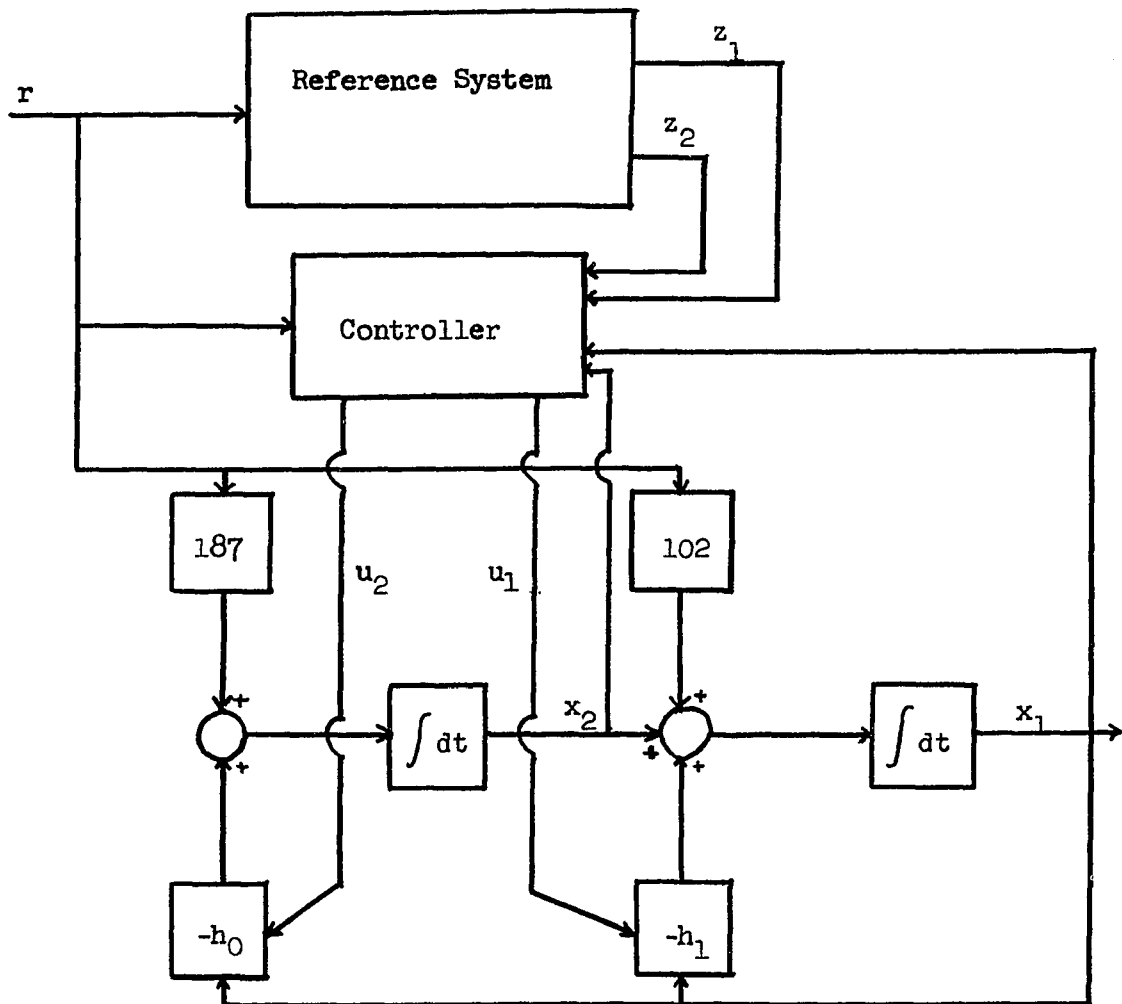


Fig. 3.6 Observable form realization for a second order model
(Two parameter adaptation)

From Equation 3.3.71 and 3.3.72 the controller equations are as follows:

$$\begin{bmatrix} \dot{u}_1 \\ \dot{u}_2 \end{bmatrix} = \begin{bmatrix} \frac{x_1}{n_{11} n_{22} - n_{12}^2} \left[(-n_{22} m_{11} + n_{12} m_{12})e_1 + (-n_{22} m_{12} + m_{22} n_{12})e_2 \right] \\ \frac{x_2}{n_{11} n_{22} - n_{12}^2} \left[(-n_{11} m_{12} + m_{11} n_{12})e_1 + (-n_{11} m_{22} + m_{12} n_{12})e_2 \right] \end{bmatrix} \quad 3.4.15$$

Note that \dot{w}_1 and \dot{w}_2 are equal to zero.

In order to satisfy Liapunov's criterion for stability that $V \geq 0$ and $\dot{V} \leq 0$ the following conditions must be satisfied:

$$n_{11} > 0$$

$$n_{22} > 0 \quad 3.4.16$$

$$n_{11} n_{22} - n_{12}^2 > 0$$

$$m_{11} > 0$$

$$m_{22} > 0 \quad 3.4.17$$

$$m_{11} m_{22} - m_{12}^2 > 0$$

The matrix D is given in terms of the elements of the M and A matrices

by

$$D = \begin{bmatrix} 2 m_{11} a_1 + 2 m_{12} a_0 & a_1 m_{12} + m_{22} a_0 - m_{11} \\ a_1 m_{12} + m_{22} a_0 - m_{11} & -2 m_{12} \end{bmatrix} \quad 3.4.18$$

Note that for this example again the D matrix depends on the unknown parameters a_1 and a_0 . The reason and justification for this is explained above in Sections 3.3.3 and 3.4.1 .

In Figures 3.7 and 3.8 are shown the time history of the parameters h_1 and h_0 and the time behaviour of the model-reference system errors e_1 and e_2 respectively. The behaviour of h_1 and h_0 and e_1 and e_0 in parameter space and error state space respectively are demonstrated in Figure 3.9. The matrices M, D, and N used in the controller design were chosen as:

$$M = \begin{bmatrix} 700 & -23.96 \\ -23.96 & 10.142 \end{bmatrix} \quad 3.4.19$$

$$D = \begin{bmatrix} 25001.68 & 0 \\ 0 & 47.92 \end{bmatrix} \quad 3.4.20$$

$$N = \begin{bmatrix} .01 & 0 \\ 0 & .01 \end{bmatrix} \quad 3.4.21$$

The starting values of the model parameters were chosen as

$$h_{10} = 2 \quad h_{00} = 200 \quad 3.4.22$$

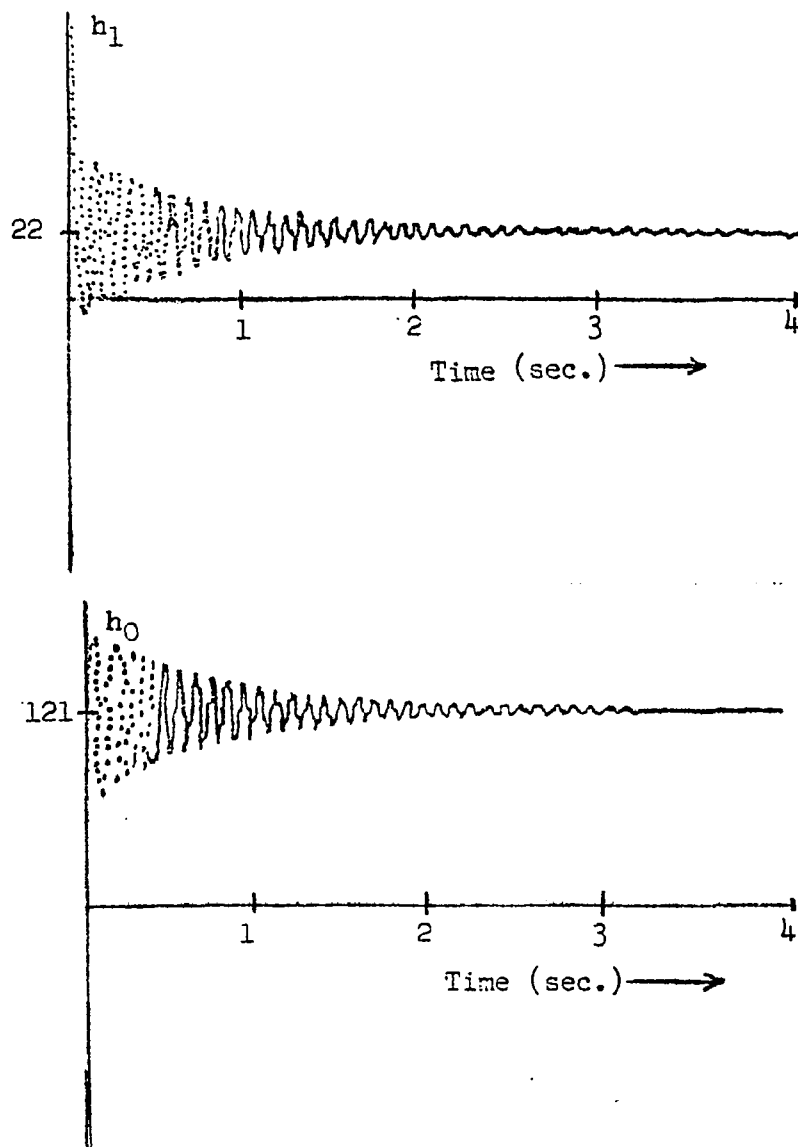


Fig. 3.7 Adaptation of parameters h_1 and h_0 (Example 2)

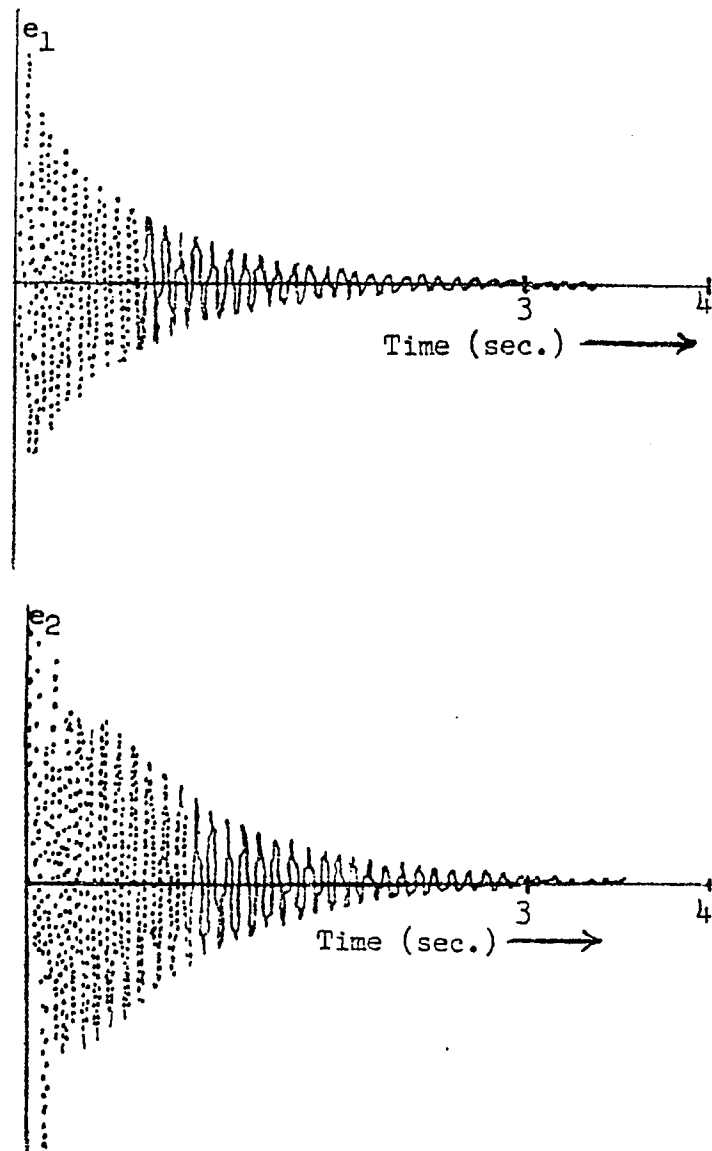


Fig. 3.8 Model-reference system errors e_1 and e_2 vs. time during adaptation (Example 2).

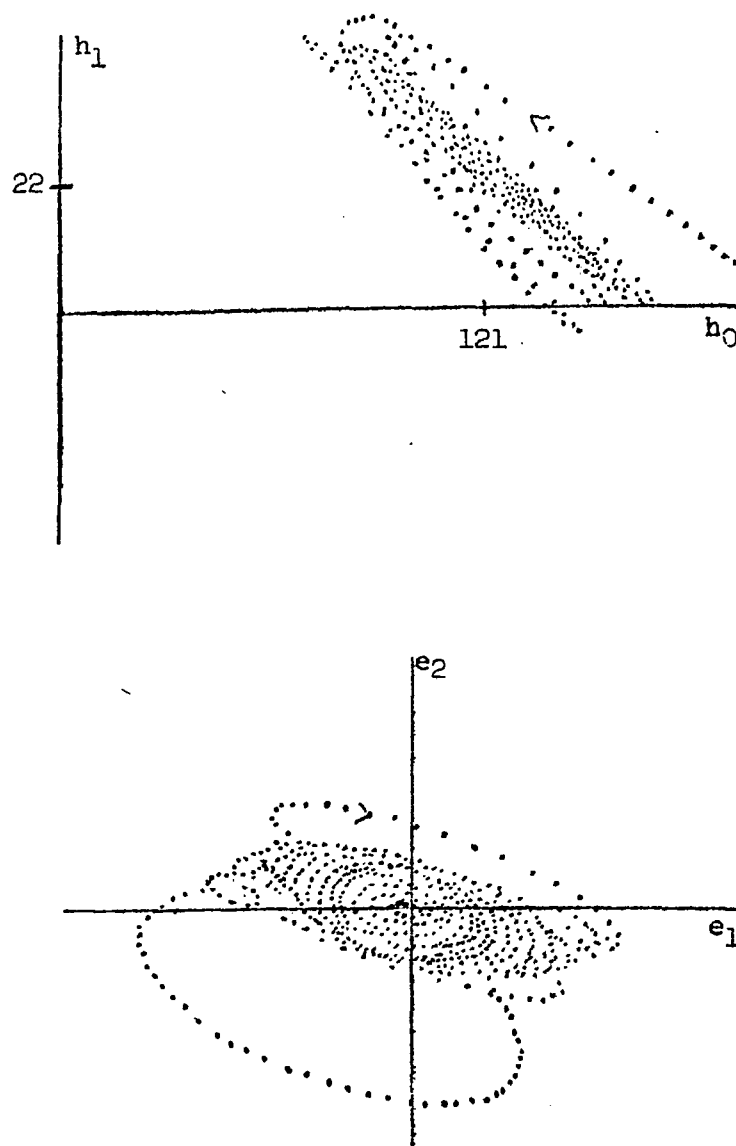


Fig. 3.9 Adaptation of parameters h_1 and h_0 in parameter space and the behavior of the errors e_1 and e_2 in error space (Example 2). Starting values of parameters $h_1 = 2$, $h_0 = 200$ final values of parameters $h_1 = 22$ and $h_0 = 121$. Errors e_1 and e_2 oscillate and decay toward zero.

3.5 Confidence Criterion for Modeling Approach

The purpose of the previous examples was to check the validity of the controller adaptive properties. Since the reference system was assumed to be known (all the parameters known) a criterion to establish identification of the model was not necessary. One can determine the identification of the model when the parameters of the model approach the reference system parameter values. However, when the reference system parameters are unknown, as is the case in physiological systems, an exact model structure for the reference system is never assured. Consequently, one must have a way of insuring with some degree of confidence that the model is representative of the processes in the reference system under investigation. Such a criterion is called a "confidence criterion" and is derived in this section. Among its features the criterion may also suggest whether additional stimulus is required to continue the adaptive process of the model.

Since the controller is designed based on a Liapunov function, the overall model reference configuration is stable and the Liapunov function value at $t = 0$ is larger than at any other time, i.e.

$V(0) \geq V(t)$. The integral of $-\dot{V}(t)$ is given by

$$\int_0^T -\dot{V} dt = V(0) - V(T) \quad \begin{array}{l} (T - \text{Identification}) \\ \text{Interval} \end{array} \quad 3.5.1$$

together with the Liapunov function at $t = 0$ may be utilized to form a "confidence criterion".

Let the "confidence criterion" be defined by:

$$\eta_1 = 1 - \frac{\int_0^T -\dot{V} dt}{V(0)} \quad 3.5.2$$

Substituting Eq.3.5.1 into Eq.3.5.2 yields:

$$\eta_1 = \frac{V(t)|_T}{V(0)|_T} \quad 3.5.3$$

If the model-reference configuration is asymptotically stable then $V(T) \rightarrow 0$ and hence $\eta_1 \rightarrow 0$.

Therefore, the smaller η_1 gets, the better the adaptation.

The negative semi-definite derivative of the Liapunov function implies that the model reference system is only stable and not asymptotically stable. Therefore adaptation could stop without having identified the proper values of parameters. One way to overcome this difficulty is to monitor the value of η_1 and keep perturbing the system until η_1 is below some present value, i.e., $\eta_1 < c$ where c is some arbitrary constant. For inexact modeling, if η_1 does not get smaller then the model has been adapted to its fullest extent.

In order to monitor η_1 over the identification interval, the derivative of the Liapunov function \dot{V} and the initial value of the Liapunov function $V(0)$ must be known.

The Liapunov function may be viewed as being composed of three parts, i.e.

$$V = V_1 + V_2 + V_3 \quad 3.5.4$$

$$\text{where } V_1 = \underline{e}^t M \underline{e} \quad 3.5.5$$

$$V_2 = \underline{u}^t N \underline{u} \quad 3.5.6$$

$$V_3 = \underline{w}^t Q \underline{w} \quad 3.5.7$$

If N and Q are chosen such that

$$M \gg N \quad 3.5.8$$

$$M \gg Q \quad 3.5.9$$

over the range of possible initial parameter errors then

$$V(0) \cong V_1(\underline{e}) + \int_0^{T_m} -\dot{V} dt \quad 3.5.10$$

and may be taken as an estimate of $V(0)$. T_m is the time at which V_1 reaches its maximum value, $V_{1\max}$.

The "confidence criterion" may then be monitored over the identification interval by substituting 3.5.10 into 3.5.2 and obtaining:

$$\eta_1 = 1 - \frac{\int_0^T -\dot{V} dt}{V_{1\max} + \int_0^{T_m} -\dot{V} dt} \quad 3.5.11$$

$$3.5.11$$

Another parameter of interest is the smallness of the error portion of the Liapunov function at the end of the identification interval compared to its initial value. Thus the following parameter may be defined:

$$\eta_2 = \frac{V_1(\underline{e})|_T}{V(0)} = \frac{V_1(\underline{e})|_T}{V_1(\underline{e})|_{T_m} + \int_0^{T_m} -\dot{V} dt} \quad 3.5.12$$

where $V_1(\underline{e})$ is given by Equation 3.5.5 and $V(0)$ is estimated by 3.5.10.

3.6 Modified Model-Reference Adaptive Controller Design

In the previous section it was shown how a "confidence criterion" for adaptation could be defined if one had knowledge of both $V(0)$, the initial value of the Liapunov function, and \dot{V} the derivative of the Liapunov function for all time. In order to alleviate some of the difficulties discussed previously such as finding the \dot{V} function and estimating the initial value of the Liapunov function $V(0)$, a modified model-reference adaptive controller is utilized (69,70).

Let the reference system be of the same form as before

$$\dot{\underline{z}} = A \underline{z} + B \underline{r} \quad 3.6.1$$

and modified model system is now chosen as

$$\dot{\underline{x}} = K \underline{x} + (H - K) \underline{z} + G \underline{r} \quad 3.6.2$$

where H and G are to be identified such that as $H \rightarrow A$ and $G \rightarrow B$ and K is an arbitrary known stable matrix. The form of K is chosen in accordance with the form of the matrix H and will be dependent on the realization desired for the model. A functional diagram of the modified model-reference configuration is shown in Figure 3.10A.

Insight into the dynamic properties of the modified model-reference adaptive system can be obtained by examining the equations and model reference configuration for the second order case.

For the second order observable form case the **modified model** equations are given by:

$$\begin{aligned} \dot{x}_1 &= -k_1 x_1 + x_2 + (-h_1 + k_1) z_1 & +g_1 r & \quad 3.6.3 \\ \dot{x}_2 &= -k_0 x_1 & + (-h_0 + k_0) z_1 & +g_0 r \end{aligned}$$

The realization is shown in Figure 3.10B. From this simple case it

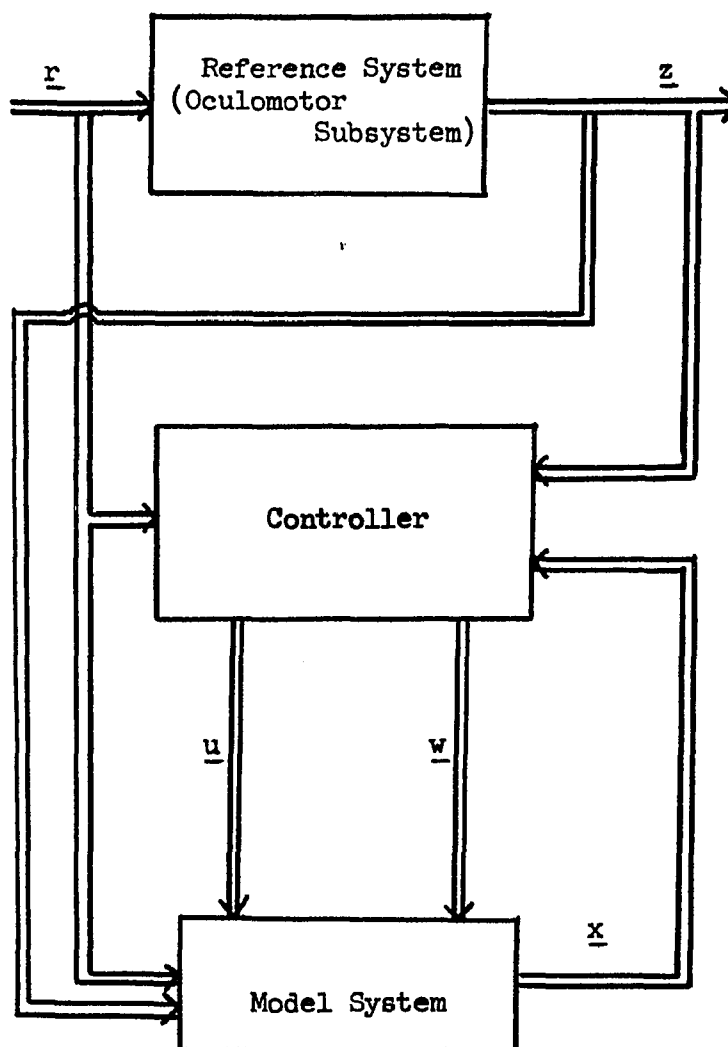


Fig 3.10 A Modified model-reference configuration for adaptation of a model in state form. Controller design is based on a Liapunov function. \underline{r} is the stimulus vector, \underline{z} and \underline{x} are the reference system and model system state vectors respectively, and \underline{u} and \underline{w} are the controller adaptation vectors.

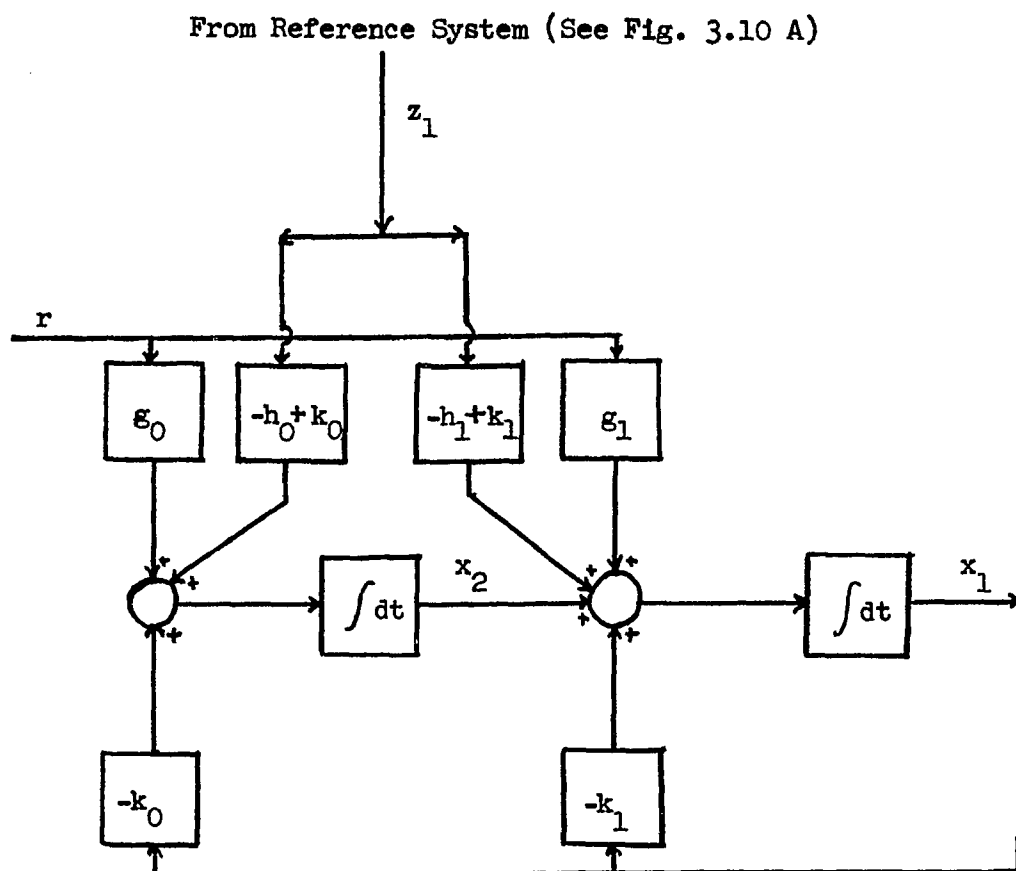


Fig. 3.10 B Second order realization of a modified model

can be seen that by changing the model-reference configuration to a modified model-reference configuration the h parameters have been altered from being feedback elements in the model to feed forward gains in the modified model. In other words, the elements of the K matrix provide the feedback gain for the model system. Since the reference system states are bounded and K can be chosen arbitrarily this will lead to greater stability in the adaptive algorithms if the eigenvalues of K are chosen negative. It also allows greater flexibility since additional parameters have been introduced via the K matrix. It must be kept in mind, however, that the h 's although altered in their role for purposes of identification still represent the parameters of the model of the "physiological" system under study.

Returning to the general case, if Equation 3.6.2 is subtracted from Equation 3.6.1 the resultant error vector differential equation yields:

$$\dot{\underline{e}} = K \underline{e} + (A - H) \underline{z} + (B - G) r \quad 3.6.4$$

This is exactly the same error equation obtained previously for the phase variable and observable form realizations of the model reference system, except that matrix K , which is the designer's choice, is multiplying \underline{e} rather than H or A which is either time varying or unknown. For the various forms of realization of the model system, the Liapunov function is chosen as in Section 3.3.2

$$V = \underline{e}^t M \underline{e} + \underline{u}^t N \underline{u} + \underline{w}^t Q \underline{w} \quad 3.6.5$$

where M , N and Q are defined by Equations 3.3.25, 3.3.26 and 3.3.27. The resultant controller dynamics for the phase variable realization

of a linear system are then exactly the same as Equations 3.3.35 and 3.3.36 and are repeated here

$$\dot{\underline{u}}^t = - \underline{z}^t N^{-1} (\underline{b}^t M \underline{e}) \quad 3.6.6$$

$$\dot{\underline{w}}^t = - \underline{r}^t Q^{-1} (\underline{d}^t M \underline{e}) \quad 3.6.7$$

For the observable form realization, the controller dynamics are obtained with z_1 replacing x_1 in Equations 3.3.67 and 3.3.68 and are given by

$$\dot{\underline{u}} = - N^{-1} M \underline{e} z_1 \quad 3.6.8$$

$$\dot{\underline{w}} = - Q^{-1} M \underline{e} r \quad 3.6.9$$

However, the derivative of the Liapunov function which is given by

$$\dot{V} = - \underline{e}^t D \underline{e} \quad 3.6.10$$

is now dependent on known chosen matrices since

$$- D = K^t M + M K \quad 3.6.11$$

where K and M are chosen in order to obtain satisfactory convergence properties.

The confidence criterion discussed in Section 3.5 may now be evaluated using Equation 3.5.2 as:

$$\eta_1 = 1 - \frac{\int_0^T \underline{e}^t D \underline{e} dt}{\underline{e}^t M \underline{e} \Big|_{T_m} + \int_0^{T_m} \underline{e}^t D \underline{e} dt} \quad 3.6.12$$

where T_m is the time at which V_1 reaches a maximum. Since D is a known matrix given by Equation 3.6.11, η_1 may be evaluated.

In the next section examples showing the convergence properties of the modified adaptive algorithm will be shown. The usefulness of the "confidence criterion" will also be demonstrated.

One may also examine

$$\eta = \sqrt{\eta_1^2 + \eta_2^2} \quad 3.6.13$$

as a check on the adaptation.

In order to evaluate 3.6.11 - 3.6.13, the time derivative of the Liapunov function (\dot{V}) would have to be known over the entire identification interval. However, to know \dot{V} at each instant of time one would need knowledge of the reference system matrix A in order to evaluate Matrix D where

$$-D = A^t M + M A \quad 3.6.14$$

since $\dot{V} = -e^t D e$. Because A required identification, V is an unknown function throughout the identification interval. Consequently, a modification in the adaptive algorithm is required to establish a viable "confidence criterion". Before such a criterion can be established a modified model reference system is considered. This is shown in Sections 3.6 and 3.7.

3.7 Examples Showing the Modified Model Reference Adaptation

In this section the same examples which were shown above in Section 3.4 are reevaluated to demonstrate the adaptive properties of the modified model reference system and to demonstrate how the "confidence criterion" defined previously may be used to give a measure of the adaptation which has taken place.

In each of these examples the reference system is assumed to be given by the differential equation:

$$\frac{d^2z}{dt^2} + a_1 \frac{dz}{dt} + a_0 z = b_1 \frac{dr}{dt} + b_0 r \quad 3.7.1$$

where a_1 , a_0 , b_1 and b_0 are specified for each example and "controllable" and "observable" form realizations for this system are identified. The model representations were chosen as

$$\begin{bmatrix} \dot{x}_1 \\ \dot{x}_2 \end{bmatrix} = \begin{bmatrix} -k_1 & 1 \\ -k_0 & 0 \end{bmatrix} \begin{bmatrix} x_1 \\ x_2 \end{bmatrix} + \begin{bmatrix} -h_1 + k_1 \\ -h_0 + k_0 \end{bmatrix} z_1 + \begin{bmatrix} g_1 \\ g_0 \end{bmatrix} r \quad 3.7.2$$

for the observable form realization and

$$\begin{bmatrix} \dot{x}_1 \\ \dot{x}_2 \end{bmatrix} = \begin{bmatrix} 0 & 1 \\ -k_0 & -k_1 \end{bmatrix} \begin{bmatrix} x_1 \\ x_2 \end{bmatrix} + \begin{bmatrix} 0 & 0 \\ -h_1 + k_1 & -h_0 + k_0 \end{bmatrix} \begin{bmatrix} z_1 \\ z_2 \end{bmatrix} + \begin{bmatrix} 0 & 0 \\ g_0 & g_1 \end{bmatrix} \begin{bmatrix} r_1 \\ r_2 \end{bmatrix} \quad 3.7.3$$

for the controllable form realization. Note that h_1 and h_0 and g_1 and g_0 are the parameters which correspond to the reference system parameters a_1 , a_0 , b_1 and b_0 respectively.* Note also $r_1=r$ and $r_2=\frac{dr}{dt}$.

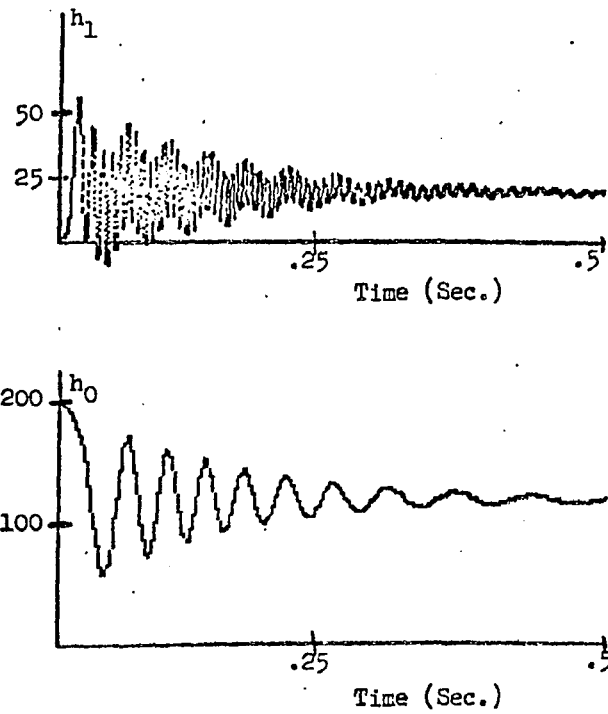
*See Section 3.6 for a detailed explanation

For each of the examples presented in this section, computer printed graphs are shown for each parameter adaptation. Below the graph the printed computer information is shown. The starting parameters at the beginning of the identification interval, the M, N, K, and D matrices used to obtain the controller dynamics are also given. The final values of the parameters are indicated by an F in front of the parameter, i.e., FHL, FHO, FGL, and FGO. Printed out are the other pertinent parameters which are related to the adaptation. The $\int_0^T -\dot{V} dt$ is denoted by INT VD, the maximum value of V_1 during the adaptation interval is denoted by VIM and the estimation of $V(0)$ is shown. The confidence criterion η_1 is evaluated in terms of INT VD and $V(0)$ and denoted by ETA1. ETA2 (η_2) is evaluated in the program as $V_1(e)/V(0)|_{T_m}$ and is a measure of how close the error signal, $e = \underline{z} - \underline{x}$, is to zero. The parameter $\eta = \sqrt{\eta_1^2 + \eta_2^2}$ is also given and is denoted by ETA.

Since $V_1(e)$ is used in estimating the value of $V(0)$, which is in turn used in defining the confidence criterion, its dynamic behaviour is shown for each example. It can be seen that V_1 reaches a maximum value very early in the identification interval and then falls off toward zero as adaptation takes place.

3.7.1 Example 1 - Two Parameter Adaptation for an Observable Form Realization

In Figure 3.11 is shown the adaptation of h_1 and h_0 for an observable form model realization. Parameters g_1 and g_0 are assumed to be the same as the corresponding reference system parameters and having the value 102 and 187 respectively. In Figure 3.12 is shown the



```

TIME=.5 STAR PAR 41-40:2 :200 M MAT:700 :-100 .37 V MAT:.01 :0 :.01
K MAT:30 :100 D MAT:22000 :0 :200
FH1= 21.4750
FH0= 122.3670
INT VD= 67.3662
VIM= 51.2413
V(0)= 65.0355
ETA1=- 0.0353 ETA2= 0.0004 ETA= 0.0359*

```

Fig. 3.11 Parameters h_1 and h_0 adaptation for modified model-reference system (Example 1)

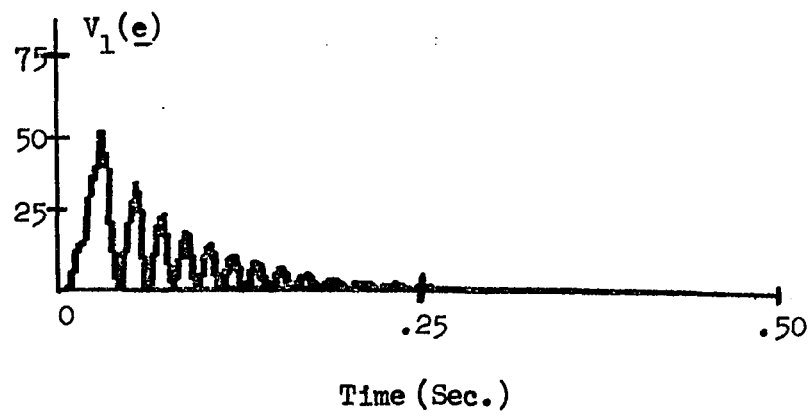


Fig. 3.12 Portion of Liapunov function ($V_1 = e^t M e$) used in evaluating confidence criterion (Example 1)

variation of the error portion of the Liapunov function $V_1(\underline{e})$ with time. The maximum value of this function is used in estimating the initial value of the Liapunov function V , i.e. $V(0)$. The time interval for the adaptation is .5 seconds. The initial values of the model parameters and the matrices used in designing the controller are:

$$h_{10} = 2 \quad h_{00} = 200 \quad 3.7.4$$

$$K = \begin{bmatrix} -30 & 1 \\ -100 & 0 \end{bmatrix} \quad 3.7.5$$

$$M = \begin{bmatrix} 700 & -100 \\ -100 & 37 \end{bmatrix} \quad 3.7.6$$

$$D = \begin{bmatrix} 22000 & 0 \\ 0 & 22000 \end{bmatrix} \quad 3.7.7$$

$$N = \begin{bmatrix} .01 & 0 \\ 0 & .01 \end{bmatrix} \quad 3.7.8$$

3.7.2 Example 2 - Three Parameter Adaptation for a Controllable Form Realization

This example demonstrates a three parameter adaptation of a second order model system whose form is a phase variable realization. Parameters h_1 , h_0 , and g_0 are identified and parameter g_1 is assumed to be known and equal to the corresponding reference system parameter

having a value $g_1 = 0$. The time for each subadaptation interval is .25 seconds and the total adaptation interval is .5 seconds. The initial values of the model parameters and the matrices used in designing the controller are:

$$h_{10} = 99 \quad h_{00} = 50 \quad g_{00} = 0 \quad 3.7.9$$

$$K = \begin{bmatrix} 0 & 1 \\ -100 & 30 \end{bmatrix} \quad 3.7.10$$

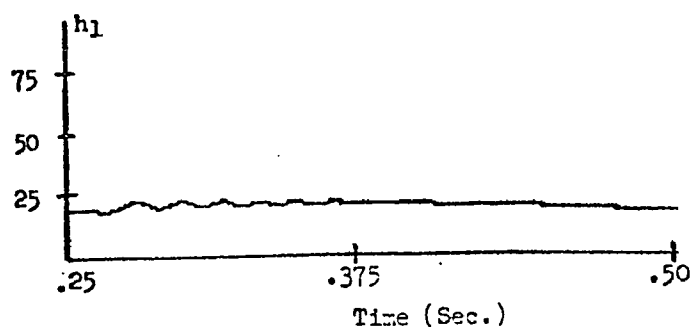
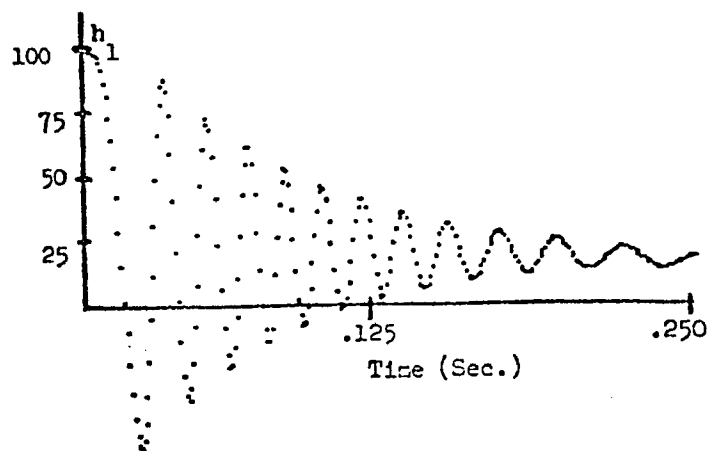
$$M = \begin{bmatrix} 3870 & -89 \\ -89 & 30 \end{bmatrix} \quad 3.7.11$$

$$D = \begin{bmatrix} 22000 & 0 \\ 0 & 220 \end{bmatrix} \quad 3.7.12$$

$$N = \begin{bmatrix} .005 & .0025 \\ .0025 & .005 \end{bmatrix} \quad 3.7.13$$

$$Q = \begin{bmatrix} .005 & .0025 \\ .0025 & .005 \end{bmatrix} \quad 3.7.14$$

The adaptation dynamics are shown in Figures 3.13, 3.14, and 3.15. In Figure 3.16 is shown the variation of the $V_1(\underline{e})$ function with time. As in example 3.7.1, the maximum value of this function is used in estimating the initial value of the Liapunov function, $V(0)$.

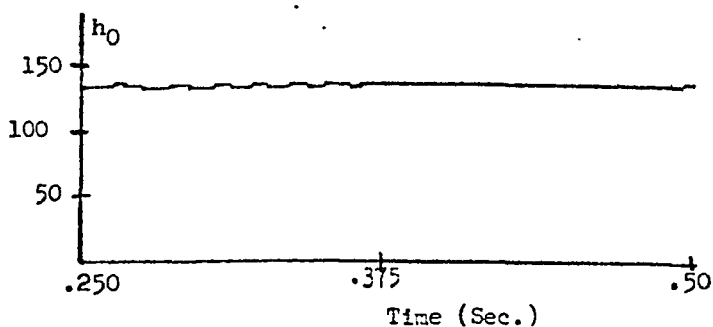
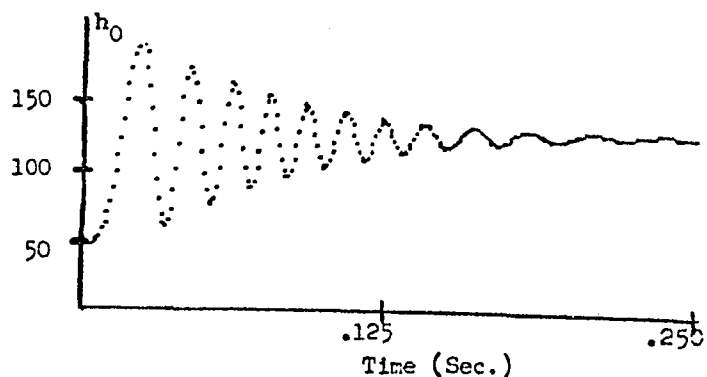


```

TIME: .25 STAR PAR H1-H0, G1-G0: 99 : 50 : 0 : 100 M MAT: 3870 : 29 : 30
K MAT: 30 : 100 D MAT: 5300 : 0 : 1742
N MAT: .005 : .0025 : .005 Q MAT: .005 : 0 : .005 DT: .001
FH1= 19.7541 FH0= 133.1950
FG1= 0.0000 FG0= 186.1370
INT VD= 86.5863
VIM= 64.5479
V(0)= 89.0030
ETA1= 0.0272 ETA2 0.0056 ETA= 0.0277
TIME: .25 STAR PAR H1-H0, G1-G0: 19.7541 : 133.1950 : 0 : 186.1370
M MAT: 3870 : 29 : 30 K MAT: 30 : 100 D MAT: 5300 : 0 : 1742
N MAT: .005 : .0025 : .005 Q MAT: .005 : 0 : .005 DT: .001
FH1= 17.0167 FH0= 134.0790
FG1= 0.0000 FG0= 187.5610
INT VD= 86.6198
VIM= 0.0255
V(0)= 89.0030
ETA1= 0.0268 ETA2= 0.0000 ETA= 0.0268

```

Fig. 3.13 Parameter h_1 adaptation for modified model-reference system (Example 2)

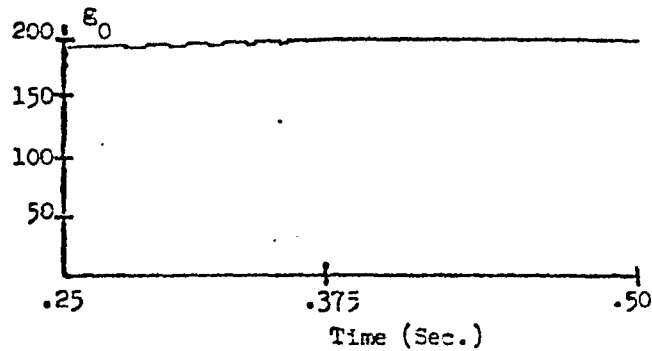
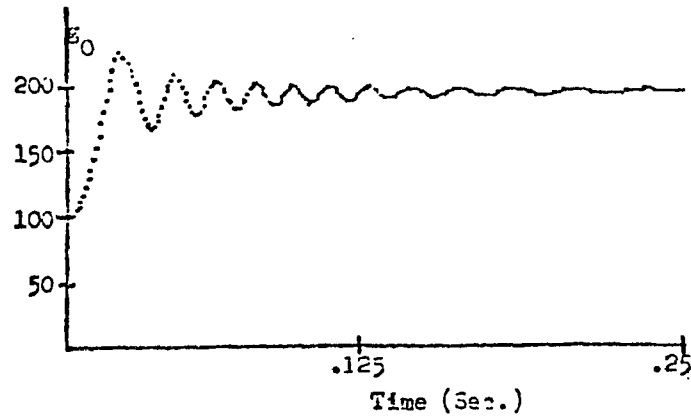


```

TIME: .25 STAR PAR 41-40, G1-G0: 99 : 50 : 0 : 100 M MAT: 3970 : 29 : 30
K MAT: 30 : 100 D MAT: 5900 : 0 : 1742
N MAT: .005 : .0025 : .005 Q MAT: .005 : 0 : .005 DT: .001
FH1= 19.7541 FH0= 133.1950
FG1= 0.0000 FGO= 186.1370
INT VD= 86.5863
VIM= 64.5479
V(0)= 99.0030
ETA1= 0.0272 ETA2 0.0056 ETA= 0.0277
TIME: .25 STAR PAR 41-40, G1-G0: 19.7541 : 133.1950 : 0 : 186.137
M MAT: 3970 : 29 : 30 K MAT: 30 : 100 D MAT: 5900 : 0 : 1742
N MAT: .005 : .0025 : .005 Q MAT: .005 : 0 : .005 DT: .001
FH1= 17.0167 FH0= 134.0790
FG1= 0.0000 FGO= 187.5610
INT VD= 86.6198
VIM= 0.0255
V(0)= 89.0030
ETA1= 0.0268 ETA2= 0.0000 ETA= 0.0268

```

Fig. 3.14 Parameter h_0 adaptation for modified model-reference system (Example 2)



```

TIME: .25 STAR PAR H1-40,G1-G0:99 : 50 : 0 : 100 M MAT: 3870 : 29 : 30
K MAT: 30 : 100 D MAT: 5800 : 0 : 1742
N MAT: .005 : .0025 : .005 Q MAT: .005 : 0 : .005 DT: .001
FH1= 19.7541 FH0= 133.1950
FG1= 0.0000 FGO= 186.1370
INT VD= 86.5863
VIM= 64.5479
V(O)= 89.0030
ETA1= 0.0272 ETA2 0.0056 ETA= 0.0277
TIME: .25 STAR PAR H1-40,G1-G0: 10.7541 : 133.1950 : 0 : 186.137
M MAT: 3870 : 29 : 30 K MAT: 30 : 100 D MAT: 5800 : 0 : 1742
N MAT: .005 : .0025 : .005 Q MAT: .005 : 0 : .005 DT: .001
FH1= 17.0167 FH0= 134.0790
FG1= 0.0000 FGO= 197.5610
INT VD= 86.6198
VIM= 0.0255
V(O)= 89.0030
ETA1= 0.0268 ETA2= 0.0000 ETA= 0.0268

```

Fig. 3.15 Parameter g_0 adaptation for modified model-reference system (Example 2)

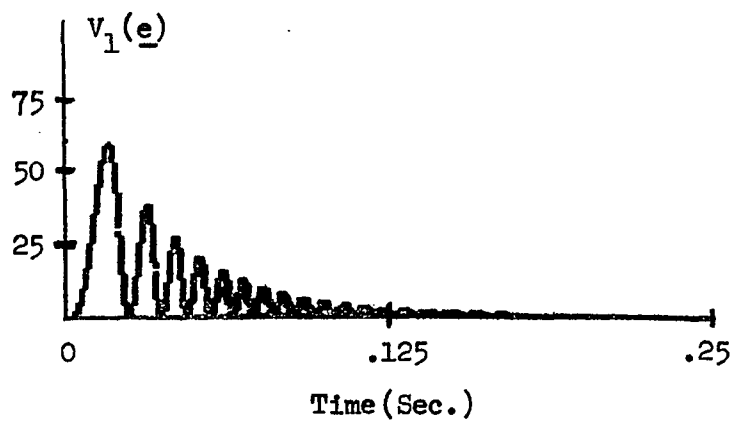


Fig. 3.16 Portion of Liapunov function ($V_1 = \underline{e}^t M \underline{e}$) used in evaluating confidence criterion (Example 2)

It should be noted that the elements of N and Q are chosen small and that under these conditions the adaptation is fairly rapid. For the first .25 sec. the value of η_1 is down to .0272 which is fairly good adaptation. A second run for next .25 sec. starting with the values attained at the end of the first .25 sec. indicates that the maximum value of $V_1 = \underline{e}'\underline{M}\underline{e}$ is .0255 as compared to 64.5479 in the previous subadaptation period. The small value of V_1 in this subinterval is because the parameters have been adapted to fairly close values to the true reference system parameters. Consequently, there is a small error ($V_1 = \underline{e}^t \underline{M} \underline{e}$) term in the next identification subinterval. This can be used as a measure of the goodness of one set of parameters over another set. Any further adaptation would give very slow convergence and does not warrant the extra effort. In some adaptation examples η_1 might go negative. This is an indication that $V(0)$ was not estimated correctly. Smaller choice of N and Q parameters usually improve the estimate of $V(0)$.

3.7.3 Example 3 - Four Parameter Adaptation for an Observable Form Realization

This example shows the adaptation of four parameters h_1 , h_0 , g_1 , and g_0 for an observable form realization. The subadaptation time interval is .25 seconds. This was repeated three times for a total adaptation interval of .75 seconds to show the decrements in η_1 and $V_{1\max}$ in each identification subinterval. This indicates that the model adaptation is improving. The dynamics are shown in Figures 3.17 - 3.22.

The initial choice for the model parameters and the matrices used in the controller design are:

$$h_{10} = 2 \quad h_{00} = 200 \quad g_{10} = 100 \quad g_{00} = 100 \quad 3.7.15$$

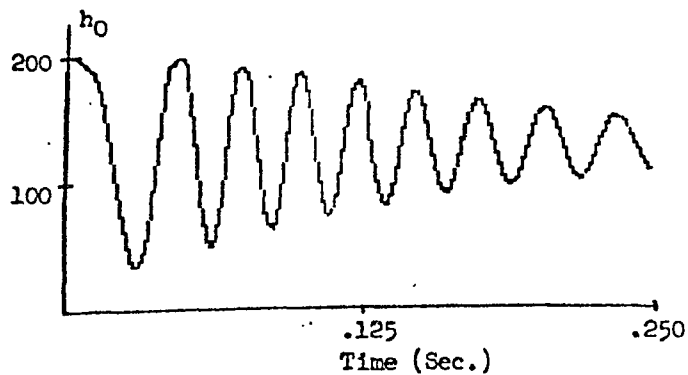
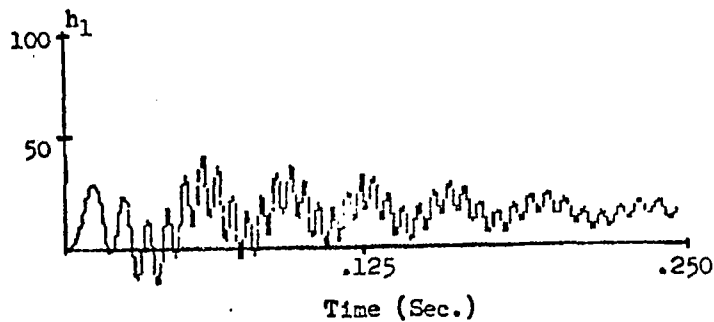
$$K = \begin{bmatrix} -30 & 1 \\ -100 & 0 \end{bmatrix} \quad 3.7.16$$

$$M = \begin{bmatrix} 700 & -100 \\ -100 & 37 \end{bmatrix} \quad 3.7.17$$

$$D = \begin{bmatrix} 22000 & 0 \\ 0 & 22000 \end{bmatrix} \quad 3.7.18$$

$$N = \begin{bmatrix} .005 & 0 \\ 0 & .005 \end{bmatrix} \quad 3.7.19$$

$$Q = \begin{bmatrix} .005 & 0 \\ 0 & .005 \end{bmatrix} \quad 3.7.20$$

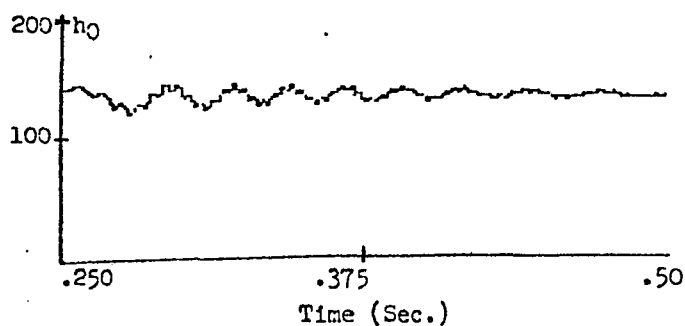
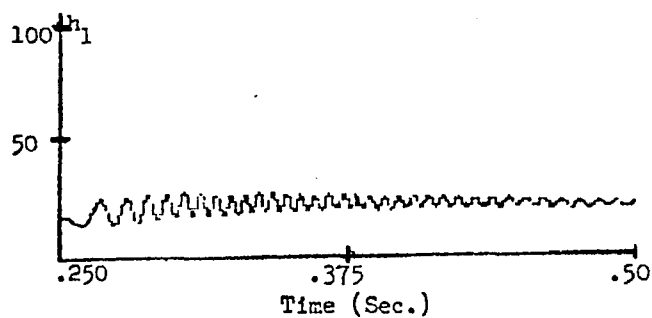


```

TIME: .25 STAR PAR H1-40, G1-G0: 2 : 200 : 100 : 100 M MAT: 700 :-100 : 37
K MAT: 30 : 100 D MAT: 22000 : 0 : 200 N MAT: .005 : 0 : .005 O MAT: .005 : 0 : -.005
DT: .0001
FH1= 11.9252 FH0= 130.9350
FG1= 73.9318 FG0= 185.2170
INT VD= 65.9483
VIM= 54.4610
V(O)= 71.0000
ETA1= 0.0712 ETA2= 0.0163 ETA= 0.0731*

```

Fig. 3.17 Parameter h_1 and h_0 adaptation for modified model-reference system (Example 3)

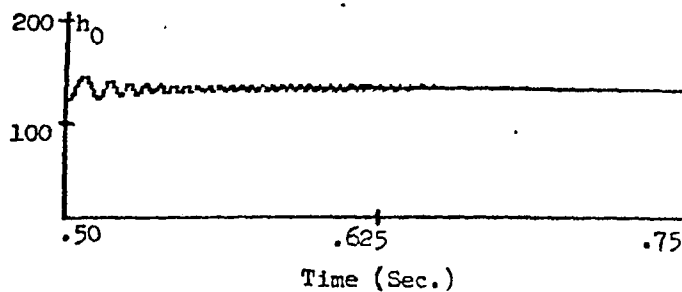
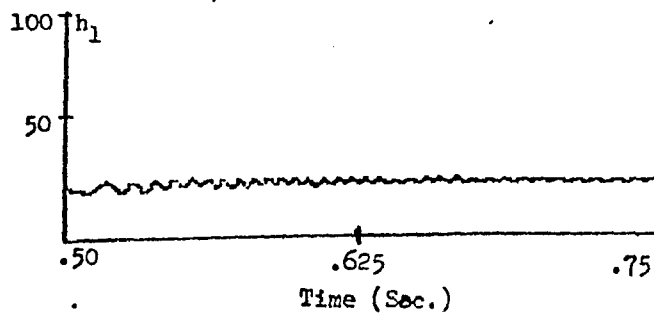


```

TIME: .25 STAR PAR H1-H0, G1-G0: 11.9252 : 130.9850 : 73.9318 : 185.217
M MAT: 700 : -100 : 37 K MAT: 30 : 100 D MAT: 22000 : 0 : 200 N MAT: .005 : 0 : .005
O MAT: .005 : 0 : .005 DT: .0001
FH1= 17.4187 FH0= 123.0070
FG1= 90.2372 FG0= 100.2230
INT VD= 4.0763
VM= 3.5504
V(O)= 71.0000
ETA1= 0.0137 ETA2= 0.0014 ETA= 0.0133*

```

Fig. 3.18 Parameters h_1 and h_0 adaptation for modified model-reference system (Example 3) (Cont.)

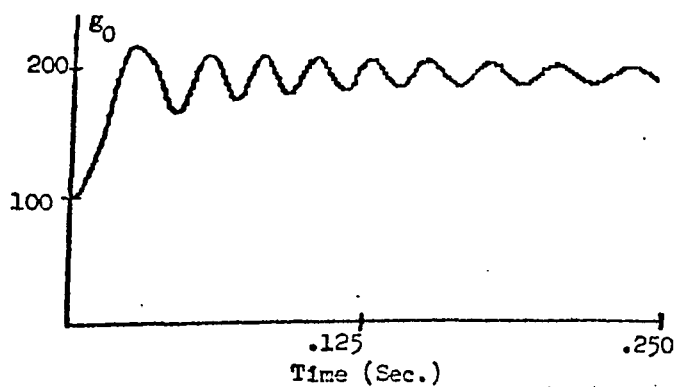
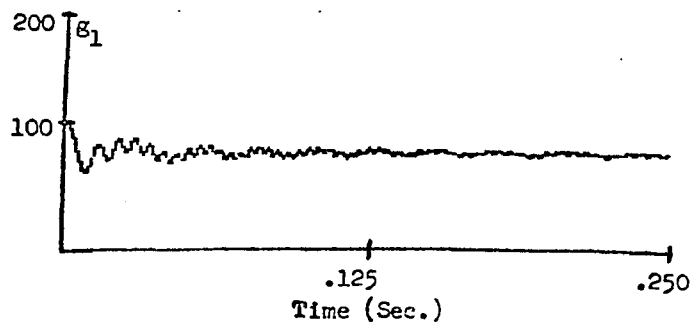


```

TIME: .25 STAR PAR H1-H0, G1-G0: 17.4137 : 123.007 : 97.2872 : 190.223
M MAT: 700 : -100 : 37 K MAT: 30 : 100 D MAT: 22000 : 0 : 200 N MAT: .005 : 0 : .005
O MAT: .005 : 0 : .005 DT=: .0001
FH1= 20.0786 FH0= 121.9060
FG1= 97.2203 FG0= 189.5140
INT VD= 0.6320
VIM= 0.6479
V(P)= 71.0000
ETA1= 0.0041 ETA2 0.0002 ETA= 0.0041*

```

Fig. 3.19 Parameters h_1 and h_0 adaptation for modified model-reference system (Example 3) (Cont.)

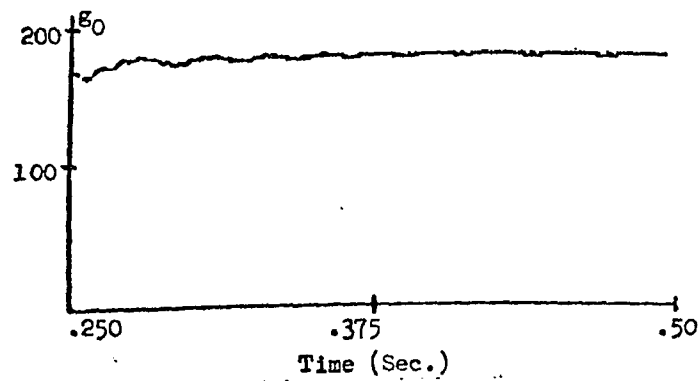
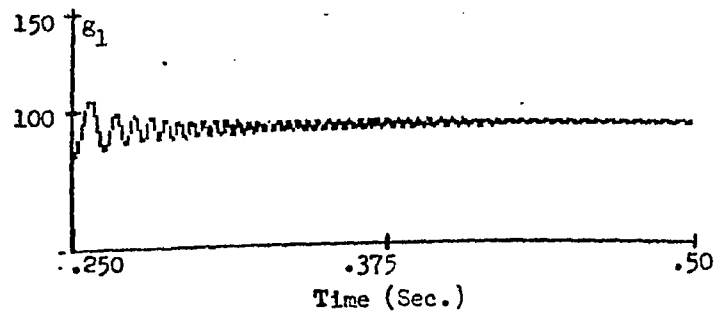


```

TIME: .25 STAR PAR H1-40, G1-G0: 2 : 200 : 100 : 100 M MAT: 700 :-100 : 37
K MAT: 30 : 100 D MAT: 22000 : 0 : 200 N MAT: .005 : 0 : -.005 Q MAT: .005 : 0 : .005
DT: .0001
FH1= 11.9252 FH0= 130.9950
FG1= 73.9313 FG0= 195.2170
INT VD= 65.9493
VIM= 54.4610
V(P)= 71.0000
ETA1= 0.0712 ETA2 0.0168 ETA= 0.0731*

```

Fig. 3.20 Parameters g_1 and g_0 adaptation for modified model-reference system (Example 3)

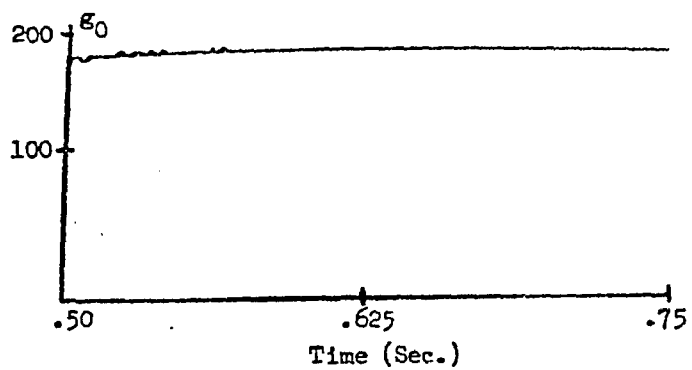
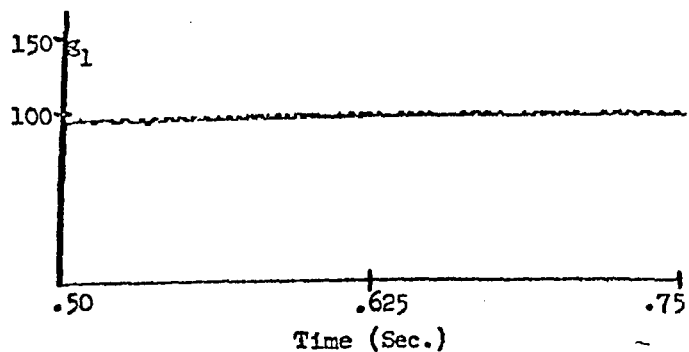


```

TIME: .25 STAR PAR H1-H0, G1-G0: 11.952 : 130.9850 : 73.9318 : 185.2170
M MAT: 700 : -100 : 37 K MAT: 30 : 100 D MAT: 22000 : 0 : 200 N MAT: .005 : 0 : .005
E MAT: .005 : 0 : .005 DT: .0001
FH1= 17.4278 FH0= 123.0060
FG1= 90.3109 FG0= 120.2220
INT VD= 4.0771
VIM= 3.5501
V(P)= 71.0000
ETA1= 0.0137 ETA2 0.0014 ETA= 0.0138*

```

Fig. 3.21 Parameters g_1 and g_0 adaptation for modified model-reference system (Example 3) (Cont.)



```

TIME: .25 STAR PAR H1-H0, G1-G0: 17.4197 : 123.007 : 90.2872 : 190.2230
M MAT: 700 : -100 : 37 K MAT: 30 : 100 D MAT: 22000 : 0 : 200 N MAT: .005 : 0 : .005
O MAT: .005 : 0 : .005 DT: -.0001
FH1= 20.0736 FH0= 121.9060
FG1= 97.2203 FG0= 139.5140
INT VD= 0.6520
VIM= 0.6479
V(O)= 71.0000
ETA1= 0.0041 ETA2 0.0002 ETA= 0.0041*

```

Fig. 3.22 Parameters g_1 and g_0 adaptation for modified model-reference system (Example 3) (Cont.)

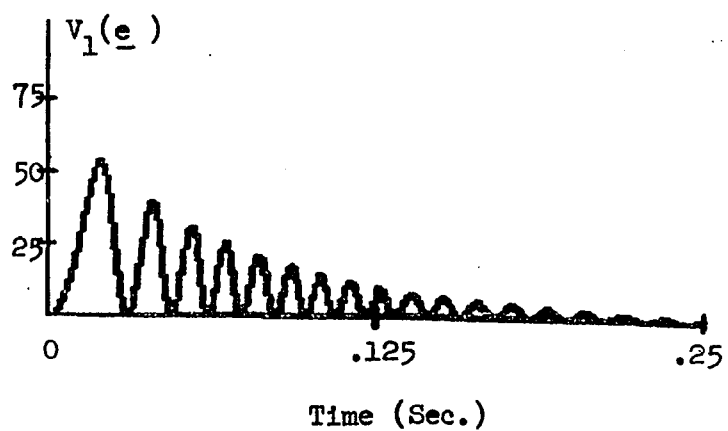


Fig. 3.23 Portion of Liapunov function ($V_1 = \underline{e}^t M \underline{e}$) used in evaluating confidence criterion (Example 3)

In this chapter the adaptation of an initially chosen model was presented. The development led to defining a "confidence criterion" which could be used to monitor the adaptation process.

In the next chapter a model for saccadic generation will be discussed from a state theoretic point of view. The model will describe saccadic generation in a "microscopic" way rather than a macroscopic input-output manner. This will lead naturally into viewing the frequency of firing of certain neurons as the state variables of the saccadic generator.

CHAPTER 4

STATE THEORETIC MODELING OF THE OCULOMOTOR SYSTEM

4.1 Introduction

In section 2.3.2 the neurophysiology of the saccadic generator was discussed. It was shown that by recording extracellularly in the paramedian zone of the pontine reticular formation (PPRF), various unit behavior can be related to quick eye movements (See Fig. 2.2). The purpose of this chapter is to conceptualize a model which will explain the observed unit activity and relate it to the overall behavior of the oculomotor system. To this end state theory or a "microscopic" approach to systems rather than an input-output "macroscopic" approach has been utilized in modeling oculomotor behavior. It is assumed that the oculomotor system is state determined. The question is what are its state variables? The answer to this question should give insight into the realization or organizational makeup of the eye movement control system.

A conceptual model for saccadic generation is shown in Fig. 4.1 A. The box labeled saccadic generator can be modeled and made to correspond to certain neuronal activity found in the brainstem. This is shown in Sec. 4.3 and analyzed in greater detail in Chapter 5. In order to formulate a model which will explain quick phase generation in terms of these neurons it will be assumed that certain types of neurons are the state variables of the saccadic generator. The state of a system represents the minimum amount of information that one needs to know about a system at a given time such that its future behavior can

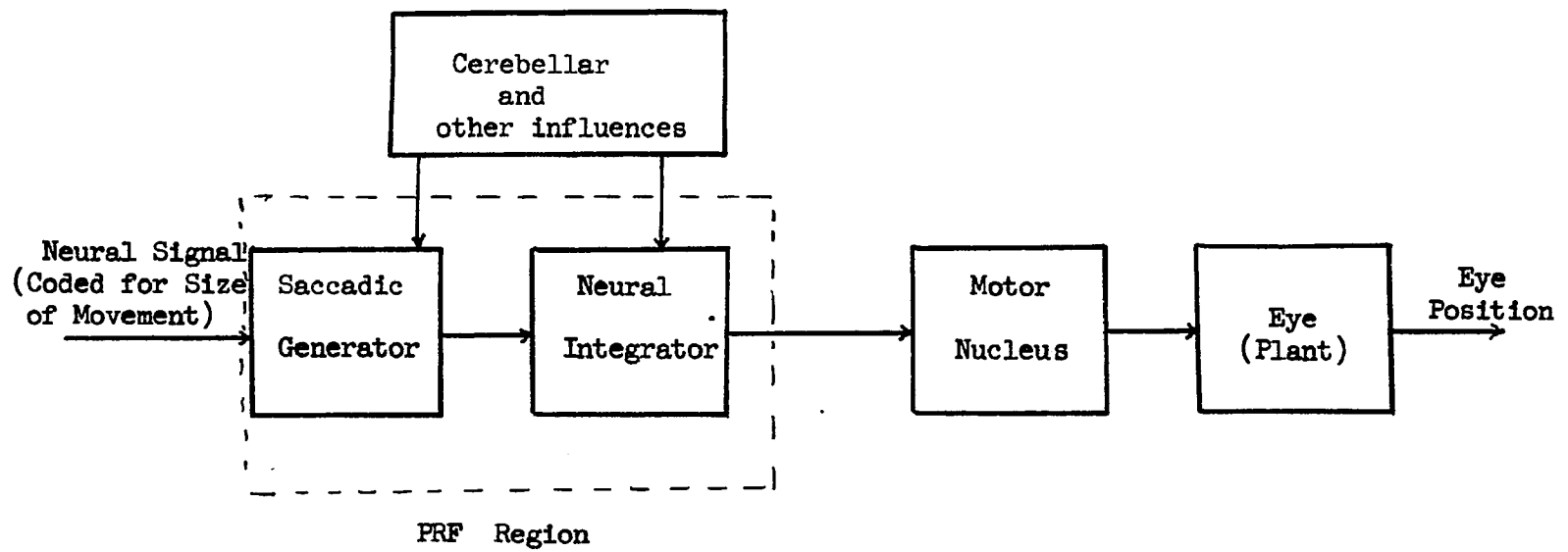


Fig. 4.1 A Conceptual model for the generation of saccadic eye movements

be determined without reference to the input before a given time. The state variables or states which characterize the system, completely determine its behavior and any variables within the system can be described in terms of the states. Since the state variables can be related to physical properties of a system, a state theoretic approach seems to be a natural way to characterize system behavior. The choice of state variables is not unique and different choices will lead to different mathematical realizations of a system (25). The particular realization which most closely agrees with the physiological data should give clues as to the structure and behavior of the physiological system. Furthermore, if one could localize the neuronal classes within the brain which may be viewed as the state variables of the oculomotor system, then he could theoretically describe all of oculomotor behavior in terms of these neurons.

The two fundamental aspects of oculomotor system behavior, i.e., saccades or quick movements and slow movements can be modeled separately. However, only a model for quick phase generator will be identified since there is no unit data available at this time which can be related directly to the slow phase movements of the oculomotor system.

4.2 Realization of Saccadic Generator Model

As described above, the PPRF of the brain stem appears to contain the neuron classes which are responsible for driving the eyes to perform saccades and quick phases of nystagmus. Neural activity in the PPRF has been classified into two broad classes: 1) Pause units and 2) burst units. The different types of units have already been discussed in Sec. 2.3.2 and are shown in Fig. 2.2.

The duration of the cessation of firing in the pause units (Fig. 2.2 e-f) is nearly linearly related to the duration of the movement and therefore these units could act as a switch which enables or disables the saccadic generator. In support of this idea, Keller (57) has recently shown that by exciting the pause units, saccadic generation could be suppressed.

The burst units* exhibit a greater variety of different activity which lead eye movements either with long, medium or short latencies. Upon closer examination of the burst units, shown in Fig. 2.2, by plots of the instantaneous spike frequency vs. time, the firing pattern of the various units are much clearer and can be seen to behave quite distinctly. These plots for the various units are shown in Fig. 4.1 B.** The unit shown in Fig. 4.1 B-c (short lead burst unit)

* Units which start firing 80 to 250 msec. before the eye movement are termed long lead burst units. Units which start firing 12 to 20 msec. before the movement are termed medium lead or short lead burst units.

** How these plots are obtained and a detailed explanation of their behavior is given in Sec. 5.2.

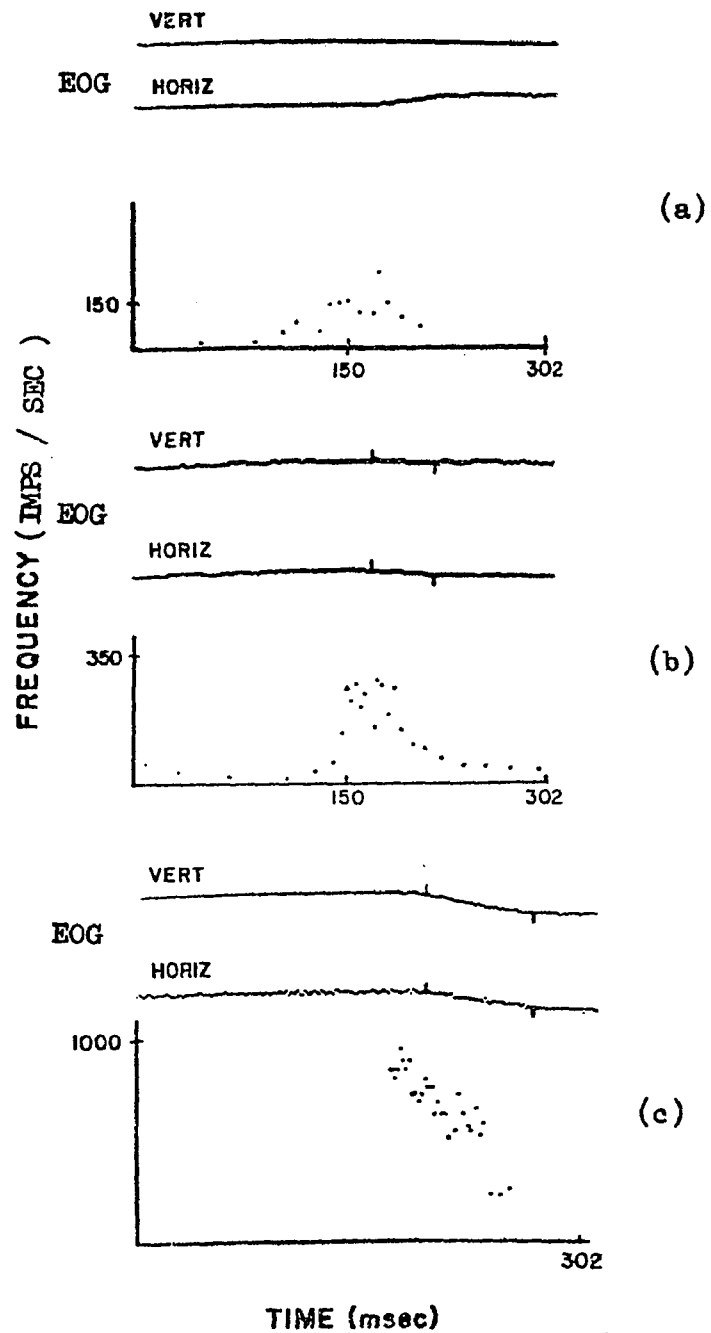


Fig. 4.1 B Instantaneous frequency vs. time behavior of burst units recorded in PPRF. Units are assumed to be associated with box labeled "Saccadic Generator" in Fig. 4.1 A.

has the property that it rises immediately to a high frequency, approximately 15 msec. before the eye movement and then falls rather sharply. The other units shown in Fig. 4.1 B-a,b (long lead burst units) have been divided into essentially two classes. There are those that rise and cut off very sharply indicating strong inhibitory influences, while the second type falls more slowly. Both types of long lead burst units have a "biphasic" dynamic character in that a slow buildup of activity precedes the period of more intense burst which precedes the eye movement by about 15 msec. This behavior suggests that these units are functionally distinct in producing quick eye movements.

The questions which need answering at this point are:

1. What role does each of these neuron types play in coding an eye movement?
2. How do these neurons act together to move the eyes?

A partial answer to these questions is obtained by setting these neurons in a mathematical framework and then inferring the internal structure and neuronal coupling coefficients of the system on the basis of the experimental data using realization theory and Liapunov's direct method to identify the system parameters.

Using this modeling approach it is assumed that the frequency of firing of the long lead burst units shown in Fig. 4.1 B are representative of the state variables of the quick phase generator. If this basic hypothesis is accepted the problem of understanding neuronal organization can be approached by realizing a model whose state variables behave as the neurons and in addition maintain the correct input-output behavior. In describing oculomotor behavior there is evidence to suggest that the nervous system is capable of performing addition, multiplication,

integration, threshold sensing, and switching. Therefore, in the model realization such functional relationships are used. The saccadic generator is moreover assumed to be completely controllable and observable. This assumption is warranted because of the close correspondence between neural activity and eye movement. In addition, it is unlikely that in such a precise, well organized mechanism, there would be neuronal modes which are uncontrollable. As a first approximation a "controllable" form realization for the model was assumed. However, a model which is more physically appealing can be realized by assuming all integration to be nonideal. A second order model was chosen because of the biphasic character of the neuronal behavior and the types of units that were available (See Fig. 4.1 B). The model may be expanded if additional unit types are located in this region of the brain.

The model for the saccadic generator with ideal integrators is shown in Fig. 4.2 A. together with the matrix state equations. The model using nonideal integrators is shown in Fig. 4.2 B. with the state equations. All delays which are inherent in the propagation of the signals have been neglected in order to reduce the complexity of the model and give greater insight into the neural activity in the brainstem. A more complete model would of course have to take delays into account and is a suitable subject for future research. The model (Fig. 4.2 B) consists of two portions: a "controlling portion" (saccadic generator) which determines the dynamic responses of the system state variables and an output portion (neural integrator) which relates state variable behavior to the motor neuron activity. The controlling part of the model

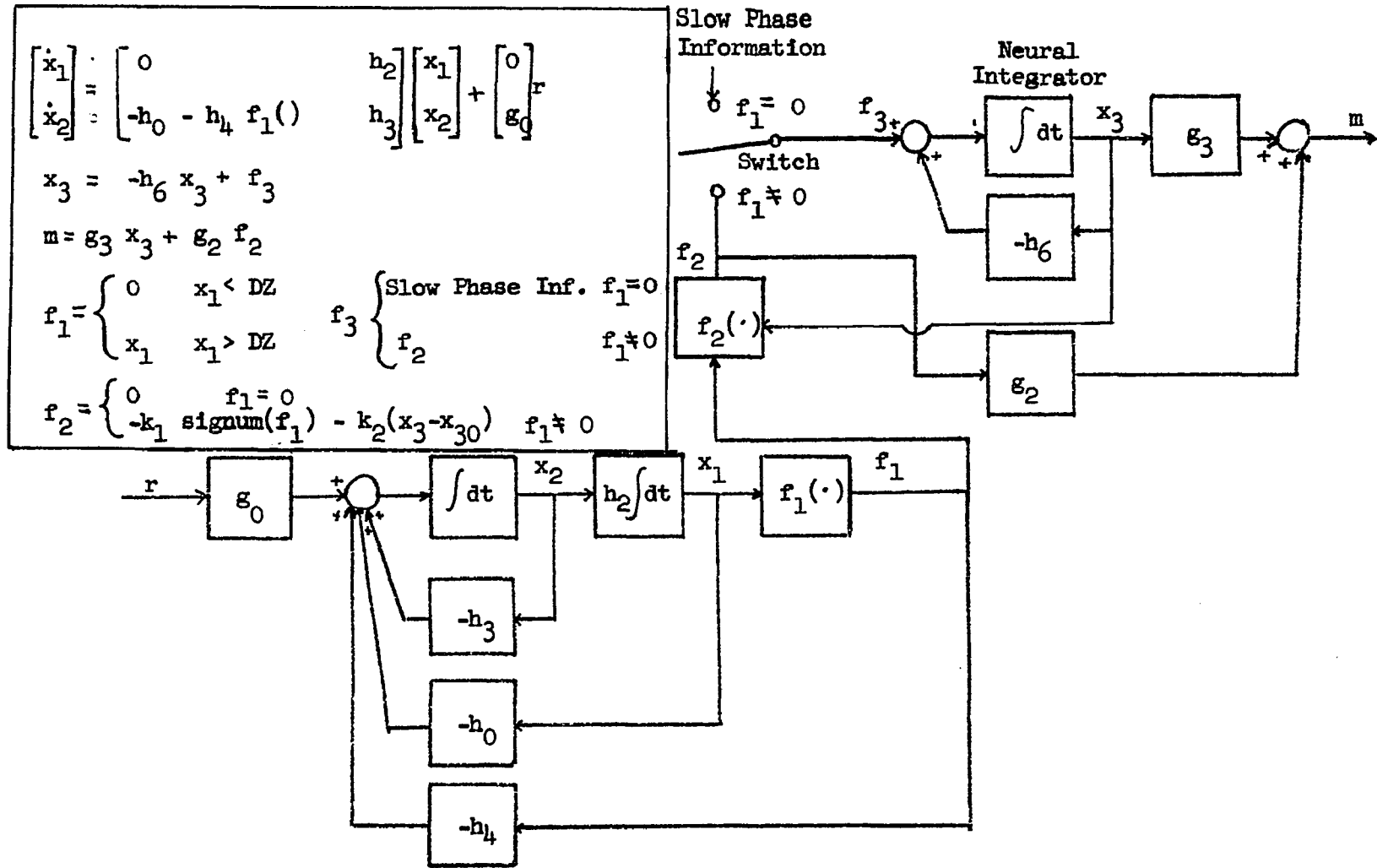


Fig. 4.2 A State realization of saccadic generator with ideal integrators (r is the signal driving the saccadic generator model and m is the signal driving the eye plant)

$$\begin{bmatrix} \dot{x}_1 \\ \dot{x}_2 \end{bmatrix} = \begin{bmatrix} -h_1 - h_0 \cdot f_1(\cdot) & h_2 \\ -h_0 - h_4 \cdot f_1(\cdot) & -h_3 \end{bmatrix} \begin{bmatrix} x_1 \\ x_2 \end{bmatrix} + \begin{bmatrix} g_1 \\ g_0 \end{bmatrix} r$$

$$\dot{x}_3 = -h_6 x_3 + f_3$$

$$m = g_3 x_3 + g_2 f_2$$

$$f_1 = \begin{cases} 0 & x_1 < DZ \\ x_1 & x_1 > DZ \end{cases}$$

$$f_2 = \begin{cases} 0 & f_1 = 0 \\ -k_1 \cdot \text{signum}(f_1) - k_2 \cdot (x_3 - x_{30}) & f_1 \neq 0 \end{cases}$$

$$f_3 = \begin{cases} \text{Slow Phase Information} & f_1 = 0 \\ f_2 & f_1 \neq 0 \end{cases}$$

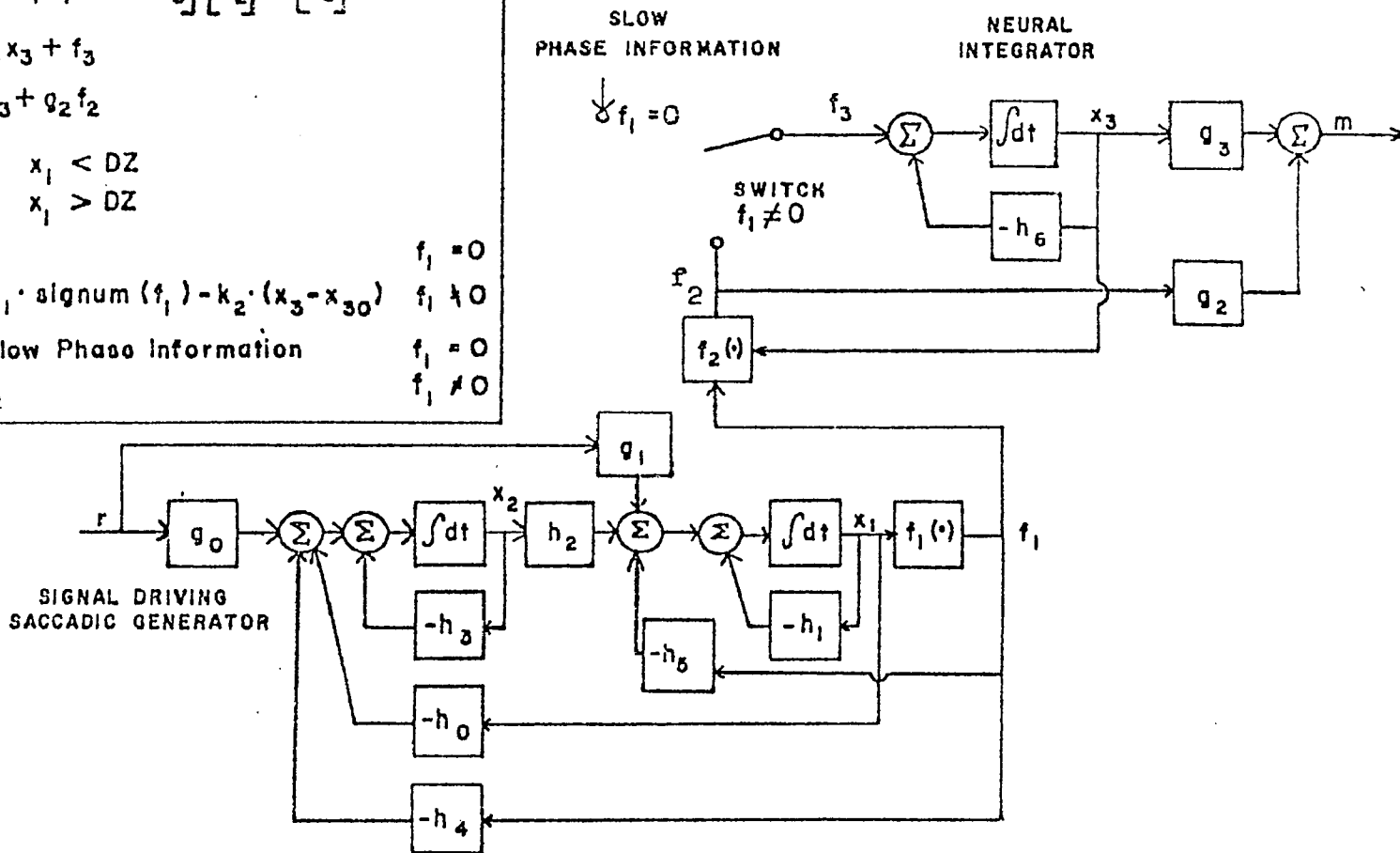


Fig. 4.2 B State realization of the saccadic generator model with nonideal integrators

behaves essentially as a "relaxation oscillator." When a perturbation is applied to the saccadic generator, there is a buildup of activity in the states x_1 and x_2 . When x_1 reaches some threshold the dynamic characteristics of the model changes due to the additional feedback through the nonlinear element $f_1(\cdot)$. This forces the generator back to its equilibrium point $x_1 = 0$, $x_2 = 0$. In terms of relaxation oscillator theory, the system has entered into a "monostable mode." This is consistent with Robinson's view (86) of the saccadic generator as a "one shot" multivibrator. When a step is applied to the input of the saccadic generator a stable condition can never be achieved since as soon as the variable x_1 is below the threshold a buildup of activity resumes. This leads to the periodic quick phases which are similar to those observed during induced nystagmus. In other words, the step or constant perturbation input has forced the system into an astable mode of behavior. A complete phase plane analysis of relaxation oscillator theory can be found in Stern (100).

By using a deadzone nonlinearity or "threshold" element for f_1 and a switching function for f_2 , a pulse is generated as the input to the neural integrator. The pulse together with the step, which is the output of the neural integrator, is the proper signal, which will drive the oculomotor plant (82). The switch in the model is activated (in the down position) when x_1 is above the threshold ($f_1 \neq 0$). The plant is not shown in this diagram as it is not of major interest in this model. For a consideration of models of the oculomotor plant see Robinson (82), Cook and Stark (23), Collins (22)

and Sobotkin (93).

If the plant is neglected then one may leave out the parameter g_2 and its direct path around the integrator in the model for purposes of simulation. This may be done since without a plant to drive, the direct pulse is unnecessary to overcome plant inertia and the variable m is directly related to the eye position.

The switch in the model is considered to be the pause units and the variables f_2 , x_1 and x_2 correspond to the various types of burst units which have been located in the brainstem (PPRF). Such units are shown in Fig. 4.6 and are compared to the variable which are generated by the idealized model shown in Fig. 4.2 A. The change in model variable m is related to motor unit activity and should correspond directly to change in eye position. This has been shown to be the case for tonic-phasic motor units (47, 85). The nonlinear control function $f_2(\cdot)$ is a switching function whose height varies as a function of x_3 , the state of the neural integrator, and is indicated in the equations in Fig. 4.2 B. This can be considered as feedback from the output of the "neural integrator." This function explains why the eyes beat on the quick phase side during nystagmus and also why the short lead burst units which are believed to input into neural integrator show a decay in their frequency vs. time behavior. This is shown in Sec. 5.2. where the frequency vs. time behavior is analyzed more closely.

Slow phase information is used by the model when $f_1 = 0$ while the saccadic generator is inhibited. There is evidence to suggest that this might be the case since there are direct vestibulo-oculomotor

pathways for vestibular slow phase generation. The visual-oculomotor pathways for slow phase generation are present but their location and characteristics are largely unknown. A realization of a slow phase generator for use in generating nystagmus is shown in Sec. 4.4.1.

However, there is no unit data available at this time to compare with the state variables of the slow phase generator and therefore remains speculative and a subject for future research.

4.3 Testing of Model to Establish Conceptual Viability

In order to test the model to see whether it was feasible to realize the saccadic system in such a fashion, various stimuli were introduced at the input to the realized saccadic generator shown in Fig. 4.2 A. This was simulated on a digital computer (PDP 8E) and the output was recorded on a digital display. Fig. 4.3 shows the response of the system to a pulse input. The output is a step or a saccade. The amplitude of the step is related to the area of the pulse. Fig. 4.4 shows that if the appropriate slow phase information is introduced when $f_1 = 0$, a step input into the saccadic generator produces nystagmus. This is in agreement with the idea that the saccadic generator uses slow phase information to produce quick phases of nystagmus. Fig. 4.5 shows the response of the overall system to a pendular stimulus. Note that the eyes beat on the quick phase side as in actual nystagmus recorded from humans and monkeys * (28, 51).

Comparisons were also made between the various variables of the model and actual neuronal firings recorded from the pontine reticular formation of an alert monkey while it was moving its eyes. This is shown in Fig. 4.6. The unit data was taken from the studies done by Cohen and Henn (14).

Figures 4.6 a-d are the model generated variables and Figs. 4.6 e-f are the recorded unit data. The dotted curve for the recorded PFRF unit (Fig. 4.6 E) is a frequency vs. time plot and the top and bottom solid curves are the horizontal and vertical EOG, respectively,

* See Fig. 2.6 (Sec. 2.4.2) and Fig. 2.8 (Sec. 2.4.3)

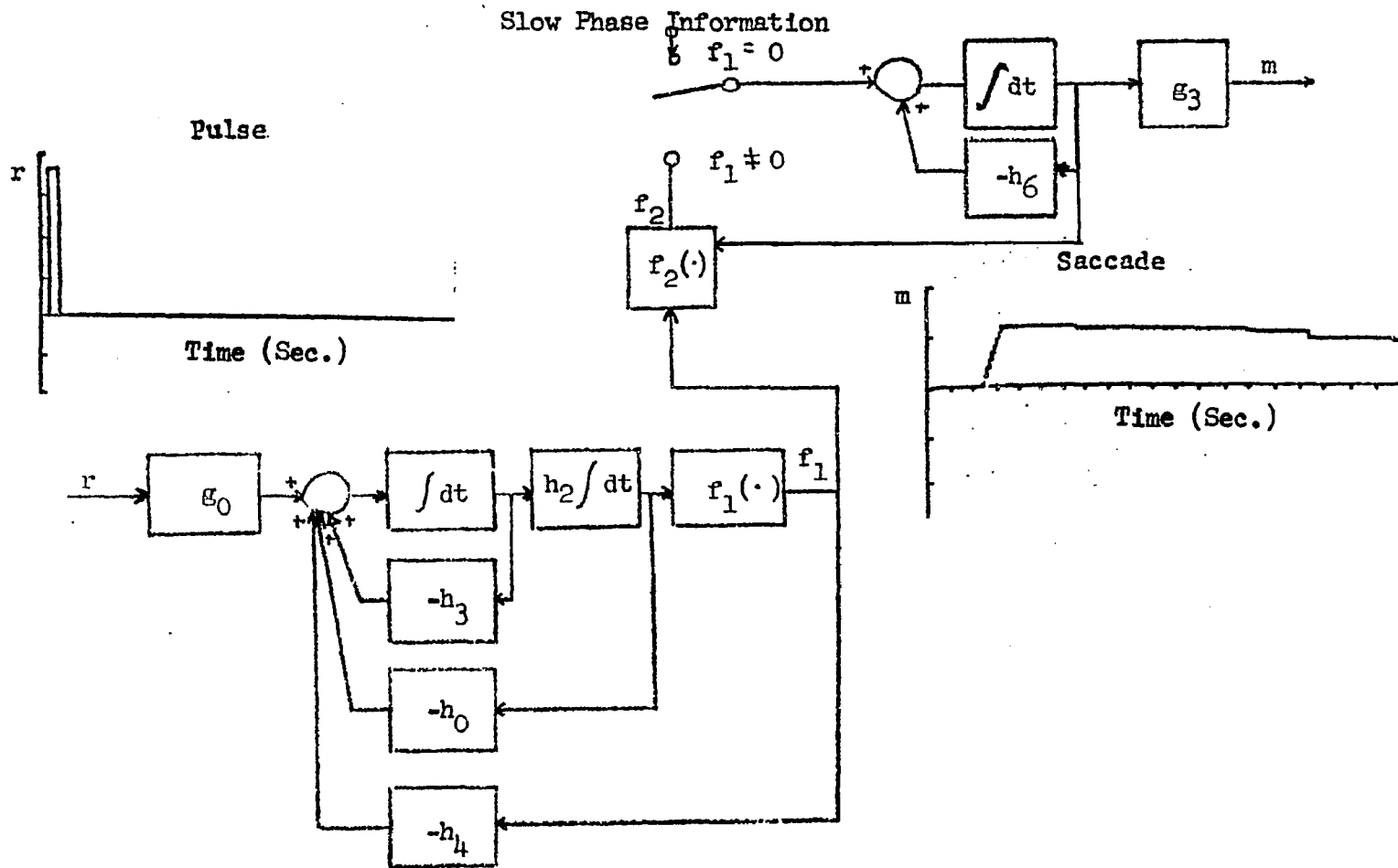


Fig. 4.3 Response of saccadic generator model to a pulse input (See Fig. 4.1 A for state variable location)

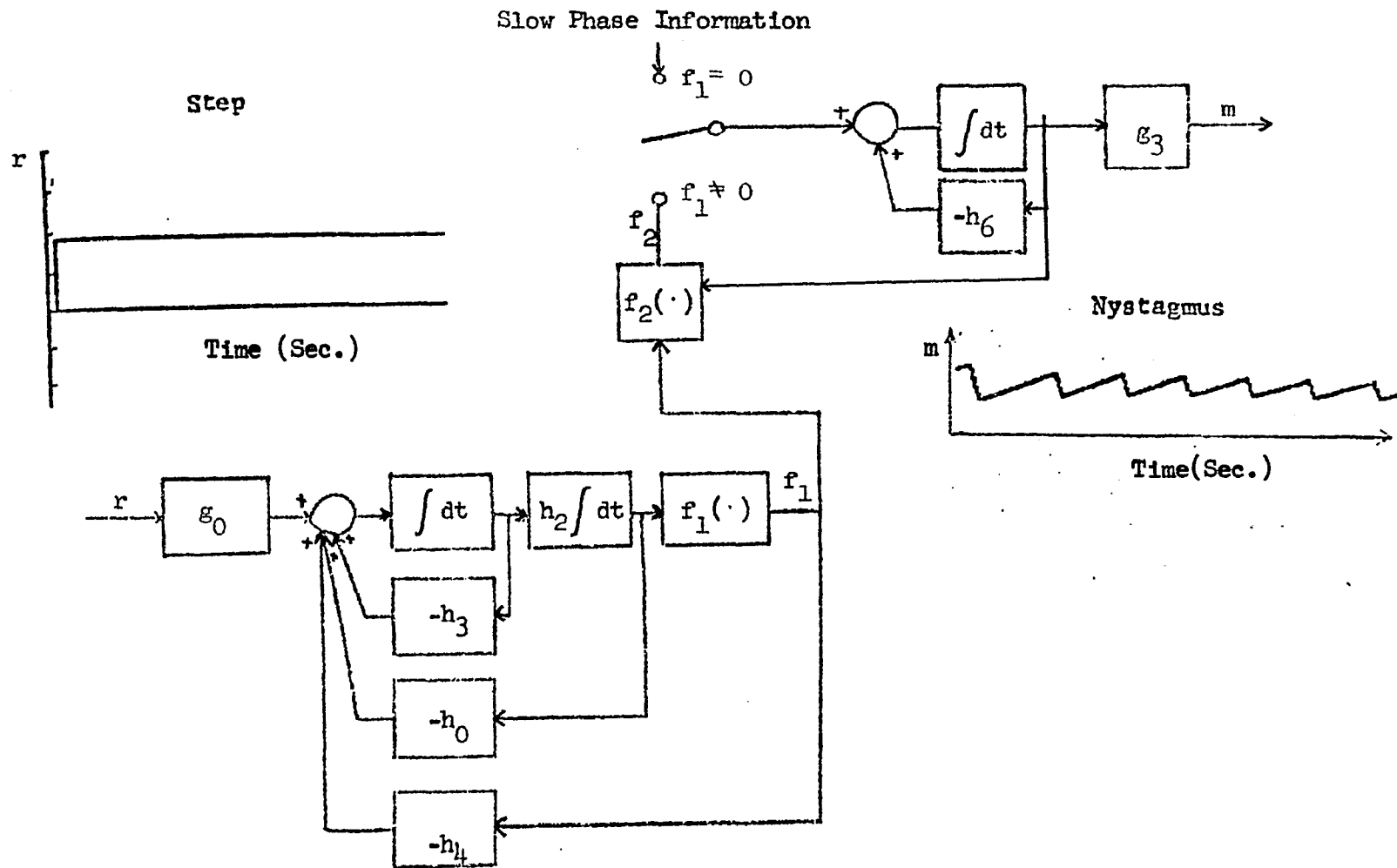


Fig. 4.4 Response of saccadic generator model to a step input (See Fig. 4.1 A for state variable location)

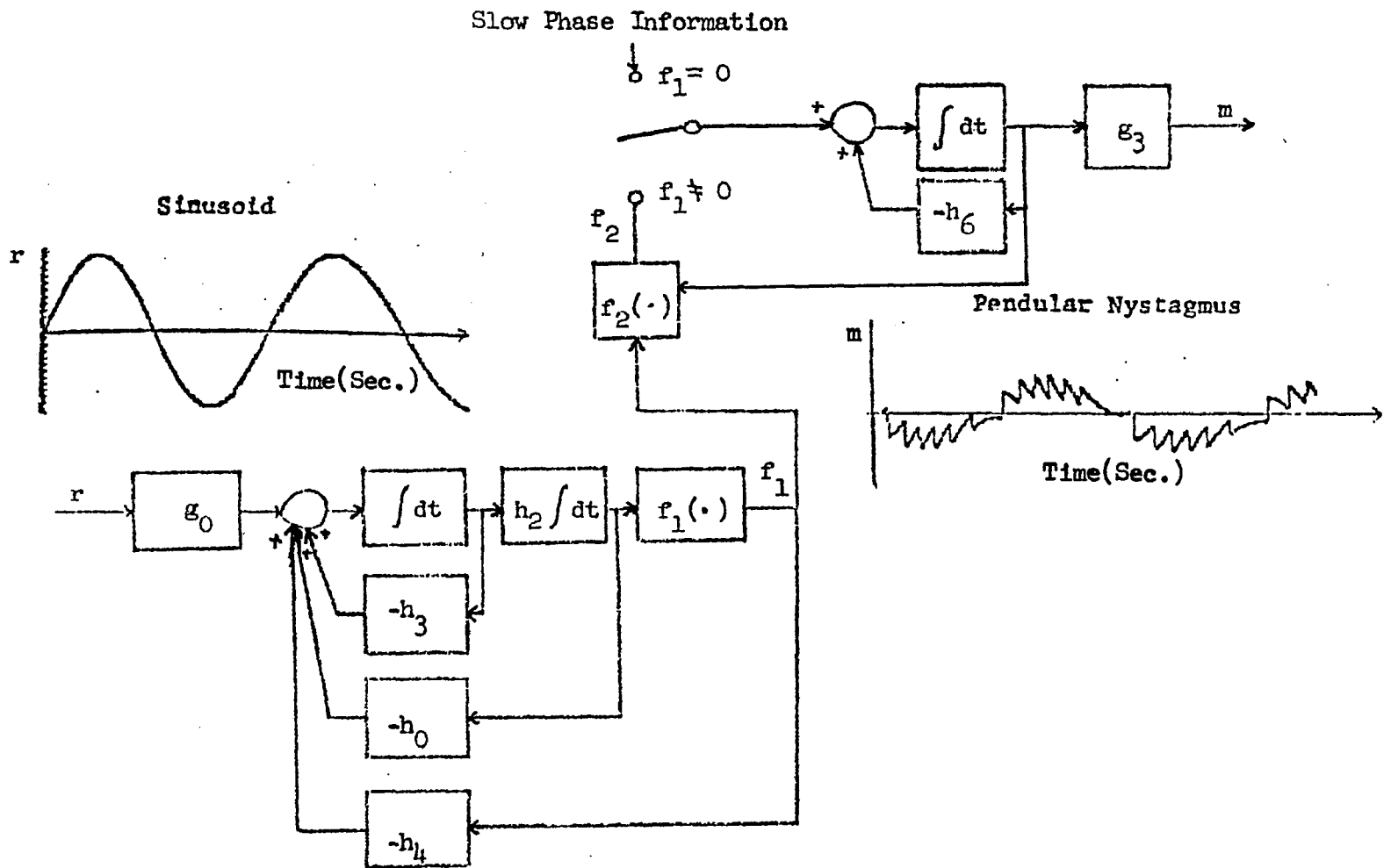


Fig. 4.5 Response of saccadic generator model to a sinusoidal input (See Fig. 4.1 A for state variable location)

showing actual eye position. The bottom trace for the model-generated variables is the variable representing horizontal eye position and the top trace frequency of firing versus time. The number of impulses in the burst for the unit in Fig. 4.6 e is linearly related to the horizontal component of movement. Excluding the differences in latency, both the actual frequency of neuronal firing and predicted variations of the f_2 variable in model (Fig. 4.6 a) fall off in approximately the same fashion. The frequency of firing of this unit could be related to the f_2 variable which inputs to the neural integrator as well as projecting directly around it to give the pulse-step which is required to drive the motor plant. The frequency of firing of the units shown in Fig. 4.6 g-h are assumed to represent the state variables of the saccadic generator and are studied further in Chapter 5 where it is shown how they are used to identify the parameters of the saccadic generator. Further electrophysiological work is required to strengthen the correspondence between the variables in the model and the neuron classes. It is to be noted, for example, that the line drawn in Fig. 4.6 d is to indicate that various thresholds could exist for each neuron and each of the variables could represent a class of neuron types with different thresholds. It is also to be noted that for Fig. 4.6 f-h the top traces are the unit recordings and the second and third traces down are the horizontal and vertical EOG respectively. For the model-generated variables (Fig. 4.6 a-d) the bottom trace is eye position versus time and the top trace is the variable representing the frequency versus time behavior of the unit.

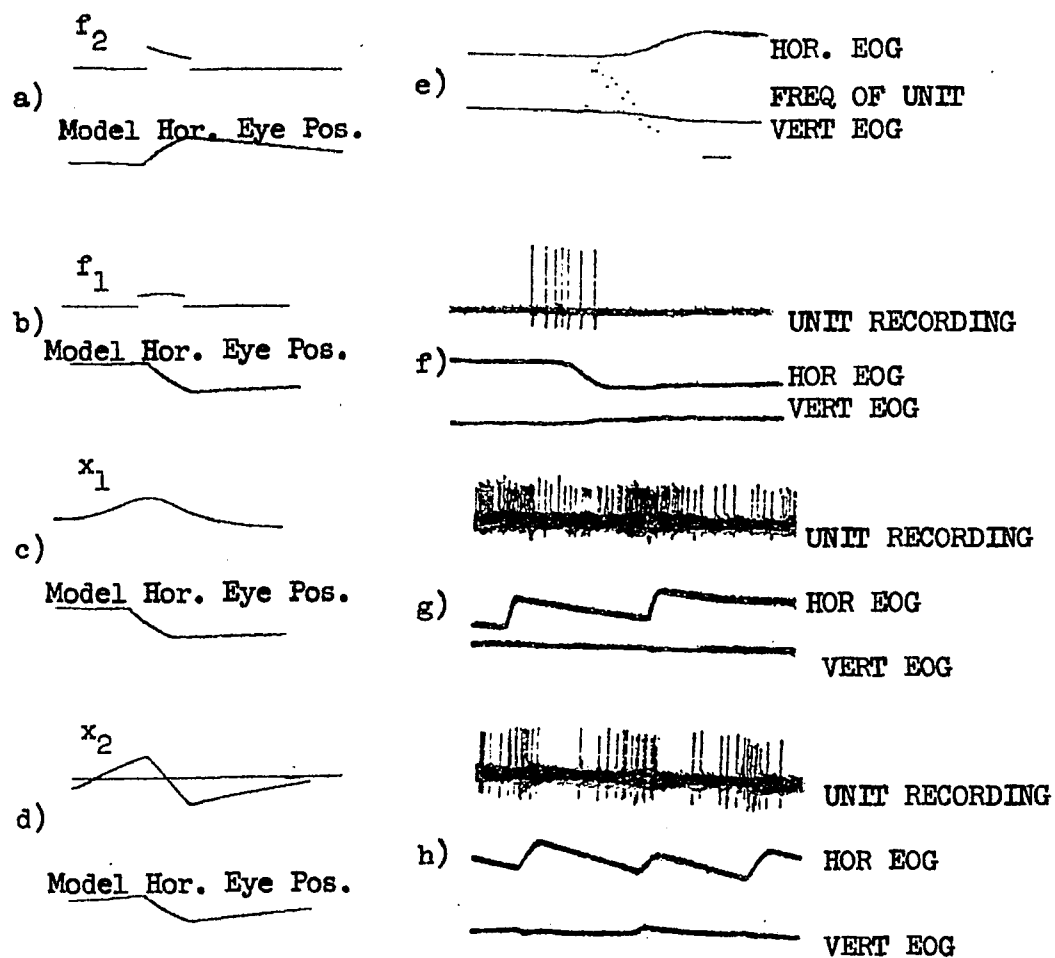


Fig. 4.6 Model variables and associated neurons. Model variables (a-d) recorded units and EOG's (e-h)

4.4 Slow Phase Generator Model

4.4.1 Introduction

A particular model realization of a slow phase generator is shown in Fig. 4.7. The motivation for choosing a realization in this form is that the brain must be monitoring the state of the end organ (semicircular canals) and therefore should be generating state variables which are in accordance with a realization of the end organ transfer function. Physiologically, neurons from the semicircular canals synapse in the rostral, medial and superior vestibular nuclei* and could generate the type of activity suggested by this realization, since the input couples into all the states directly. In Sec. 4.4.2 it is shown how such a realization may be formulated from the transfer functions which have been proposed for the vestibular system. This model was formulated for purposes of completeness to show how the modeling philosophy used in this dissertation can be applied to a different aspect of oculomotor control. Whether the state variables postulated in the slow phase generator model are actually generated internally as frequency of firing of various units is speculative at this point. Recently, though, there have been reports of slow phase velocity related units in the vestibular nuclei and cerebellum. The parameters chosen for this slow phase generator model are in accordance with a known transfer function between the input-output behavior of the vestibular system. It is then shown how this may be generalized to include an optokinetic slow phase generator with coupling between

* See Sec. 2.4.2

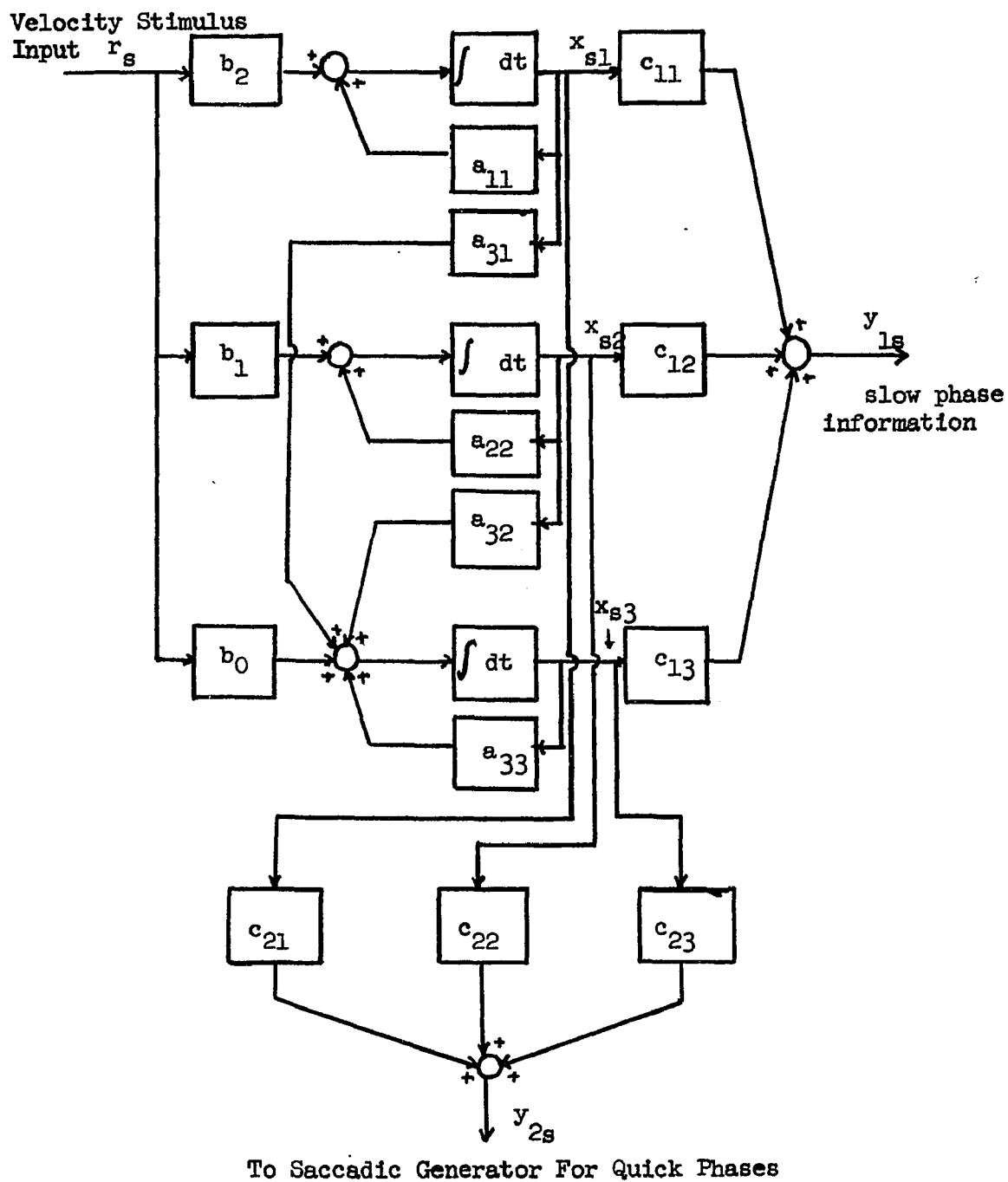


Fig 4.7 A state realization for a slow phase generator

the optokinetic slow phase state variables and the vestibular system slow phase states.

4.4.2 Realization of a Slow Phase Generator Model

Before considering the realization of a particular slow phase generator model, some general concepts of realization theory are discussed. For a state determined system, the system may be described by the equation

$$\dot{x}_s = A x_s + \underline{b} r_s \quad 4.1$$

$$y_s = C^t x_s \quad 4.2$$

where the subscript s denotes that these state variables are referred to the slow phase generator. Taking the Laplace transform of Eqs. 4.1 and 4.2 and assuming the initial state vector to be zero, the following is obtained:

$$s X_s(s) = A X_s(s) + \underline{b} R_s(s) \quad 4.3$$

$$Y_s(s) = C^t X_s(s) \quad 4.4$$

where $X_s(s)$, $Y_s(s)$, and $R_s(s)$ are the Laplace transforms of x_s , y_s and r_s respectively. Solving for $X_s(s)$ one obtains

$$X_s(s) = (s I - A)^{-1} \underline{b} R_s(s) \quad 4.5$$

$$Y_s(s) = C^t (s I - A)^{-1} \underline{b} R_s(s) \quad 4.6$$

where $(s I - A)^{-1} = \underline{\Phi}(s)$ is the Laplace transform of the state transition matrix. Therefore

$$Y_s(s) = C^t \underline{\Phi}(s) \underline{b} R_s(s) \quad 4.7$$

Hence

$$H(s) = C^t \Phi(s) \underline{b} \quad 4.8$$

is called the transfer function matrix. Eq. 4.7 may be rewritten as:

$$Y_s(s) = H(s) R_s(s) \quad 4.9$$

The problem in realization theory is: given a transfer function matrix $H(s)$, find matrices C , A , and vector \underline{b} such that $C^t (s I - A)^{-1} \underline{b} = H(s)$. A discussion of this equation can be found in Zadeh and Desoer(120).

In this section it is shown how the transfer function used for the vestibular system may be realized in the form shown in Fig. 4.7.

From the original work of Steinhausen(99), who compared the semicircular canal to a damped torsion pendulum, one finds the transfer function between the canal output to head velocity input to be given by

$$\frac{Y_{1s}(s)}{R_s(s)} = H_1(s) = \frac{s}{(1 + sT_1)(1 + sT_2)} \quad 4.10$$

This has been discussed in Sec. 2.4.2. The time constants in Eq. 4.10 are related to the coefficients of Eq. 2.1 in the following way:

$$a_1 = \frac{1}{T_1} + \frac{1}{T_2}, \quad a_0 = \frac{1}{T_1 T_2}, \quad b_1 = \frac{1}{T_1 T_2} \quad 4.11$$

Barnes and Benson(2) suggest that the transfer function between information going to the quick phase generator and head velocity is given by

$$\frac{Y_{2s}(s)}{R_s(s)} = H_2(s) = \frac{s(1 + sT_3)}{(1 + sT_1)(1 + sT_2)(1 + sT_4)} \quad 4.12$$

Therefore the transfer function vector $H(s)$ for the system is given by:

$$H(s) = \begin{bmatrix} H_1(s) \\ H_2(s) \end{bmatrix} = \begin{bmatrix} \frac{s}{(1+sT_1)(1+sT_2)} \\ \frac{s(1+sT_3)}{(1+sT_1)(1+sT_2)(1+sT_4)} \end{bmatrix} \quad 4.13$$

Eq. 4.13 is now realized in state form, i.e. matrices C , A , and vector \underline{b} are found. From Fig. 4.7, the state equations are given by:

$$\begin{bmatrix} \dot{x}_{1s} \\ \dot{x}_{2s} \\ \dot{x}_{3s} \end{bmatrix} = \begin{bmatrix} a_{11} & 0 & 0 \\ 0 & a_{22} & 0 \\ a_{31} & a_{32} & a_{33} \end{bmatrix} \begin{bmatrix} x_{1s} \\ x_{2s} \\ x_{3s} \end{bmatrix} + \begin{bmatrix} b_2 \\ b_1 \\ b_0 \end{bmatrix} r \quad 4.14$$

$$\begin{bmatrix} y_{1s} \\ y_{2s} \end{bmatrix} = \begin{bmatrix} c_{11} & c_{12} & c_{13} \\ c_{21} & c_{22} & c_{23} \end{bmatrix} \begin{bmatrix} x_{1s} \\ x_{2s} \\ x_{3s} \end{bmatrix} \quad 4.15$$

where y_{1s} is the slow phase signal driving the neural integrator and y_{2s} is the signal driving the saccadic generator. Matrices A , C^t , and vector \underline{b} are given by

$$A = \begin{bmatrix} a_{11} & 0 & 0 \\ 0 & a_{22} & 0 \\ a_{31} & a_{32} & a_{33} \end{bmatrix} \quad 4.16$$

$$\underline{b} = \begin{bmatrix} b_2 \\ b_1 \\ b_0 \end{bmatrix} \quad 4.17$$

$$c^t = \begin{bmatrix} c_{11} & c_{12} & c_{13} \\ c_{21} & c_{22} & c_{23} \end{bmatrix} \quad 4.18$$

The Det (s I - A) = (s - a₁₁)(s - a₂₂)(s - a₃₃).

Using the above equations, the Laplace transform of the state transition matrix is found to be

$$\tilde{\Phi}(s) = \begin{bmatrix} \frac{1}{s-a_{11}} & 0 & 0 \\ 0 & \frac{1}{(s-a_{22})} & 0 \\ \frac{a_{31}}{(s-a_{11})(s-a_{33})} & \frac{a_{32}}{(s-a_{22})(s-a_{33})} & \frac{1}{(s-a_{33})} \end{bmatrix} \quad 4.19$$

From Eqs. 4.8, 4.17, 4.18, and 4.19, the elements of the matrix H(s) in terms of the elements of matrices A, C, and vector b are found to be

$$H_1(s) = \frac{\begin{aligned} & [b_2 c_{11} + b_1 c_{12} + b_0 c_{13}] s^2 + [b_2 c_{13} a_{31} + b_1 c_{13} a_{32} \\ & - b_2 c_{11} (a_{22} + a_{33}) - b_1 c_{12} (a_{11} + a_{33}) - b_0 c_{13} (a_{11} + a_{22})] s \\ & + [b_2 c_{11} a_{22} a_{33} + b_1 c_{12} a_{11} a_{33} + b_0 c_{13} a_{11} a_{22} \\ & - b_2 c_{13} a_{31} a_{22} - b_1 c_{13} a_{32} a_{11}] \end{aligned}}{(s-a_{11})(s-a_{22})(s-a_{33})} \quad 4.20$$

$$H_2(s) = \frac{\begin{aligned} & [b_2 c_{21} + b_1 c_{22} + b_0 c_{23}] s^2 + [b_2 c_{23} a_{31} + b_1 c_{23} a_{32} \\ & - b_2 c_{21} (a_{22} + a_{33}) - b_1 c_{22} (a_{11} + a_{33}) - b_0 c_{23} (a_{11} + a_{22})] s \\ & + [b_2 c_{21} a_{22} a_{33} + b_1 c_{22} a_{11} a_{33} + b_0 c_{23} a_{11} a_{22} \\ & - b_2 c_{23} a_{31} a_{22} - b_1 c_{23} a_{32} a_{11}] \end{aligned}}{(s-a_{11})(s-a_{22})(s-a_{33})} \quad 4.21$$

Comparing Eqs. 4.20 and 4.21 with Eqs. 4.10 and 4.12, the values of the a 's and c 's may be chosen to get the appropriate transfer function.

By choosing

$$a_{11} = -\frac{1}{T_1} \quad a_{22} = -\frac{1}{T_2} \quad a_{33} = -\frac{1}{T_4} \quad c_{13} = 0 \quad c_{22} = 0 \quad c_{21} = 0 \quad 4.22$$

$H_1(s)$ and $H_2(s)$ become

$$H_1(s) = \frac{(b_2 c_{11} + b_1 c_{12})s - (b_1 c_{12} a_{11} + b_2 c_{11} a_{22})}{(s-a_{11})(s-a_{22})} \quad 4.23$$

$$H_2(s) = \frac{b_0 c_{23} s^2 + [b_2 c_{23} a_{31} + b_1 c_{23} a_{32} - b_0 c_{23} (a_{11} + a_{22})] s - b_2 c_{23} a_{31} a_{22} + c_{23} b_0 a_{11} a_{22} - b_1 c_{23} a_{32} a_{11}}{(s-a_{11})(s-a_{22})(s-a_{33})} \quad 4.24$$

By further constraining Eqs. 4.23 and 4.24 as follows:

$$b_2 c_{11} + b_1 c_{12} = \frac{1}{T_1 T_2} \quad 4.25$$

$$b_1 c_{12} a_{11} + b_2 c_{11} a_{22} = 0 \quad 4.26$$

$$b_0 c_{23} = \frac{T_3}{T_1 T_2 T_4} \quad 4.27$$

$$c_{23} [b_2 a_{31} + b_1 a_{32} - b_0 a_{11} - b_0 a_{22}] = \frac{1}{T_1 T_2 T_4} \quad 4.28$$

$$-b_2 a_{31} a_{22} + b_0 a_{11} a_{22} - b_1 a_{32} a_{11} = 0 \quad 4.29$$

The following transfer functions $H_1(s)$, and $H_2(s)$ are obtained:

$$H_1(s) = \frac{\frac{1}{T_1 T_2}}{(s - \frac{1}{T_1})(s - \frac{1}{T_2})} \quad 4.30$$

$$H_2(s) = \frac{\frac{1}{T_1 T_2 T_4} s (1 + T_3 s)}{(s + \frac{1}{T_1})(s + \frac{1}{T_2})(s + \frac{1}{T_4})} \quad 4.31$$

A more general slow phase generator model should contain optokinetic state variables and vestibular state variables . Using the state theoretic approach the interaction between the two sets of state variables may be examined and coefficients of coupling found.*

To formulate this mathematically, assume that the vestibular system is state determined and may be described by the state equations

$$\dot{\underline{x}}_v = A_v \underline{x}_v + B_v \underline{r}_v \quad 4.32$$

where \underline{x}_v is the vestibular system state vector, \underline{r}_v is the vestibular system input velocity signal and the elements of matrices A_v and B_v govern the system response. The optokinetic system may be similarly described by the state equations

$$\dot{\underline{x}}_o = A_o \underline{x}_o + B_o \underline{r}_o \quad 4.33$$

where the subscript, o, indicates that this equation is referred to the optokinetic system. Eqs. 4.32 and 4.33 may be combined to form the composite equation:

* The interactive effects have been discussed in Section 2.5.

$$\begin{bmatrix} \dot{x}_v \\ \vdots \\ \dot{x}_o \end{bmatrix} = \begin{bmatrix} A_v & \vdots & 0 \\ \vdots & \ddots & \vdots \\ 0 & \vdots & A_o \end{bmatrix} \begin{bmatrix} x_v \\ \vdots \\ x_o \end{bmatrix} + \begin{bmatrix} B_v & \vdots & 0 \\ \vdots & \ddots & \vdots \\ 0 & \vdots & B_o \end{bmatrix} \begin{bmatrix} r_v \\ \vdots \\ r_o \end{bmatrix} \quad 4.34$$

If the coupling matrices A_{vo} , B_{vo} , A_{ov} , and B_{ov} are introduced to account for visual-vestibular interaction, then a complete slow phase generator may be formulated as follows

$$\begin{bmatrix} \dot{x}_v \\ \vdots \\ \dot{x}_o \end{bmatrix} = \begin{bmatrix} A_v & \vdots & A_{vo} \\ \vdots & \ddots & \vdots \\ A_{ov} & \vdots & A_o \end{bmatrix} \begin{bmatrix} x_v \\ \vdots \\ x_o \end{bmatrix} + \begin{bmatrix} B_v & \vdots & B_{vo} \\ \vdots & \ddots & \vdots \\ B_{ov} & \vdots & B_o \end{bmatrix} \begin{bmatrix} r_v \\ \vdots \\ r_o \end{bmatrix} \quad 4.35$$

Once the state variables for the visual and vestibular systems slow phase generator are determined, analysis techniques similar to those used in this dissertation for studying quick phase generation may be utilized to identify the parameters of the slow phase generator.

In the next chapter, the parameters of the model for quick phase generation (Fig. 4.2 B) is identified using the parameter adaptive technique derived in Chapter 3.

CHAPTER 5

APPLICATION OF PARAMETER ADAPTIVE APPROACH
TO THE OCULOMOTOR SYSTEM MODEL (QUICK PHASE GENERATION)5.1 Introduction

In Chapter 4 a model for saccade generation was developed assuming that the frequency of firing of the neurons found in the brain stem were the state variables of the saccadic generator. It is now necessary to identify the parameters h_i and g_i of the saccadic generator model so that a better quantitative association might be established between the neuronal activity and model behavior. The parameter adaptive technique based on a Liapunov function, which was developed and shown to be a viable identification scheme in Chapter 3 will now be applied to identify the parameters of the saccadic generator while executing nystagmus. In order to accomplish this, the reference system must be established and the adaptive identification algorithm must be implemented. In section 5.2 it is shown how the reference system is formulated on digital tapes for use in the model reference configuration. The experimental technique is described and a description of data processing that was done to obtain it in a form so that it could be used in the analysis will be indicated. In section 5.4 the implementation of the controller dynamics is given. In section 5.5 some interesting conclusions about the implications of the adapted parameters will be discussed.

5.2 Experimental Procedure for Data Acquisition*and Reference

System Formulation

Monkeys are used in the extracellular unit studies. Under anesthesia a plug which accepts a microelectrode housing is implanted on the skull and fixed in place with screws and dental acrylic resin cement. The bone at the base of the plug is removed, but the dura is left intact. Etched insulated tungsten electrodes of 2-12 Megohms resistance are used for recording unit activity. They are introduced into regions of interest in a guide tube through the implanted plug. Microelectrodes are advanced using a hydraulic microdrive. Action potentials are recorded with RC-coupled amplifiers with a bandpass of from 200-5000 Hz. Eye movements are recorded by electro-oculography (EOG). Platinum needle electrodes are placed at the lateral margins and above and below the eyes, or silver-silver chloride electrodes are implanted in the bone around the eyes. The horizontal and vertical EOG's are recorded differentially using DC-coupled amplifiers. Eye movement and unit data are displayed on an oscilloscope and are recorded on FM magnetic tape along with stimulus information. A time code accurate to the nearest second is simultaneously recorded on one channel of tape to provide accurate identification of segments of tape.

During experiments monkeys are alert and sit restrained in a chair. The head is bolted to the chair and the chest and arms restrained in a breast plate. Small doses of amphetamine (0.2 mg/Kg) are sometimes given to maintain alertness but this is generally

* From Cohen and Henn (14)

unnecessary. The monkeys look about spontaneously, and OKN or rotational nystagmus is induced. OKN is evoked by an internally-lighted rotating OKN drum which surrounds the animal, or by an OKN belt which can be moved in horizontal, vertical or oblique directions. Rotational nystagmus is induced by a rim-driven rotating platform. Each of these devices is servo-controlled for velocity or for position and can be externally driven by a wave form generator. The velocity of the OKN drum and belt is determined by measuring the passage of drum or belt stripes, or by registering feedback voltages. The EOG is calibrated using slow phase velocity (1). It is assumed the animal's eyes move at the velocity of the OKN drum for speeds up to 90 deg./sec.

Unit activity and horizontal and vertical EOG's are digitized and recorded on digital magnetic tape using a PDP 8/E computer. A tape search unit identifies predetermined sections of FM magnetic tapes and signals the computer when to start and stop the digitizing. The horizontal and vertical EOG's are digitized each 1.6 msec. and the unit activity which occurs between these digitizations is coded to the nearest 100 μ sec. Periods of up to 145 seconds can be put on one decatape. Programs have been written to mark the beginning and end of eye movements, and occurrence of blinks. Tape files are generated which contain measures of the position of the eyes at the beginning and end of eye movement, the duration of eye movement and periods of fixation, and the duration and mean frequency of unit firing during eye movements and periods of fixation. In addition, programs have been written which display the frequency vs. time behavior of the

neuron. The frequency vs. time curve for the units was obtained by recording the time of occurrence of each spike on a decatape to the nearest 100 microseconds. A program was then written to calculate the interspike interval each time a spike occurred. The reciprocal of this time interval was then plotted as a function of time to obtain the traces shown in Figs. 5.1 and 5.2. The values obtained are then approximated by a polynomial and thus the reference system state variables z_1 and z_2 are obtained.

In Fig. 5.1 are shown typical EOG (electro-oculogram) and frequency vs. time traces of PPRF neurons which are assumed to be representative of the state variables which govern the dynamic response of saccadic generation. The traces are those of neuron types shown in Fig. 2.2 and 4.6 where the actual recorded AP's (action potentials) are shown. In Fig. 5.2 is shown the frequency characteristics of a burst unit which is believed to drive the neural integrator. This type of unit has been analyzed by Cohen and Henn (17), the number of spikes having been shown to be linearly related to saccade size. In order to obtain the correct temporal relationships between the neuron types shown in Fig. 5.1, the data was displayed on a digital display and lined up so that the corresponding eye movement (EOG) started approximately at the same time. This is shown in Fig. 5.3 by a dotted line. Eye movements of approximately the same size were chosen (approximately 10-12 degrees). The neuron shown in Fig. 5.1 A has the very interesting characteristic that it turns off very drastically a few milliseconds after the start of the movement. This indicates very strong inhibitory effects on the neuron cell. This

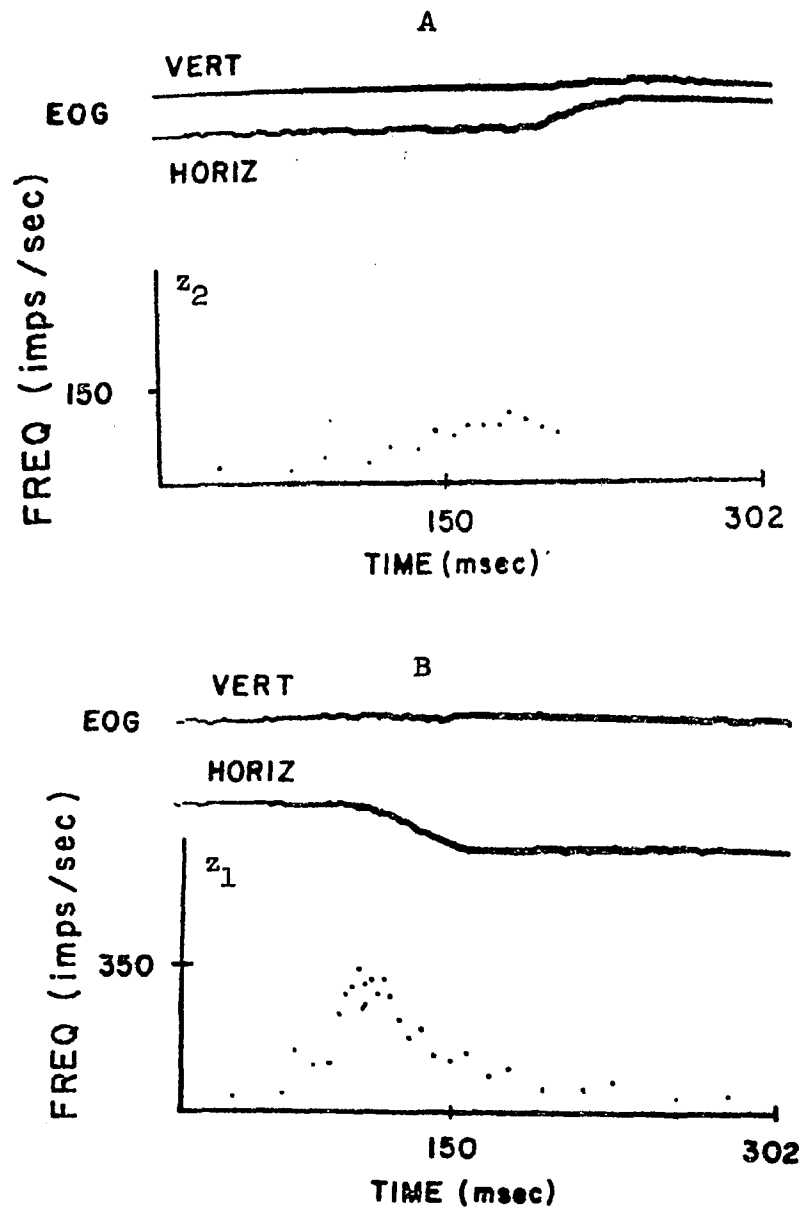


Fig. 5.1 Frequency (Impulses per sec.) vs. time for
 A) One type of long lead burst unit
 B) Different type of long lead burst unit

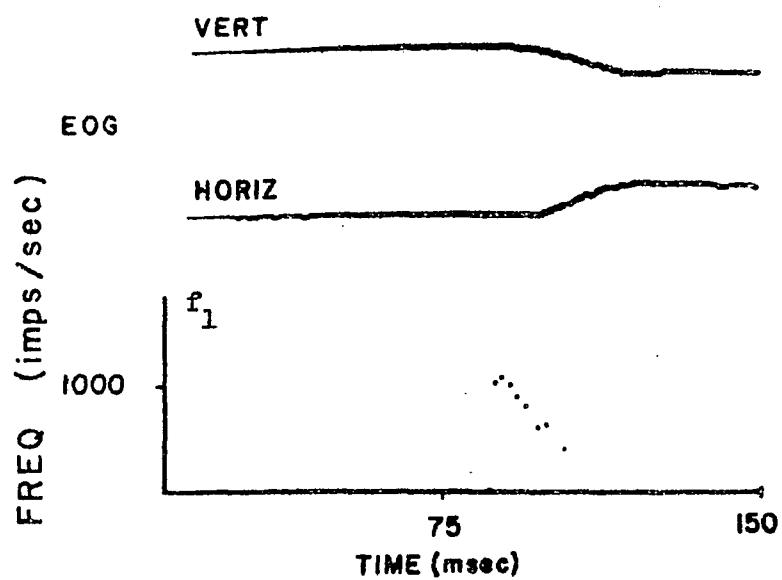


Fig. 5.2 Frequency (Impulses per Sec.) vs. time for short lead burst unit (medium lead burst unit)

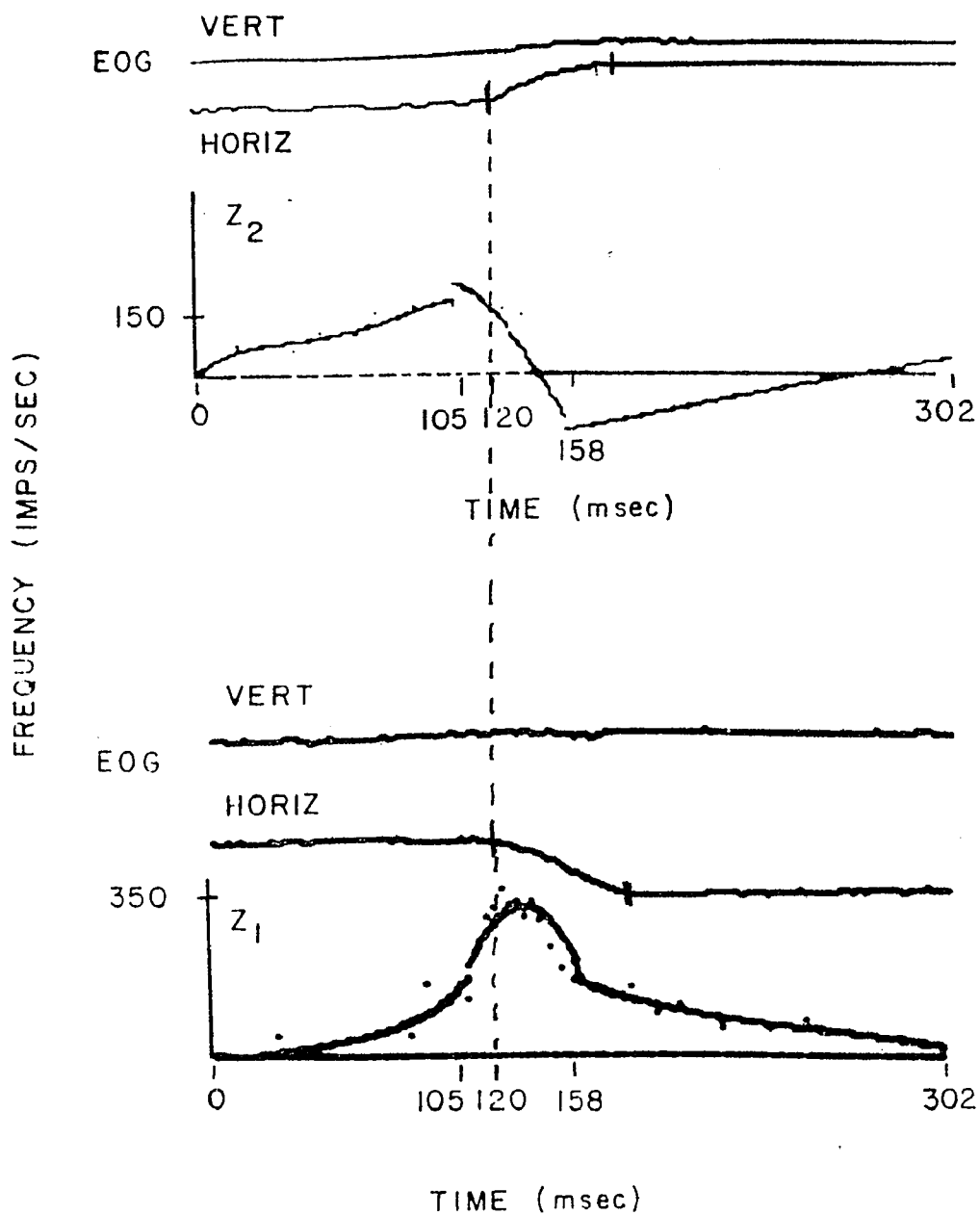


Fig 5.3 Polynomial fits to frequency (Impulses /sec) vs. time plots for different neuron types

behavior has been approximated by a negative going waveform which passes through zero a few milliseconds after turning off. Although this function is conjectured, it can be seen in intracellular recordings of hyperpolarized cells (49). "Following lead burst units" as reported by Keller (57) could be responsible for this activity since they start firing at the beginning or slightly after the start of the eye movement and could be coding this activity. This is in contrast to the type of activity seen in the neuron shown in Fig. 5.1 B where a slower decline in neural activity can be seen. The data representing the frequency vs. time behavior (Fig. 5.3) were approximated by polynomials in three regions:

$$0 \leq t \leq .105, \quad .105 \leq t \leq .158, \quad .158 \leq t \leq .320$$

The computer generated curves representing the polynomials are shown superimposed on the data in Fig. 5.3. The polynomial approximation expressions* used are as follows:

$$z_1 = -1.04422 + .797122 t + 11812.7 t^2 \quad 0 \leq t \leq .105 \quad 5.2.1$$

$$z_1 = -12214.5 + 216863 t - 763908 t^2 - 3726550 t^3 - 19017400 t^4 \quad .105 \leq t \leq .158 \quad 5.2.2$$

$$z_1 = 733.038 - 5504.6 t + 7813.95 t^2 + 37354.4 t^3 - 94383.5 t^4 \quad .158 \leq t \leq .302 \quad 5.2.3$$

$$z_2 = 3.71795 + 3773.05 t - 96174 t^2 - 1200950 t^3 - 4779200 t^4 \quad 0 \leq t \leq .105 \quad 5.2.4$$

$$z_2 = 1042.37 - 39156.6 t + 53156 t^2 - 2641540 t^3 - 3451200 t^4 \quad .105 \leq t \leq .158 \quad 5.2.5$$

* See Appendix B.

$$z_2 = -240.176 + 696.524 t + 274.783 t^2 + 4950.77 t^3 - 12397.75 t^4$$

5.2.6
.158 ≤ t ≤ .302

For the region of data $.158 \leq t \leq .302$, z_2 was cut off (no data points) and therefore this region was not identified. A curve has been drawn in Fig. 5.3 to indicate that the variable should theoretically rise toward zero. The exact nature of the rise is not known but can only be conjectured. The polynomial approximation to the data was used because continuous functions are needed in the Liapunov designed controllers used in this dissertation. A flow diagram showing the experimental procedure for data acquisition and the reference system formulation is given in Fig. 5.4.

In the next section the controller equations for adapting the model formulated in Chapter 4 are derived.

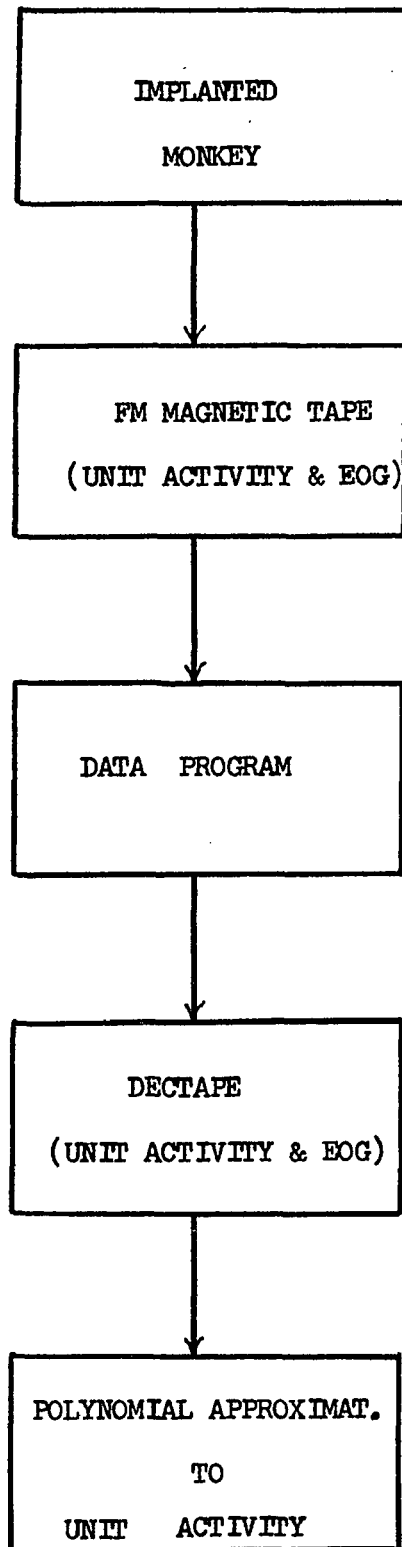


Fig. 5.4 Flow graph of reference system formulation

5.3 Controller Design for Adaptation of Parameters of the Quick Phase Generator Model

The parameters of the saccadic generator model are identified by assuming a piecewise linear model and applying the parameter adaptive approach using Liapunov's direct method as developed in Chapter 3. The model of the saccadic generator is divided into two linear models, when $f_1 = 0$ and when $f_1 \neq 0$. This can be seen by examining the state equations for the saccadic generator shown in Fig. 4.2 B. The reference system structure is assumed to be of the same form as the model which is based on physiological arguments and formulated in Chapter 4. The problem is now to identify its parameters from the observed data. Corresponding to the model state variable behavior for $f_1 = 0$, the reference system states are assumed to be the neuronal behavior for $0 \leq t \leq .105$ sec.

Therefore, for $f_1 = 0$ the reference system is assumed to be given by:

$$\begin{bmatrix} \dot{z}_1 \\ \dot{z}_2 \end{bmatrix} = \begin{bmatrix} -a_1 & a_2 \\ -a_0 & -a_3 \end{bmatrix} \begin{bmatrix} x_1 \\ x_2 \end{bmatrix} + \begin{bmatrix} b_1 \\ b_0 \end{bmatrix} r \quad 5.3.1$$

where z_1 and z_2 are obtained from the polynomial approximation to the unit data and are given by Eqs. 5.2.1 and 5.2.4*. The model is chosen as:

$$\begin{bmatrix} \dot{x}_1 \\ \dot{x}_2 \end{bmatrix} = \begin{bmatrix} -k_1 & 1 \\ -k_0 & 0 \end{bmatrix} \begin{bmatrix} x_1 \\ x_2 \end{bmatrix} + \begin{bmatrix} -(h_1 - k_1) & h_2 - 1 \\ -(h_0 - k_0) & -h_3 \end{bmatrix} \begin{bmatrix} z_1 \\ z_2 \end{bmatrix} + \begin{bmatrix} g_1 \\ g_0 \end{bmatrix} r \quad 5.3.2$$

* Note this is the polynomial approximation for the section of data $0 \leq t \leq .105$.

based on the state equations for Fig. 4.2 B when $f_1 = 0$. The formulation of the model in this fashion is so that a modified model adaptation algorithm might be implemented. The details of formulating the model in this way and its advantages are described in Sec. 3.6.

The error equation is formulated as:

$$\begin{bmatrix} \dot{e}_1 \\ \dot{e}_2 \end{bmatrix} = \begin{bmatrix} -k_1 & 1 \\ -k_0 & 0 \end{bmatrix} \begin{bmatrix} e_1 \\ e_2 \end{bmatrix} + \begin{bmatrix} -(a_1 - h_1) & (a_2 - h_2) \\ -(a_0 - h_0) & -(a_3 - h_3) \end{bmatrix} \begin{bmatrix} z_1 \\ z_2 \end{bmatrix} + \begin{bmatrix} b_1 - g_1 \\ b_0 - g_0 \end{bmatrix} r \quad 5.3.3$$

The equation may be rewritten in the form:

$$\begin{bmatrix} \dot{e}_1 \\ \dot{e}_2 \end{bmatrix} = \begin{bmatrix} -k_1 & 1 \\ -k_0 & 0 \end{bmatrix} \begin{bmatrix} e_1 \\ e_2 \end{bmatrix} + \begin{bmatrix} -(a_1 - h_1) \\ -(a_0 - h_0) \end{bmatrix} z_1 + \begin{bmatrix} (a_2 - h_2) \\ -(a_3 - h_3) \end{bmatrix} z_2 + \begin{bmatrix} (b_1 - g_1) \\ (b_0 - g_0) \end{bmatrix} r \quad 5.3.4$$

This equation is essentially the same as that obtained for the observable form realization.

Eq. 5.3.4 may be rewritten concisely as:

$$\dot{\underline{e}} = \underline{K} \underline{e} + \underline{u} z_1 + \underline{v} z_2 + \underline{w} r \quad 5.3.5$$

where

$$\underline{K} = \begin{bmatrix} -k_1 & 1 \\ -k_0 & 0 \end{bmatrix} \quad 5.3.6$$

$$\underline{u} = \begin{bmatrix} u_1 \\ u_2 \end{bmatrix} = \begin{bmatrix} -(a_1 - h_1) \\ -(a_0 - h_0) \end{bmatrix} \quad 5.3.7$$

$$\underline{v} = \begin{bmatrix} v_1 \\ v_2 \end{bmatrix} = \begin{bmatrix} (a_2 - h_2) \\ -(a_3 - h_3) \end{bmatrix} \quad 5.3.8$$

$$\underline{w} = \begin{bmatrix} w_1 \\ w_2 \end{bmatrix} = \begin{bmatrix} b_1 - g_1 \\ b_0 - g_0 \end{bmatrix} \quad 5.3.9$$

The vectors \underline{z} , \underline{e} , are the reference system state vector and the model reference state error vector respectively. One may now choose a Liapunov function as follows:

$$V = \underline{e}^t M \underline{e} + \underline{u}^t N \underline{u} + \underline{v}^t L \underline{v} + \underline{w}^t Q \underline{w} \quad 5.3.10$$

Because of the form of the error equation (5.3.4) the controller equations will be those obtained for an observable form realization.

The solution of the controller dynamics are then using Eqs. 3.3.67 and 3.3.68.

$$\dot{h}_1 = \frac{-z_1}{n_{11} n_{22} - n_{12}^2} \left[(n_{22} m_{11} - n_{12} m_{12}) e_1 + (n_{22} m_{12} - n_{12} m_{22}) e_2 \right] \quad 5.3.11$$

$$\dot{h}_0 = \frac{-z_1}{n_{11} n_{22} - n_{12}^2} \left[(n_{11} m_{12} - m_{11} n_{12}) e_1 + (n_{11} m_{22} - m_{12} n_{12}) e_2 \right] \quad 5.3.12$$

$$\dot{h}_2 = \frac{-z_2}{l_{11} l_{22} - l_{12}^2} \left[(l_{22} m_{11} - l_{12} m_{12}) e_1 + (l_{22} m_{12} - l_{12} m_{22}) e_2 \right] \quad 5.3.13$$

$$\dot{h}_3 = \frac{-z_2}{l_{11} l_{22} - l_{12}^2} \left[(l_{11} m_{12} - l_{12} m_{11}) e_1 + (l_{11} m_{22} - l_{12} m_{12}) e_2 \right] \quad 5.3.14$$

$$\dot{g}_0 = \frac{r}{q_{11} q_{22} - q_{12}^2} \left[(q_{11} m_{12} - m_{11} q_{12}) e_1 + (q_{22} m_{12} - q_{12} m_{22}) e_2 \right] \quad 5.3.15$$

$$\dot{g}_1 = \frac{r}{q_{11} q_{22} - q_{12}^2} \left[(q_{22} m_{11} - q_{12} m_{12}) e_1 + (q_{22} m_{12} - q_{12} m_{22}) e_2 \right] \quad 5.3.16$$

The process of adaptation can be performed on this section of data until the "confidence criterion" is at some value. This will be considered and explained in the next section where the adaptation is shown.

For $f_1 \neq 0$ the reference system is assumed to have entered a different mode of behavior and is given by:

$$\begin{bmatrix} \dot{z}_1 \\ \dot{z}_2 \end{bmatrix} = \begin{bmatrix} -a_1 & a_2 \\ -a_0 & -a_3 \end{bmatrix} \begin{bmatrix} z_1 \\ z_2 \end{bmatrix} + \begin{bmatrix} b_1 \\ b_0 \end{bmatrix} r \quad 5.3.17$$

where z_1 and z_2 are obtained from the polynomial expression for the unit data given by Eqs. 5.2.2 and 5.2.5*. The model is chosen as in the previous case as:

$$\begin{bmatrix} \dot{x}_1 \\ \dot{x}_2 \end{bmatrix} = \begin{bmatrix} -k_1 & 1 \\ -k_0 & 0 \end{bmatrix} \begin{bmatrix} x_1 \\ x_2 \end{bmatrix} + \begin{bmatrix} -(h'_1 - k_1) & h_2 - 1 \\ -(h'_0 - k_0) & -h_3 \end{bmatrix} \begin{bmatrix} z_1 \\ z_2 \end{bmatrix} + \begin{bmatrix} g_1 \\ g_0 \end{bmatrix} r \quad 5.3.18$$

Comparing this with the model in Fig. 4.2 B it can be seen that

$$h'_1 = h_1 + h_5 \quad 5.3.19$$

$$h'_0 = h_4 + h_1 \quad 5.3.20$$

* Note this is the polynomial approximation for the section of data $.105 \leq t \leq .158$.

Since h_2, h_3, g_1, g_0, h_1 and h_0 have been identified in the mode corresponding to $f_1 = 0$, h_4 and h_5 can be found by first identifying h'_1 and h'_0 in the mode $f_1 \neq 0$.

The equations used to identify h'_1 and h'_0 are the same as Eqs. 5.3.11 and 5.3.12 with h'_1 and h'_0 replacing h_1 and h_0 .

$$\dot{h}'_1 = \frac{-z_1}{n_{11} n_{22} - n_{12}^2} \left[(n_{22} m_{11} - n_{12} m_{12}) e_1 + (n_{22} m_{12} - n_{12} m_{22}) e_2 \right] \quad 5.3.11'$$

$$\dot{h}'_0 = \frac{-z_1}{n_{11} n_{22} - n_{22}^2} \left[(n_{11} m_{12} - m_{11} n_{12}) e_1 + (n_{11} m_{22} - m_{12} n_{12}) e_2 \right] \quad 5.3.12'$$

From Eqs. 5.3.19 and 5.3.20 h_4 and h_5 may be found as:

$$h_4 = h'_0 - h_0 \quad 5.3.21$$

$$h_5 = h'_1 - h_1 \quad 5.3.22$$

The next section shows the implementation of these equations in identifying the parameters of the saccadic generator model.

5.4 Identification of Parameters

To identify the parameters h_1 , h_0 , h_2 , h_3 , g_1 , g_0 of the saccadic generator model during nystagmus, a computer program (See Fig. 5.5) was written which generates the polynomial expressions for z_1 and z_2 given by Eqs. 5.2.1 - 5.2.4 at each instant of time, compares these values to the generated model state variables x_1 and x_2 at that instant and updates the parameters according to Eqs. 5.3.11 - 5.3.16. An input of 45 deg./sec. was used in exciting the saccadic generator model as it is assumed that a constant velocity signal is used in driving the saccadic generator during nystagmus.

In the identification of the parameters of the model for $f_1 \approx 0$, the matrices M, D, K, L, N and Q were chosen as follows:

$$M = \begin{bmatrix} 1 & -.1 \\ -.1 & .133 \end{bmatrix} \quad 5.4.1$$

$$D = \begin{bmatrix} 54 & 0 \\ 0 & .2 \end{bmatrix} \quad 5.4.2$$

$$K = \begin{bmatrix} -30 & 1 \\ -30 & 0 \end{bmatrix} \quad 5.4.3$$

$$N = \begin{bmatrix} .05 & 0 \\ 0 & .05 \end{bmatrix} \quad 5.4.4$$

$$Q = \begin{bmatrix} .05 & 0 \\ 0 & .05 \end{bmatrix} \quad 5.4.5$$

$$L = \begin{bmatrix} .05 & 0 \\ 0 & .05 \end{bmatrix} \quad 5.4.6$$

The initial choices of the H matrix H_0 and the \underline{g} vector \underline{g}_0 were

$$H_0 = \begin{bmatrix} -30 & 35 \\ -(-25) & -30 \end{bmatrix} \quad \underline{g}_0 = \begin{bmatrix} 0 \\ 80 \end{bmatrix} \quad 5.4.7$$

The M matrix was chosen considerably smaller than the examples presented in Chapter 3. This was because the adaptive algorithms were implemented on a digital computer and the range of the state variables is about 100 times as great. Therefore, if one wishes to have the advantages of digital adaptation with a reasonable time interval, then smaller values of the elements of M and D are required. This points out again the flexibility of the Liapunov designed controller. Since the model can never give an exact fit to the data, the parameters may never reach a steady state level but rather will tend to oscillate. It is in this case that the confidence criterion is useful in establishing some "degree of confidence" in the adapted parameter values. For exact model matching as shown in the examples in Chapter 3 the parameters of the model system will eventually converge to those of the reference system. Once the adaptation is complete further identification will give $-\int_0^T \dot{V} dt = 0$, $V(0) = 0$ and the confidence criteria, η_1 , will be indeterminate for this identification interval. However, for inexact modelling $V(0)$ can never be zero for any given identification interval since the reference system and model can never be matched. This produces an

interesting effect on the confidence criterion, η_1 . As the model parameters oscillate in parameter space, η_1 , will tend to some value

$$\eta_1 = 1 - \frac{\int_0^T \underline{e}^t D \underline{e} dt}{V(0)} \quad 5.4.8$$

If the D matrix is chosen to be diagonal as is done here

$$\eta_1 = 1 - \frac{d_{11} \int_0^T e_1^2 dt + d_{22} \int_0^T e_2^2 dt}{V(0)} \quad 5.4.9$$

This value will depend on the choice made for matrices M and D. The identification of a particular phase of data behavior will be terminated, therefore, when it is felt that η_1 has reached some relatively unchanging value. The final choice of parameters for the system depends on the values obtained by the "confidence criterion" after the identification interval and stability considerations for the model. Because of the inexact modeling there exists a region in parameter space which would establish the model as an adequate representation of the physiological system under study.

In Fig. 5.6 are shown the model adapted parameters as the adaptation is run for the interval of data between 0 and .105 sec., since this is the approximate duration of the slow buildup of activity of the long lead burst units and is assumed to correspond to the phase $f_1 \approx 0$. The adaptation was repeatedly done for this interval to obtain a final set of adapted parameters for this phase. A stimulus of 45 deg./sec. was applied at the start of each subinterval to

perturb the systems. This magnitude stimulus was used since from Figs. 2.9 and 2.10 it is seen that the amplitude of a quick phase movement at 45 deg./sec. is about 10 degrees which is the amplitude of the quick movement in this problem. The total adaptation duration for this phase was equivalent to .945 sec. The final adapted parameters of the model for each identification subinterval were used as starting parameters for the next identification subinterval. These values are indicated in Fig. 5.6 as FH1, FH2, FH0, FH3, FG1, and FG0. Functions V_{lmax} , and $\int_0^T -V dt$, $V(0)$, and η_1 have been denoted by VIM, INT VD, V(0), and ETAL. The program used to generate the corrective dynamics for identification was written in Focal for a PDP 8/E computer and displayed on a VT8/E digital display. A listing of the programs is shown in Fig. 5.5.

```

01.10 E
01.11 A P0(1), P1(1), P2(1), P3(1), P4(1), F0(2), F1(2), P2(2), P3(2), F4(2)
01.20 A P, H1, H0, H2, H3, G1, G0, M1, M3, M4, X1, X0, X2, X3, D1, D4, N1, N3, N4, DT
01.28 S DN=N1*N4-N3*2; S S1=(N4*M1-N3*M3)/DN; S S2=(N4*M3-N3*M4)/DN
01.29 S S3=(N1*M3-N3*M1)/DN; S S4=(N1*M4-N3*M3)/DN; S D=FDIS()
01.40 A X1, X2; S R=45; S P1=199/P; F T=0, DT, F; D 2
01.50 S V(0)=V2+V3; S ET(1)=1-VI/V(0); S ET(2)=V1/V(0)
01.60 T "FH1="H1," FH2="H2, !," FH0="H0," FH3="H3, !," FG1="G1," FG0="G0, !
01.90 T "INT VD="VI, !," VIM="V2, !," V(0)="V(0), !," ETA1"ET(1)," ETA2"ET(2)
01.99 0

02.01 S V1=M1*E1*2+2*M3*E1*E2+M4*E2*2; I (V1-V2)2.02; S V2=V1; S V3=VI
02.02 S VI=VI+DT*D1*E1*2+DT*D4*E2*2; S D=FDIS(F1*T-94, H1)
02.10 S Z1=P0(1)+F1(1)*T+F2(1)*T*2+F3(1)*T*3+F4(1)*T*4
02.11 S Z2=P0(2)+F1(2)*T+F2(2)*T*2+F3(2)*T*3+F4(2)*T*4
02.40 S XD(1)=X1*E1-E2-H1*Z1+H2*Z2+G1*F; S X1=X1+XD(1)*DT; S E1=Z1-X1
02.45 S XD(2)=X0*E1-H0*Z1-H3*Z2+G0*F; S X2=X2+XD(2)*DT; S E2=Z2-X2
02.50 S H6=-S1*E1*Z1-S2*E2*Z1; S H7=-S3*E1*Z1-S4*E2*Z1
02.60 S H8=S1*E1*Z2+S2*E2*Z2; S H9=-S3*E1*Z2-S4*E2*Z2
02.65 S H1=H1+H6*DT; S H0=H0+H7*DT; S H2=H2+DT*H2; S H3=H3+DT*H3
02.70 S G1=R*S1*E1*DT+R*S2*E2*DT+G1; S G0=S3*E1*F*DT+S4*E2*F*DT+G0
*
```

Fig. 5.5 Program for Saccadic Generator Model Parameter Identification

The dynamics of the adaptation are shown in Fig. 5.7 - 5.12. As can be seen, the parameters tend to oscillate with smaller amplitudes in the final identification interval than in the first. Also by examining the values of η_1 in each subinterval it can be seen that η_1 tends to some constant value indicating that the model adaptation has gone as far as it can. In the last few subintervals there is very little gained by the adaptation as can be inferred by the small changes in η_1 and additional identification, it is felt, is not warranted as has already been explained previously. Another indication that further adaptation is not warranted is the repeated oscillations of the parameters. The final adapted parameters for the total interval have, therefore, been taken to be as:*

$$\begin{array}{lll} h_1 = 19.5 & h_2 = 35.6 & g_1 = -18.52 \\ h_0 = 17.46 & h_3 = 46.157 & g_0 = 88.04 \end{array} \quad 5.4.10$$

The identification of the parameter values for $f_1 \neq 0$ were done in the same fashion as described previously for $f_1 = 0$. The M, D, N and Q matrices were chosen as before and the starting parameters at each new subinterval were chosen to be those at the end of the previous subinterval. The starting parameters of the model for the interval of data corresponding to $f_1 \neq 0$ are the final adapted parameters for $f_1 = 0$ and are given by equation 5.4.10. Only new values for h_1 and h_0 were identified. The identification interval was taken to be .053 seconds and was obtained from estimating the time duration of the burst of activity in Fig. 5.3. Repeated adaptation for this interval is given in Fig. 5.13 and the dynamics are shown in Fig. 5.14 and 5.15. As can

* The significance of these parameters in terms of the physiology is discussed in Sec. 5.5.

be seen from Fig. 5.13 η_1 has settled at the level $\eta_1 = .788$ and therefore the adaptation was terminated. The values obtained for h_1 and h_0 are to be considered as h'_1 and h'_0 as described in Sec. 5.3. This is so as not to confuse these values with h_1 and h_0 for the case $f_1 = 0$. Parameters h_4 and h_5 can then be computed as follows:

$$h_4 = h'_0 - h_0$$

$$h_5 = h'_1 - h_1$$

From Fig. 5.13 the following values were taken as the final parameters values h'_0 and h'_1 :

$$h'_0 = 157.53$$

$$h'_1 = -41.9$$

Therefore:

$$h_4 = 157.53 + 17.46 = 174.99$$

$$h_5 = -41.9 - 19.5 = -61.4$$

In order to simulate the physiological data the obtained parameters were used in the model. The model horizontal eye movement was obtained by setting the output parameters in Fig. 4.2 B, i.e., g_2 , g_3 , h_6 appropriately to obtain a 12 degree movement. Parameter h_6 was chosen small so as to give the final neural integrator a large time constant ($h_6 = .1$). Parameter g_2 was set to zero (0) because the plant was neglected. Parameter k_1 , which corresponds to the peak firing frequency of the short lead burst units, was chosen to be $k_1 = 800$. Parameter k_2 was chosen to be $k_2 = 20$ to correspond to the falling behavior of these

short lead burst units. Parameter g_3 may then be adjusted to give a 12 degree step for 45 deg./sec. input into the saccadic generator. This is purely a scaling problem.

Upon putting these values into the model equations and driving it with a 45 deg./sec. stimulus, the curves generated in Fig. 5.16 result. This compares favorably with the real data generated in Fig. 5.3. Fig. 5.17 shows the model in response to a 45 deg./sec. stimulus showing the model generated nystagmus and pendular nystagmus with the f_2 variable. Fig. 5.18 shows a comparison between the model variables and the physiological unit data.

The next section discusses some of these results in terms of the parameters which have been found for simulating the characteristics of the quick phase generator.

FH1=	23.9007	FH2=	41.4572	FH1=	20.2559	FH2=	36.3114
FH0=-	13.0391	FH3=	49.2353	FH0=-	16.3563	FH3=	45.4353
FG1=-	9.5265	FG0=	69.9715	FG1=-	13.7762	FG0=	87.5063
INT VD=	10.4652			INT VD=	6.9285		
VIM=	23.2409			VIM=	12.1307		
V(0)=	29.7561			V(0)=	16.5640		
ETA1=	0.6483	ETA2=	0.0103*	ETA1=	0.5317	ETA2=	0.0027*
FH1=	21.1914	FH2=	40.9293	FH1=	19.3574	FH2=	35.9569
FH0=-	13.5302	FH3=	47.5713	FH0=-	16.3030	FH3=	45.7931
FG1=-	19.9119	FG0=	81.3392	FG1=-	18.6932	FG0=	87.3044
INT VD=	7.2065			INT VD=	6.3227		
VIM=	23.4139			VIM=	11.8133		
V(0)=	27.6337			V(0)=	16.1917		
ETA1=	0.7397	ETA2=	0.3473*	ETA1=	0.5736	ETA2=	0.0030*
FH1=	21.0355	FH2=	33.4670	FH1=	19.5159	FH2=	35.6033
FH0=-	13.3290	FH3=	44.5063	FH0=-	17.4595	FH3=	46.1575
FG1=-	22.7036	FG0=	87.1767	FG1=-	13.5223	FG0=	83.0479
INT VD=	7.0134			INT VD=	6.7613		
VIM=	13.9593			VIM=	11.5533		
V(0)=	13.4773			V(0)=	15.9195		
ETA1=	0.6202	ETA2=	0.0911*	ETA1=	0.5753	ETA2=	0.0029*
FH1=	21.2923	FH2=	37.0420				
FH0=-	14.3379	FH3=	43.8304				
FG1=-	21.2647	FG0=	87.8310				
INT VD=	10.4133						
VIM=	13.4452						
V(0)=	20.5350						
ETA1=	0.4941	ETA2=	0.0013*				
FH1=	21.1752	FH2=	30.6566				
FH0=-	15.2534	FH3=	44.3554				
FG1=-	19.5527	FG0=	37.3450				
INT VD=	9.2020						
VIM=	13.5173						
V(0)=	19.3196						
ETA1=	0.5312	ETA2=	0.0010*				
FH1=	20.7326	FH2=	36.5530				
FH0=-	15.3443	FH3=	44.9351				
FG1=-	13.3320	FG0=	37.2506				
INT VD=	7.5731						
VIM=	12.6263						
V(0)=	17.6365						
ETA1=	0.5703	ETA2=	0.0015*				

Fig. 5.6 Model parameter values at end of each adaptation subinterval for $f_1 = 0$. See Fig. 5.7-5.12 for first and last subinterval identification dynamics.

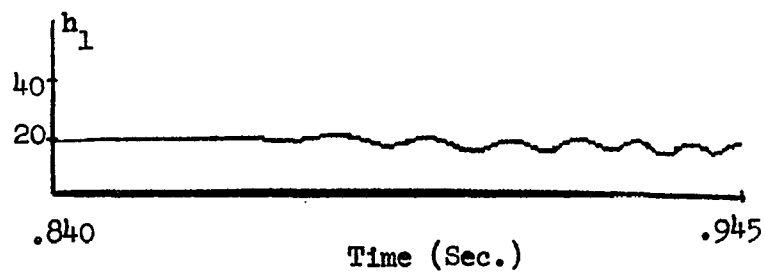
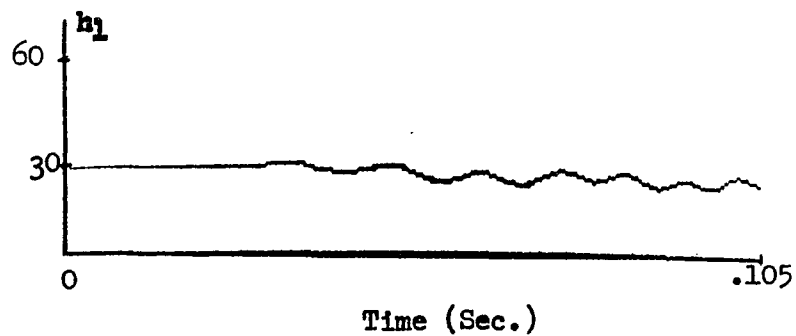


Fig. 5.7 Adaptation of parameter h_1 of saccadic generator model for $f_1 = 0$. The corresponding data interval is $0 \leq t \leq .105$. The first and last subintervals of adaptation are shown. (See Fig. 5.6 for initial and final parameter values for each subinterval)

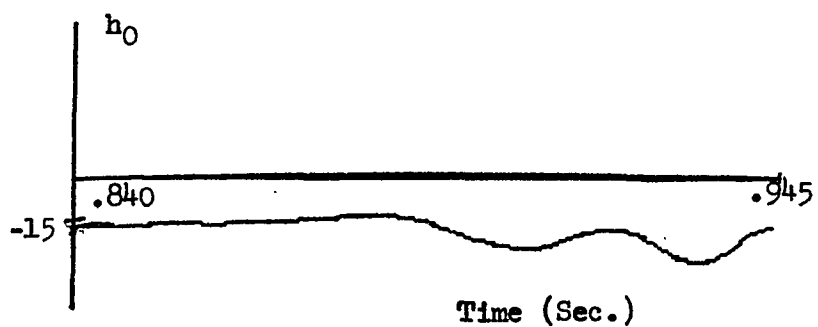
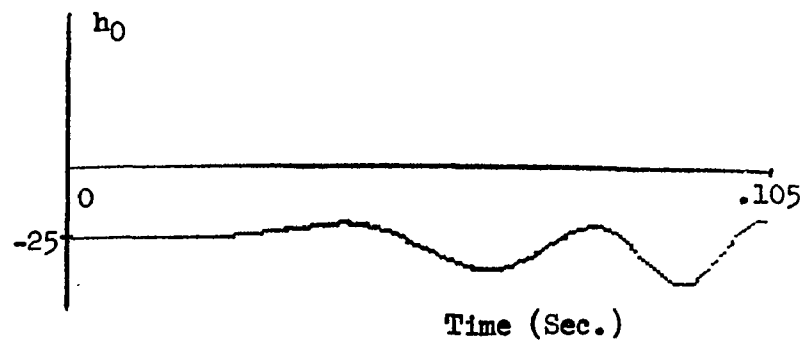


Fig. 5.8 Adaptation of parameter h_0 of saccadic generator model for $f_1 = 0$. The corresponding data interval is $0 \leq t \leq .105$. The first and last subintervals of adaptation are shown. (See Fig. 5.6 for initial and final parameter values for each subinterval)

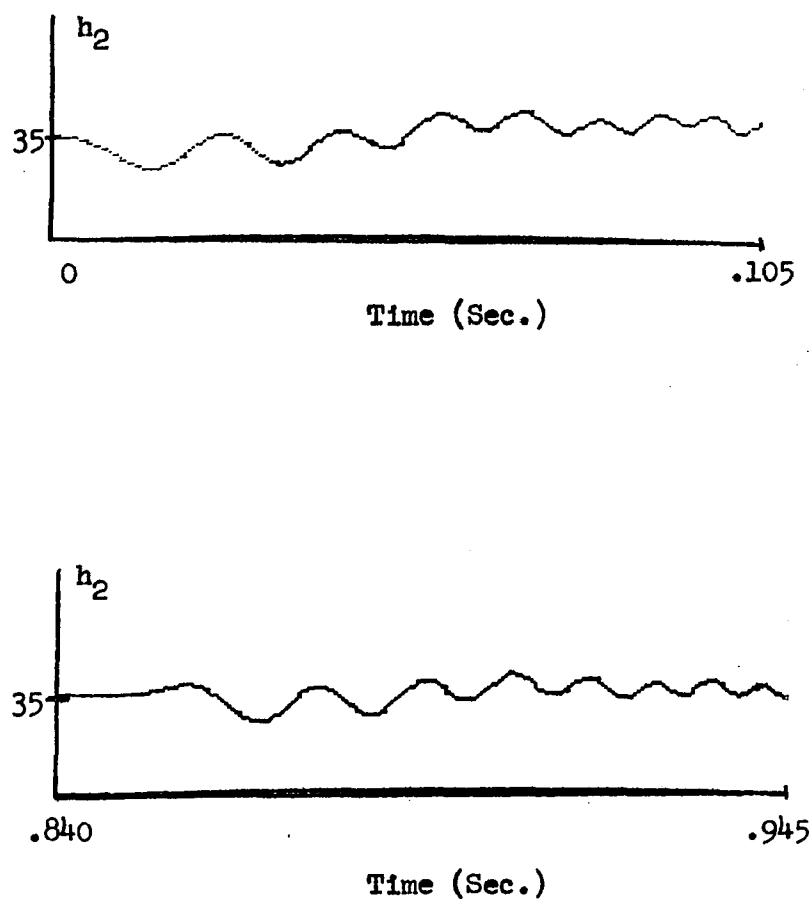


Fig. 5.9 Adaptation of parameter h_2 of saccadic generator model for $f_1 = 0$. The corresponding data interval is $0 \leq t \leq 0.105$. The first and last subintervals of adaptation are shown. (See Fig. 5.6 for initial and final parameter values for each subinterval)

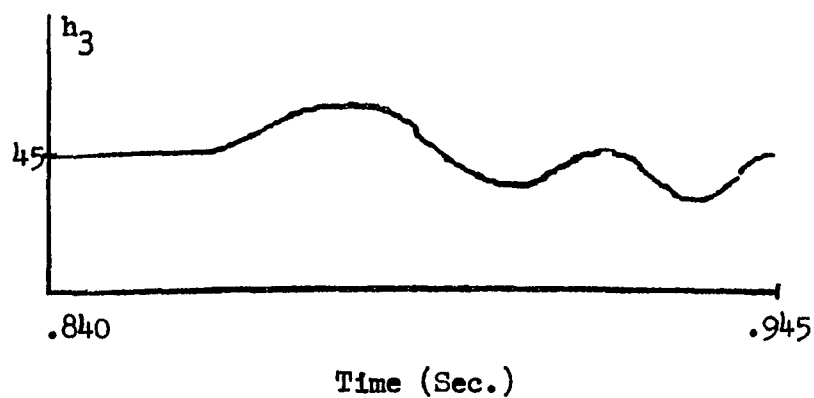
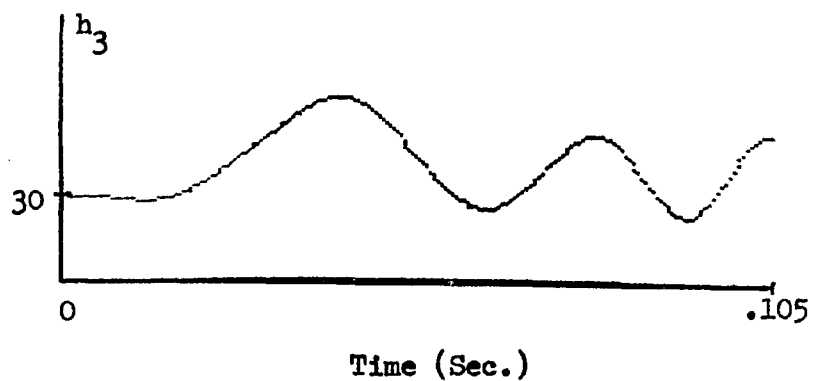


Fig. 5.10 Adaptation of parameter h_3 of saccadic generator model for $f_1 = 0$. The corresponding data interval is $0 \leq t \leq .105$. The first and last subintervals of adaptation are shown. (See Fig. 5.6 for initial and final parameter values for each subinterval)

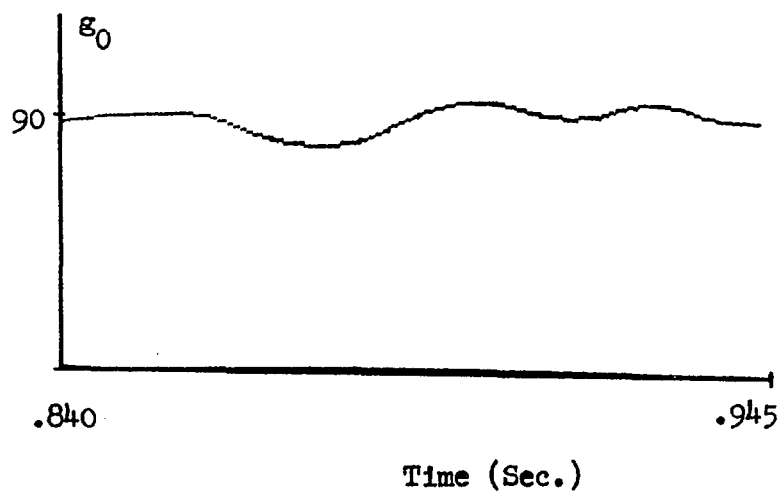
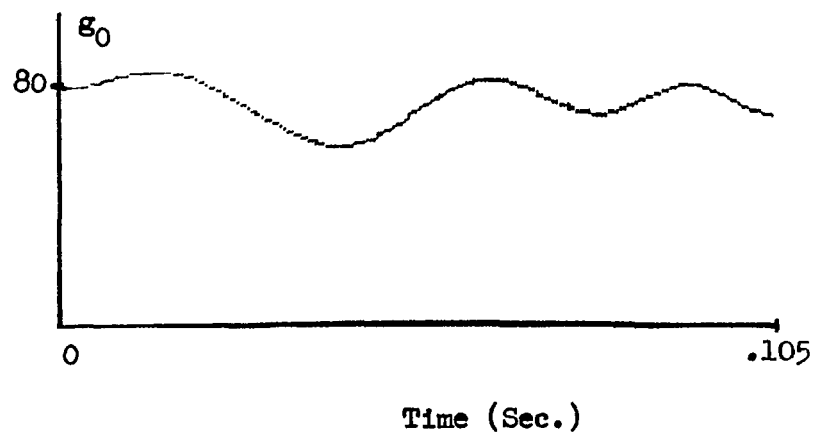


Fig. 5.11 Adaptation of parameter g_0 of saccadic generator model for $f_1 \approx 0$. The corresponding data interval is $0 \leq t \leq .105$. The first and last subintervals of adaptation are shown. (See Fig. 5.6 for initial and final parameter values for each subinterval)

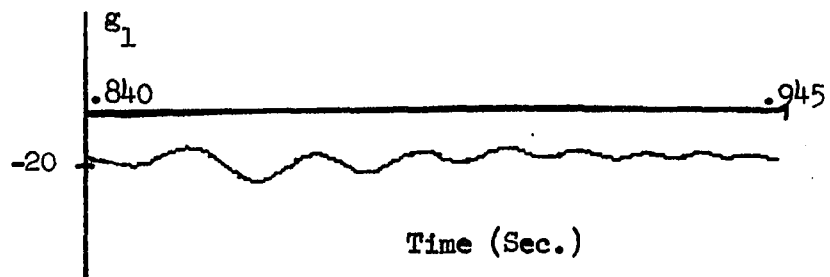
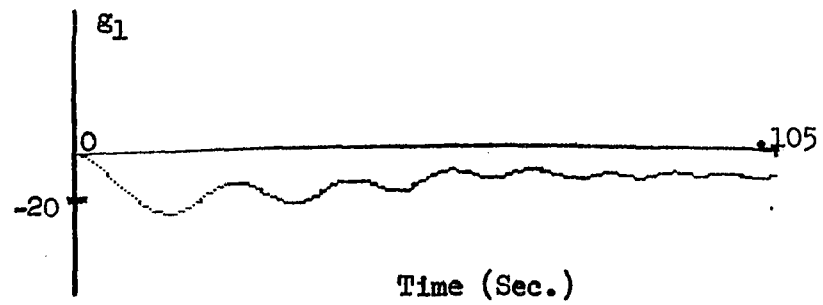


Fig. 5.12 Adaptation of parameter g_1 of saccadic generator model for $f_1 = 0$. The corresponding data interval is $0 \leq t \leq .105$. The first and last subintervals of adaptation are shown. (See Fig. 5.6 for initial and final parameter values for each subinterval)

```

*FH1= - 73.9358 FH2= 35.6000
FH0= 163.0010 FH3= 46.1600
FG1=- 18.5230 FG0= 88.0500
INT VD= 623.9750
VIM= 817.6300
V(0)= 911.4660
ETA1 0.3154 ETA2 0.2511

*FH1= - 30.2395 FH2= 35.6000
FH0= 155.7110 FH3= 46.1600
FG1=- 18.5230 FG0= 88.0500
INT VD= 325.0600
VIM= 1791.1500
V(0)= 2046.0100
ETA1 0.8411 ETA2 0.3076

*FH1= - 46.7397 FH2= 35.6000
FH0= 158.2770 FH3= 46.1600
FG1=- 18.5230 FG0= 88.0500
INT VD= 440.2640
VIM= 1785.4200
V(0)= 1897.6700
ETA1 0.7680 ETA2 0.3330

*FH1= - 40.5180 FH2= 35.6000
FH0= 157.3100 FH3= 46.1600
FG1=- 18.5230 FG0= 88.0500
INT VD= 378.7470
VIM= 1751.5600
V(0)= 2054.0100
ETA1 0.8156 ETA2 0.3049

*FH1= - 42.8621 FH2= 35.6000
FH0= 157.6750 FH3= 46.1600
FG1=- 18.5230 FG0= 88.0500
INT VD= 399.4590
VIM= 1761.8400
V(0)= 1858.4100
ETA1 0.7851 ETA2 0.3330

*FH1= - 41.9793 FH2= 35.6000
FH0= 157.5390 FH3= 46.1600
FG1=- 18.5230 FG0= 88.0500
INT VD= 391.3040
VIM= 1757.1200
V(0)= 1850.5400
ETA1 0.7885 ETA2 0.3330

```

Fig. 5.13 Model parameter values at end of each adaptation subinterval for $f_1 \neq 0$. See Figs. 5.14-5.15 for first and last subinterval identification dynamics.

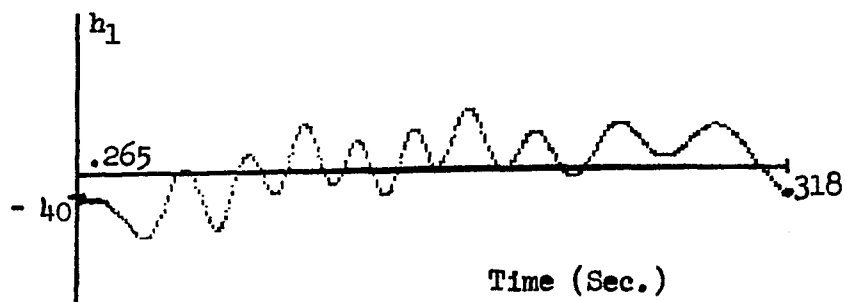
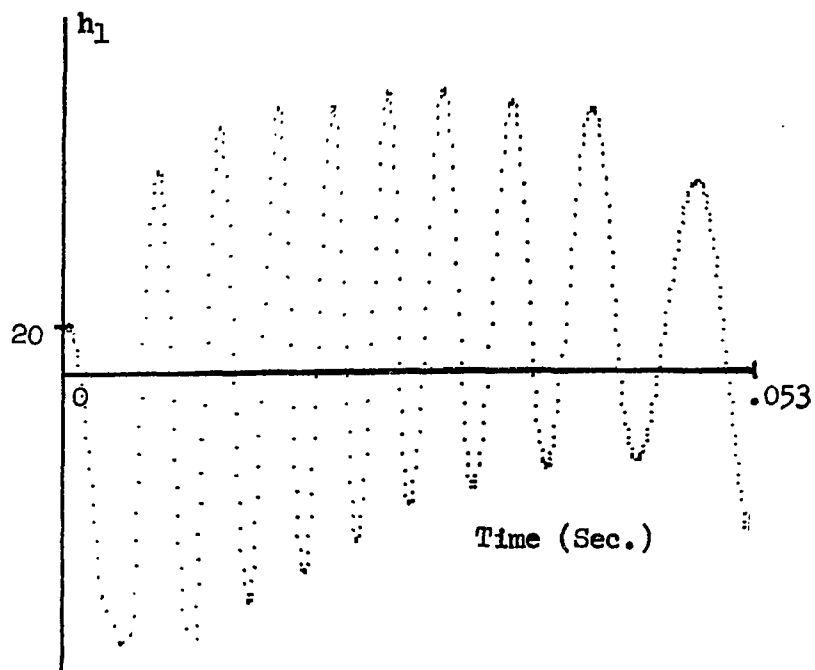


Fig. 5.14 Adaptation of parameter h_1 of saccadic generator model for $f_1 \neq 0$. The corresponding data interval is $.105 \leq t \leq .158$. The first and last subintervals of adaptation are shown (See Fig. 5.13 for initial and final parameter values for each subinterval)

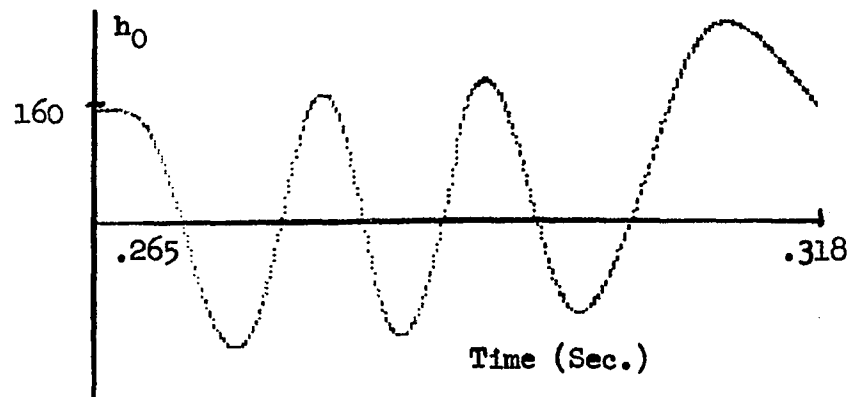
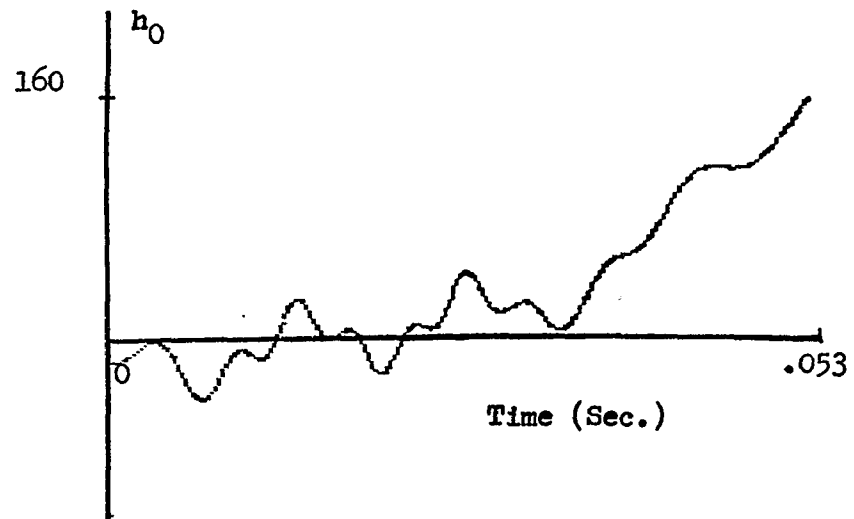


Fig. 5.15 Adaptation of parameter h_0 of saccadic generator model for $f_1 \neq 0$. The corresponding data interval is $.105 \leq t \leq .158$. The first and last subintervals of adaptation are shown (See Fig. 5.13 for initial and final parameter values for each subinterval)

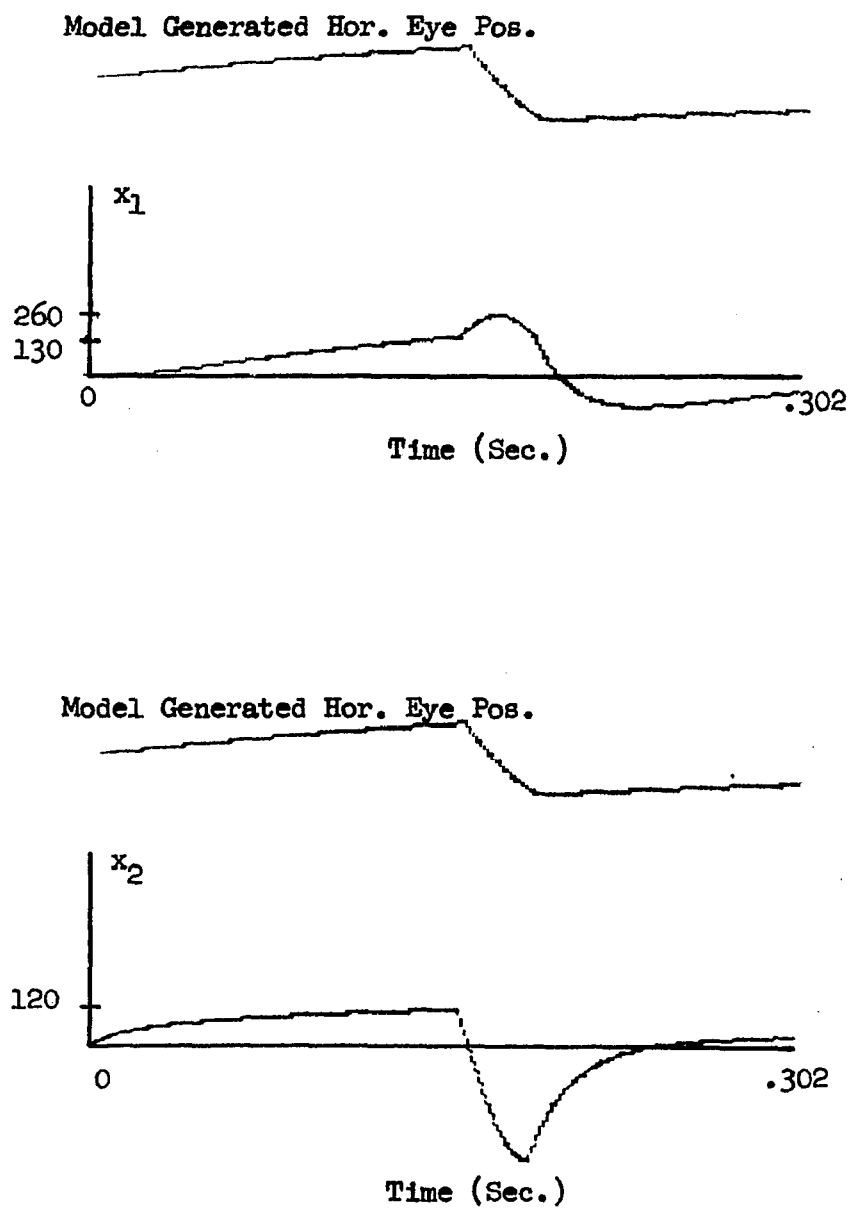


Fig. 5.16 Model generated state variables for a quick phase movement
(The size of the movement was made to correspond to approx
12 degrees as described on pages 157 and 158)

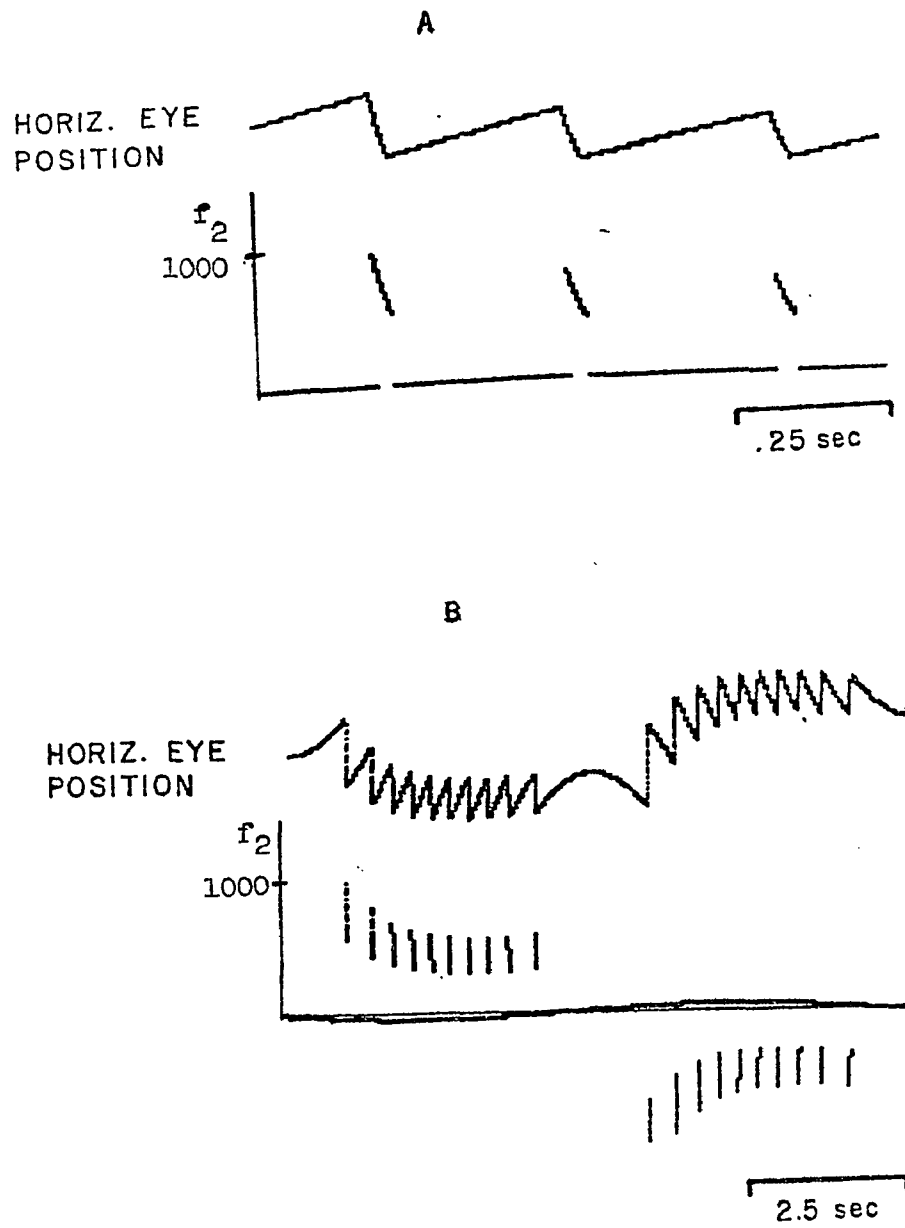


Fig. 5.17 Model nystagmus generation
 A- Constant velocity nystagmus
 B- Pendular nystagmus

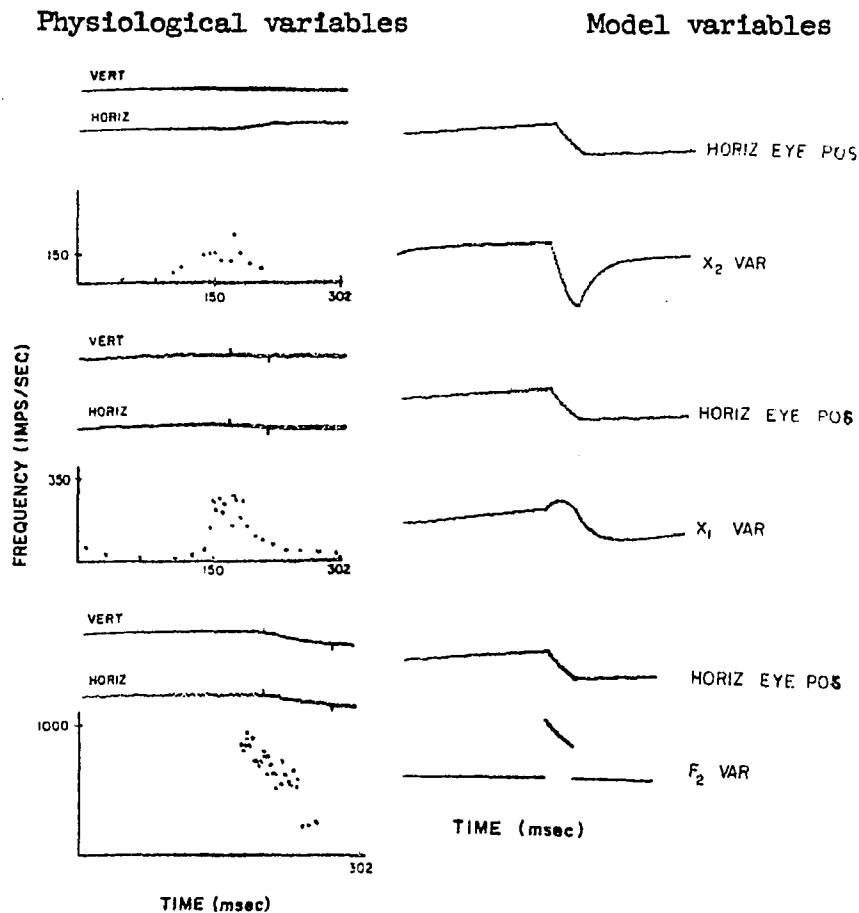


Fig. 5.18 Comparison of physiological variables (Frequency of firing of units) with state variables and variable f_2 of the model. The size of the quick phase eye movement is approximately 10-12 degrees.

5.5 Discussion of Results

The parameters of the model have been adapted by the controller to the following values for $f_1 = 0$:

$$h_1 = 19.5159$$

$$h_0 = -17.4595$$

$$h_2 = 35.6033$$

$$h_3 = 46.1575$$

$$g_1 = -18.5228$$

$$g_0 = 88.0479$$

This corresponds to the following state equation for $f_1 = 0$

$$\begin{bmatrix} \dot{x}_1 \\ \dot{x}_2 \end{bmatrix} = \begin{bmatrix} -19.5159 & 35.6033 \\ 17.4595 & 46.1575 \end{bmatrix} \begin{bmatrix} x_1 \\ x_2 \end{bmatrix} + \begin{bmatrix} -18.5228 \\ 88.0479 \end{bmatrix} r$$

The parameters of the saccadic generator model h_1 , h_0 , h_2 , h_3 , g_1 , and g_0 are assumed to determine the dynamic response of the neurons found in the PPRF, and some interesting observations can be made about the nature of the signal processing in the PPRF from the adapted parameter values. For the system matrix H given by:

$$H = \begin{bmatrix} -h_1 & h_2 \\ -h_0 & -h_3 \end{bmatrix}$$

The characteristic equation is

$$\det (sI - H) = 0$$

or

$$s^2 + (h_1 + h_3)s + (h_1 h_3 + h_2 h_0) = 0$$

where in this case $h_1 + h_3 = 65.9075$ and $h_0 h_2 + h_1 h_3 = 279.1893379$. The damping coefficient and natural oscillation frequency is found to be $\zeta = 1.972$ and $\omega_n = 16.709$ respectively. This implies that the system is overdamped in its initial response.

An interesting point arises for these parameter values. Because h_0 is negative ($h_0 < 0$) the quantity $h_1 h_3 + h_0 h_2$ may become negative if h_1 and h_3 take on values such that $h_1 h_3 + h_0 h_2 < 0$. This would make the saccadic generator unstable and result in spontaneous oscillations. This type of phenomena is observed in patients with lesions in the PPRF region.

It is also interesting to note that the parameters $1/h_1$ and $1/h_3$ represent the time constants of the integrators in the model. These values are about 20 - 50 msec. This implies that the brain has different integration mechanisms to perform different functions. In the PPRF, where quick eye movements are processed, integrators with short time constants are all that is necessary. The integrator mediating activity from the PPRF to the motor nucleus has a long time constant since it is necessary that the eyes be held in positions of fixation for extended periods with little drift.

Figs. 5.19 - 5.21 summarize the model behavior by showing where in the model the various unit types appear during a quick phase movement. The top two traces in the upper left hand corner represent the EOG and show the actual movement of the eye. This could be realized by putting output m of the model into an appropriate plant representing the eye muscles.*

* See Sobotkin (93), Robinson (82).

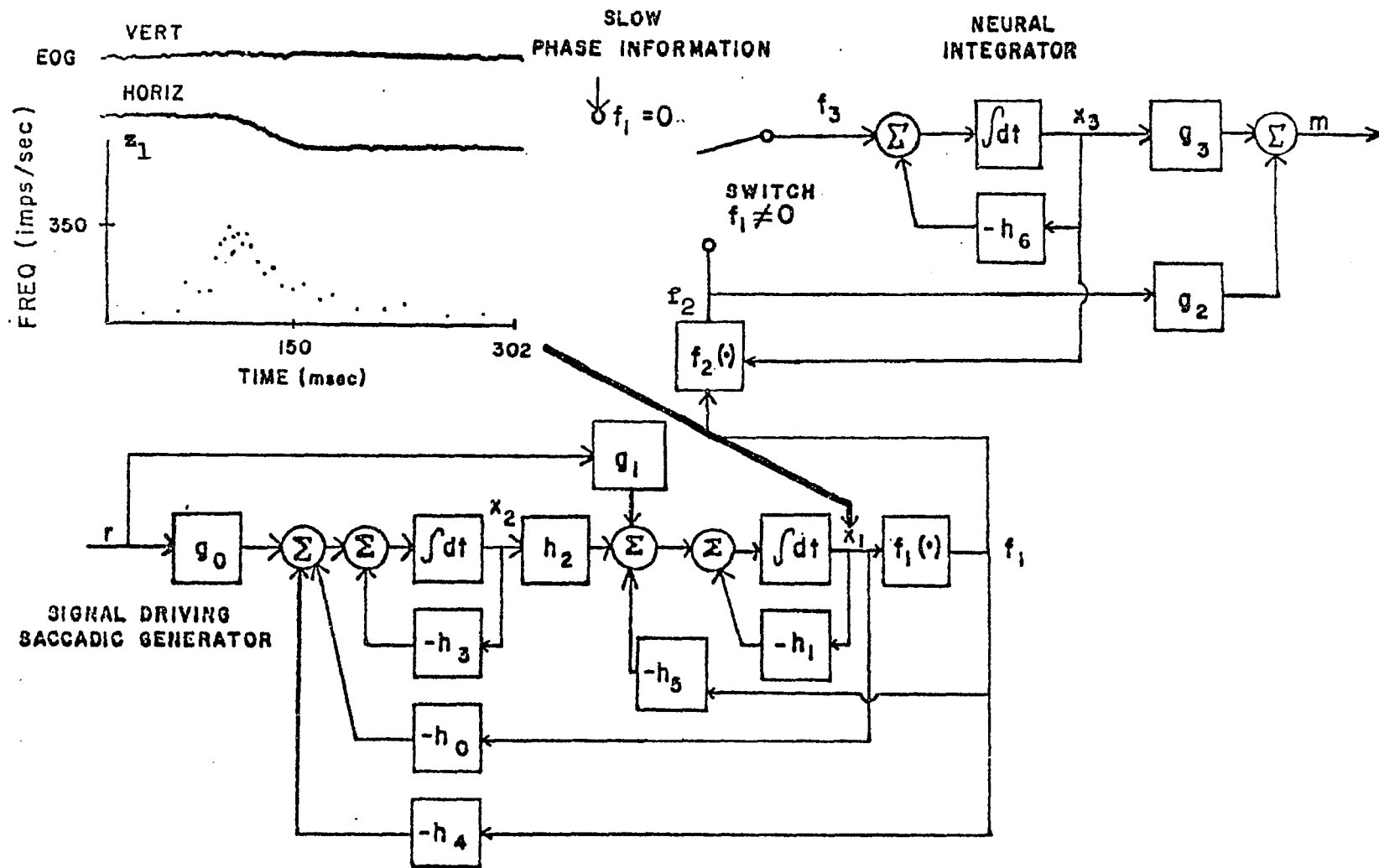


Fig. 5.19 Location of neuron type z_1 in saccadic generator model

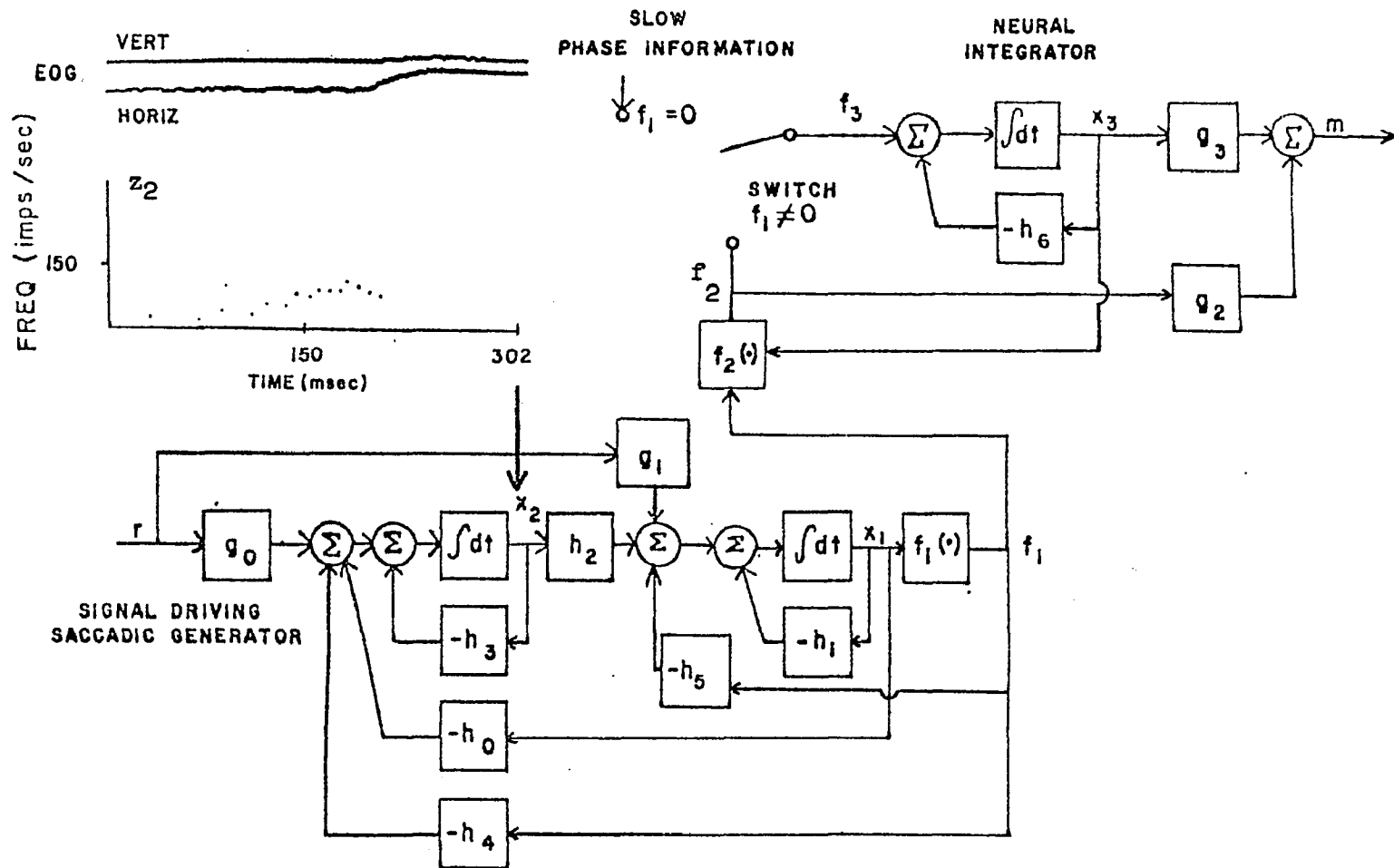


Fig. 5.20 Location of neuron type z_2 in saccadic generator model

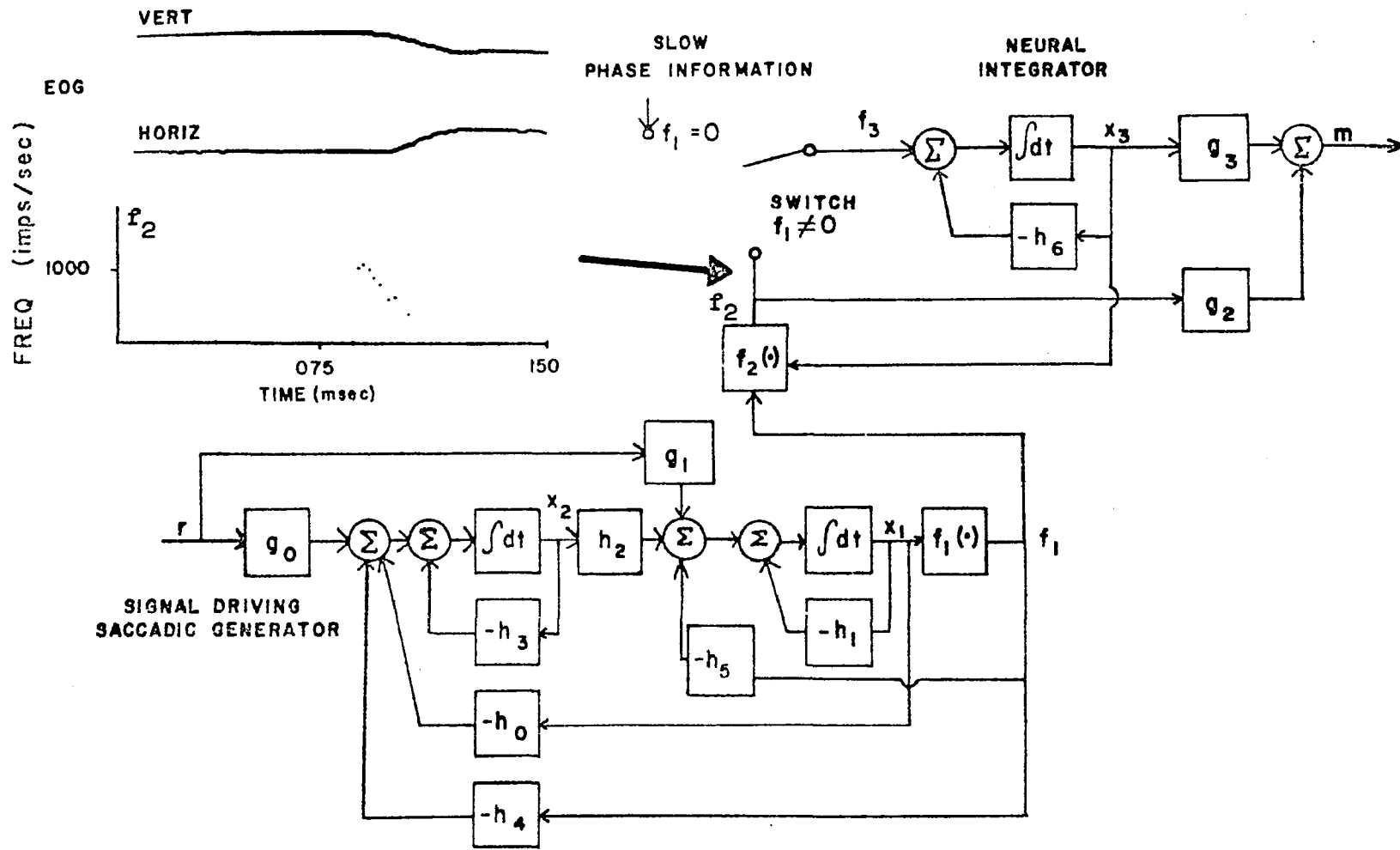


Fig. 5.21 Location of neuron type f_2 in saccadic generator model

CHAPTER 6

SUMMARY AND CONCLUSIONS

6.1 Summary

In this dissertation a combined neurophysiological and system theoretic technique has been utilized in studying the behavior of the oculomotor system and how it might relate to neural units recorded in the PPRF. Rather than study the overall system from an input-output point of view an attempt was made to establish a theoretical basis for explaining oculomotor response in terms of recorded unit activity in the brain stem.

One of the major postulates of this dissertation is that the oculomotor system is state determined and that there exists classes of neurons in the brain whose frequency of firing as a function of time can be considered the state variables of the oculomotor system. It was then shown in Chapter 4 that by realizing a second order non-linear system in a particular fashion, based on physiological arguments, various frequency patterns of units found in the brain stem could be simulated. In other words it was demonstrated that there are sufficient neurons in the PPRF to realize a pulse generator capable of producing quick eye movements.

Once a conceptually viable model had been demonstrated, quantitative agreement between model state variables and neural activity was obtained. This was accomplished using a model reference adaptive approach. The controller which was used to adapt the parameters was designed using Liapunov's direct method. The adaptive algorithms for the parameter controller to identify the model were derived for two types

of reference systems in Secs. 3.3.2 and 3.3.3. In Sec. 3.4 the algorithms were implemented by adapting two realizations of a model to a known reference system. The reference systems for identification used in the examples were assumed linear, controllable, observable, and having constant parameters. This technique is extended in Chapter 5 to piecewise linear reference systems when it is applied to the identification of the saccadic generator. Under the influence of the controller, the model's postulated parameters are modified in a manner such as to cause the model reference system state error vector to approach zero or to remain on a surface in error space (stability region) and the model parameter values to approach those of the reference system. The identification controller's adaptive algorithms were derived using Liapunov's Direct method.

The design based on Liapunov's second method insures the convergence of the adaptive algorithm and furthermore guarantees that for inexact modeling the state error vector stays within some bound which can be given in terms of the Liapunov function. In Chapter 3 a criterion has been established which gives estimates on the "goodness" of the adaptation. Using this criterion, engineering judgment can then be exercised to determine whether the mathematical model suitably approximates the process under investigation. This performance criterion is particularly important in modeling biological systems where the class of input functions to the reference system is limited and in many cases might have to be inferred from the observed response. Also the use of Liapunov's second method in designing the adaptive controller leads to algorithms which do not require large arrays of computer space

and can be easily programmed to run on a minicomputer. This is an extremely important practical consideration in electrophysiological research since the minicomputer has become an extensively used tool for data analysis.

The identification controller is derived in Chapter 3 where various examples were simulated to demonstrate the convergence properties of the adaptive algorithms.

A phase variable form and observable form realization were studied to gain insight into the type of adaptation expected for different realizations for a given system. By introducing "leaky" integrators into the quick phase generator model realization a more appropriate system matrix was obtained. The observable form realization also seems to have promise in the identification of systems where only a single state variable is measurable.

In the examples in Sec. 3.4 it was pointed out that the elements of the M , N , and Q matrices were important in determining the dynamic properties of the controller. However, the elements of M , N , and Q were dependent on the unknown reference system or on the time varying system parameters. In order to alleviate this difficulty a modified model-reference approach was used to derive the adaptive algorithms which enable the defining of a "confidence criterion" in Sec. 3.5 that estimates the controller's adaptive properties.

In Sec. 4.3 the model for the eye movement control system saccadic generator is presented. The conceptual viability is then demonstrated by introducing pulse, step, and sinusoidal inputs into the system with appropriate slow phase information introduced at the switch site.

It was also shown in Chapter 4 that there exist neurons in the brain stem (in particular the paramedian zone of the pontine reticular formation) whose frequency vs. time behavior is very similar to the time behavior of the state variables of a model for the saccadic generator.

In Chapter 5 minimum mean square error polynomials were found which approximated the neural activity of different neuron types recorded in the PPRF. The parameter adaptive technique developed in Chapter 3 was then applied by using these polynomials in identifying the saccadic generator model parameters.

The state theoretic approach in viewing the oculomotor system is conceptually pleasing as it offers a theoretical basis for understanding unit behavior and its relation to overall oculomotor response. In particular, it was shown that the saccadic generator can be looked at as a relaxation oscillator whose behavior is determined by the type of input introduced. When a pulse is applied to the saccadic generator it enters into an astable mode of behavior and a step is produced which is similar to a saccade. When a step is introduced via the slow phase generator, then nystagmus results. When a sinusoidal stimulus is used as an input to the slow phase generator, then pendular nystagmus is produced at the output. By introducing feedback from the neural integrator state to the saccadic generator the neuron type which rises rapidly and decays sharply can be simulated. This neuron type is assumed to drive the neural integrator as well as feeding directly onto the motoneurons.

An interesting conclusion of this research is that if the PPRF is looked at as a state determined system, then the quick phases of

nystagmus and saccadic generation can be explained by the same saccadic generator.

6.2 Recommendations for Future Research

Future research in this area could be approached on two levels. From the mathematical point of view, the following areas of research are extensions of this work:

1. To develop further criteria for "model adequacy." The criteria developed in this dissertation could be extended by defining vector valued distance functions as has recently appeared in the literature (81).
2. Develop a complete approach to non-perfect model matching in terms of these "model adequacy" criteria.
3. Investigate new forms of Liapunov functions from which new controllers may be designed.
4. Examine controller design for larger classes of nonlinear systems.

From the applications point of view:

1. Do more unit recordings and establish the model further as well as indicate modifications.
2. Examine the body repair mechanism in terms of a controller which exists in the brain and updates parameters (repairs) based on a normal model copy which also resides in the brain.
3. Apply similar techniques to study other physiological systems.

APPENDIX A

THEORY OF STABILITY IN THE SENSE OF LIAPUNOV (44, 59, 60)

Liapunov in 1892 introduced a criterion called the direct method for studying the stability of the equilibrium solution of nonlinear systems. This criterion gives information about stability or instability by making use only of the form of the equations describing the systems but without requiring the explicit knowledge of the solution. The underlying idea of the direct method of Liapunov is based on the existence of a positive definite scalar function $V(\underline{x})$ of the state variables \underline{x} with the following properties:

- a) $V(\underline{x})$ is continuous and has continuous first partial derivatives in a certain region R about the equilibrium point $\underline{x}=0$, where the origin is chosen as the equilibrium point.
- b) $V(0) = 0$
- c) Outside the origin and always in region R , $V(\underline{x})$ is positive and vanishes only at the origin. The origin is an isolated minimum of $V(\underline{x})$.

Since $V(\underline{x})$ has first partial derivatives it has a gradient ∇V , and one can get $\dot{V}(\underline{x}) = (\nabla V)' \underline{x}$ as its time derivative. $(\nabla V)'$ is the transpose of ∇V . If in addition $V(\underline{x}) \geq 0$ in R , $V(\underline{x})$ is called a Liapunov function. With these definitions, Liapunov's stability theory can be summarized by the following theorems:

1. Stability Theorem. If there exists in some neighborhood ϵ of the origin a Liapunov function $V(\underline{x})$ then the origin is stable.
2. Asymptotic Stability Theorem. If, in addition to the requirements of Theorem 1, $\dot{V}(\underline{x})$ is negative definite $\dot{V}(\underline{x}) \leq 0$ in ϵ then the stability is asymptotic.
3. Instability Theorem. If $V(\underline{x}) \geq 0$, $V(0) = 0$ and $\dot{V}(\underline{x}) > 0$ in ϵ then the origin is unstable.
4. Global Asymptotic Stability Theorem. If the Liapunov function $V(\underline{x})$ satisfies further the conditions: (a) $V(\underline{x}) \rightarrow \infty$ as $\underline{x} \rightarrow \infty$ and (b) $V(\underline{x})$ not identically zero along a solution of the system other than the origin, the system is globally asymptotically stable.

From the above theorems it is seen that stability in the sense of Liapunov rests upon the relative sign of the function V and its time derivative \dot{V} .

APPENDIX B
WEIGHTED MINIMUM MEAN SQUARE ERROR

POLYNOMIAL APPROXIMATION TO DATA (45)

This appendix describes the polynomial curve fitting technique which was used in this dissertation.

Given M measurements (observations) (x_1, y_1) we wish to fit a polynomial of degree N where N is much less than M , typically about 3 to 10 times smaller for cubics or higher-degree polynomials. Let the calculated data be given by $y(x_1)$ where

$$y(x) = P_0 + P_1 x + P_2 x^2 + \dots + P_N x^N \quad \text{B.1}$$

and the weighted sum of the squares of the differences (residuals) be given by

$$w_1 (y(x_1) - y_1)^2 = F(a_0, a_1, a_2, \dots, a_N) \quad \text{B.2}$$

where w_1 is the weight assigned to each data point $y(x_1)$ is the value of the polynomial at x_1 and y_1 is the value of the actual data at x_1 . With $N+1$ parameters we have the $N+1$ partial derivatives to equate to zero

$$\frac{\partial F}{\partial P_j} = 2 \sum_{i=1}^M w_1 (y(x_1) - y_1) x_1^j = 0 \quad \text{B.3}$$

or

$$P_0 \left(\sum_{i=1}^M w_1 x_1^j \right) + P_1 \left(\sum_{i=1}^M w_1 x_1^{j+1} \right) + \dots + P_N \left(\sum_{i=1}^M w_1 x_1^{j+N} \right) = \sum_{i=1}^M w_1 x_1^j y_1 \quad \text{B.4}$$

For ease, in notation we set

$$\sum_{i=1}^M w_1 x_1^k = S_k \quad \text{and} \quad \sum_{i=1}^M w_1 x_1^j y_1 = T_k \quad \text{B.5}$$

The equations then become

$$\sum_{i=1}^M P_i S_{i,j} = T_j \quad j = 0, 1, \dots, N \quad \text{B.6}$$

and are called the normal equations.

The normal equations are $N-1$ linear equations in $N-1$ unknowns P_i , whose determinant is shown not to be zero. Considering the homogeneous equations

$$\sum_{i=1}^M P_i S_{i+j} = 0 \quad \text{B.7}$$

it is shown that they have only the trivial solution $P_j=0$ for all j from which it follows that the determinant is not zero. Multiplying the j th equation by P_j and summing for all j

$$\sum_{j=0}^N \sum_{l=1}^M P_j P_l S_{l+j} = \sum_{j=0}^N \sum_{l=1}^M P_j P_l \sum_{n=1}^N x_l^j x_l^n = \left(\sum_{l=1}^M P_l x_l^j \right) \left(\sum_{n=0}^N P_n x_l^n \right) \\ \sum y^2(x_l) = 0 \quad \text{B.8}$$

This means that $y(x)=0$ and $P_j=0$ for all j . We have therefore proved that the determinant is not zero and that the nonhomogeneous equations can be solved for the coefficients of the least-squares polynomial.

In principle the problem of finding the least-squares polynomial is solved; in practice it is not very easy to solve the normal equations when N is very large, say greater than 10. To see why this is so, suppose that the x_i are more or less uniformly distributed in the interval $0 \leq x \leq 1$. Then

$$S_k = \sum_{j=1}^M x_j^k = M \int_0^1 x^k dx = \frac{M}{k+1} \quad \text{B.9}$$

The resulting determinant (suppressing the factors M) is the well-known Hilbert determinant

$$\left| \frac{1}{j+k+1} \right| \quad j, k = 0, 1, \dots, N \quad \text{B.10}$$

The Hilbert determinant of order N has the value

$$H_N = \frac{N!(N+1)! \cdots (2N-1)!}{[(1! 2! 3! \cdots (N-1)!)^3]} \quad \text{B.11}$$

which approaches zero very rapidly and suggests that the system of normal equations will be difficult to solve when N is even moderate in size. For $N=4$, which is the maximum order used in this dissertation the Hilbert determinant H_N is 1.7×10^{-7} .

For the fourth order polynomial approximation the following normal equations are obtained for the coefficients of the polynomial

$$S_0 P_0 + S_1 P_1 + S_2 P_2 + S_3 P_3 + S_4 P_4 = T_0 \quad \text{B.12}$$

$$S_1 P_0 + S_2 P_1 + S_3 P_2 + S_4 P_3 + S_5 P_4 = T_1 \quad \text{B.13}$$

$$S_2 P_0 + S_3 P_1 + S_4 P_2 + S_5 P_3 + S_6 P_4 = T_2 \quad \text{B.14}$$

$$S_3 P_0 + S_4 P_1 + S_5 P_2 + S_6 P_3 + S_7 P_4 = T_3 \quad \text{B.15}$$

$$S_4 P_0 + S_5 P_1 + S_6 P_2 + S_7 P_3 + S_8 P_4 = T_4 \quad \text{B.16}$$

Gauss's elimination process (45) can be used to solve these equations for the polynomial coefficients. The computer program to do this was written for a PDP 8/12 using Focal and is shown in Fig. B-1.

```

01.01 E
01.02 A S0, S1, S2, S3, S4, S5, S6, S7, S8, T0, T1, T2, T3, T4
01.10 S A1=S0; S A2=S1; S A3=S2; S A4=S3; S A5=S4
01.20 S E1=S1; S E2=S2; S E3=S3; S E4=S4; S E5=S5
01.30 S C1=S2; S C2=S3; S C3=S4; S C4=S5; S C5=S6
01.40 S D1=S3; S D2=S4; S D3=S5; S D4=S6; S D5=S7
01.50 S E1=S4; S E2=S5; S E3=S6; S E4=S7; S E5=S8
01.70 S T1=T1-T0*A1/A1; S T2=T2-T0*C1/A1; S T3=T3-T0*D1/A1
01.80 S F2=F2-A2*A1/A1; S B3=B3-A3*A1/A1; S F4=F4-A4*A1/A1
01.90 S E5=E5-A5*A1/A1; S C2=C2-A2*C1/A1; S C3=C3-A3*C1/A1

02.10 S C4=C4-A4*C1/A1; S C5=C5-A5*C1/A1
02.20 S D2=D2-A2*D1/A1; S D3=D3-A3*D1/A1; S D4=D4-A4*D1/A1
02.30 S D5=D5-A5*D1/A1; S E2=E2-A2*E1/A1; S E3=E3-A3*E1/A1
02.40 S E4=E4-A4*E1/A1; S E5=E5-A5*E1/A1; S T4=T4-T1*E1/A1
02.50 S F1=0; S C1=0; S D1=0; S E1=0
02.60 S C3=C3-F3*C2/F2; S C4=C4-F4*C2/F2; S C5=C5-F5*C2/F2
02.70 S T2=T2-T1*C2/F2; S D3=D3-F3*D2/F2; S D4=D4-F4*D2/F2
02.80 S D5=D5-F5*D2/F2; S T3=T3-T1*D2/F2; S E3=F3-F3*E2/F2
02.90 S E4=E4-F4*E2/F2; S E5=E5-F5*E2/F2; S T4=T4-T1*E2/F2

03.10 S C2=0; S D2=0; S E2=0; S D4=D4-C4*D3/C3; S D5=D5-C5*D3/C3
03.20 S E4=E4-C4*E3/C3; S E5=E5-C5*E3/C3; S T3=T3-T2*D3/C3
03.30 S T4=T4-T2*E3/C3; S D3=0; S E3=0; S E5=E5-D5*E4/D4
03.40 S T4=T4-T3*E4/D4; S E4=0

04.10 S F4=T4/E5; S F3=(T3-D5*E4)/D4; S F2=(T2-C5*F4-C4*F3)/C3
04.20 S F1=(T1-E5*F4-F4*F3-E3*F2)/F2
04.30 S F0=(T0-A5*F4-A4*F3-A3*F2-A2*F1)/A1
04.40 T Z, !, "F0="F0, !, "F1="F1, !, "F2="F2, !, "F3="F3, !, "F4="F4, !!
04.50 T "TYPE (D 5) FOR POLY EXAM:":0

05.10 A "TIME="T;I (T)4.5
05.20 S Y=F0+F1*T+F2*T^2+F3*T^3+F4*T^4; T "F(T)="Y, !; G 5.1
*
```

Fig. B-1 Computer Program for Obtaining Polynomial Approximation To Data

APPENDIX C

COMPUTER PROGRAMS USED TO GENERATE CORRECTIVE DYNAMICS

FOR EXAMPLES IN SECTION 3.4

Example 1

```

01.10 E
01.15 C 410=99;400=50;M11=30;M12=20;M22=30;N11=1;N12=.5;N22=1
01.20 A "TIME="F,"ST FOR 41-40"41,40,"M MAT"M1,M3,M4,"V MAT"V1,V3,V4
01.30 S D=FDISC();S S1=M3/(N1*N4-N3*N3);S S2=M4/(N1*N4-N3*N3)
01.40 S F1=180/F;S DT=.001;S F1=1;F T=0,DT,F;D 2
01.00 T "FIN41="41,1,"FIN40="40
01.70 0

02.10 S D=FDISC(F1*T-94,41);S F2=0;I (-T)2.2;S F2=1/DT
02.20 S Z4=-121*Z1-22*Z2+197*F1+102*F2;S Z2=Z2+DT*Z4;S Z1=Z1+DT*Z2
02.60 S X4=-40*X1-41*X2+197*F1+102*F2;S X2=X2+DT*X4;S X1=X1+DT*X2
02.80 S E1=Z1-X1;S E2=Z2-X2
02.90 S H4=-V4*S1*E1*X1-V4*S2*X1*E2+V3*X2*S1*E1+V3*X2*S2*F2
02.95 S H3=-V1*S1*E1*X2-V1*S2*X2*E2+V3*S1*X1*E1+V3*S2*X1*E2
02.97 S H0=40+DT*H4;S 41=41+DT*H3

```

Example 2

```

01.10 E
01.11 C 410=0;400=200;M11=700;M12=-200;M22=23.26
01.15 A "TIME="I,"ST FOR 41-40"41,40,"M MAT"M1,M3,M4,"V MAT"V1,V3,V4
01.20 S F1=180/F;S D=FDISC();S DT=.001;F T=0,DT,F;D 2
01.40 T "FIN41="41,1,"FIN40="40
01.50 0

02.10 S D=FDISC(F1*T-94,41);S Z3=-22*Z1+Z2+102;S Z4=-121*Z1+197
02.20 S Z1=Z1+DT*Z3;S Z2=Z2+DT*Z4;I (-T)2.4
02.30 S G1=Z1/D1;S G2=Z2/DT
02.40 S X3=-11*X1+X2+G1;S X4=-40*X1+G2;S X1=X1+X3*DT
02.50 S X2=X2+DT*X4;S E1=Z1-X1;S E2=Z2-X2;S H3=-X1*14000*E1+X1*2000*F2
02.60 S H4=X1*2000*E1-470.2*X1*E2;S 41=41+DT*H3;S 40=40+DT*H4

```

APPENDIX D

COMPUTER PROGRAMS USED TO GENERATE CORRECTIVE DYNAMICS

FOR EXAMPLES IN SECTION 3.7

Example 1

```

01.10 E
01.20 A "TIME" P, "STAR PAR H1-H0" H1, H0, "M MAT" M1, M3, M4, "V MAT" V1, N3, N4
01.25 A "X MAT" K1, K0, "D MAT" D1, D3, D4
01.28 S DN=V1*N4-N3*2; S S1=(N4*M1-N3*M3)/DN; S S2=(N4*M3-M4*N3)/DN
01.29 S S3=(V1*M3-M1*N3)/DN; S S4=(V1*M4-M3*N3)/DN
01.40 S F1=188/P; S D=FDIS(); S DT=.001; F T=0, DT, P; D 2
01.45 S V(0)=V2+V3
01.50 S ET(1)=1-V1/V(0); S ET(2)=V1/V2; S ET(3)=FSQT(ET(1)+2+ET(2)+2)
01.60 T "FH1="H1, !, "FH0="H0, !, "INT VD="V1, !, "VIM="V2, !
01.99 T "V(0)="V(0), !, "ETA1="ET(1), " ETA2"ET(2), " ETA="ET(3); 0

02.01 S VD=D1*E1+2+D4*E2+2; S VI=VI+DT*VD
02.02 S V1=M1*E1+2+2*M3*E1+E2+M4*E2+2; I (V1-V2) 2.1; S V2=V1; S V3=VI
02.10 S D=FDIS(P1*T-94, H1); S Z3=-22*Z1+Z2+102; S Z4=-121*Z1+187
02.20 S Z1=Z1+DT*Z3; S Z2=Z2+DT*Z4; I (-T) 2.4
02.30 S G1=Z1/DT; S G0=Z2/DT
02.40 S X3=-H1*Z1+K1*E1+X2+G1; S X4=-H0*Z1+K0*E1+G0; S X1=X1+X3*DT
02.50 S X2=X2+DT*X4; S E1=Z1-X1; S E2=Z2-X2; S H3=-Z1*S1*E1-Z1*S2*E2
02.60 S H4=-Z1*S3*E1-S4*Z1*E2; S H1=H1+DT*H3; S H0=H0+DT*H4
*
```

Example 2

```

01.10 E
01.20 A "TIME" P, "STAR PAR H1-H0, G1-G0" H1, H0, G1, G0, "M MAT" M1, M3, M4
01.23 A "X MAT" K1, K0, "D MAT" D1, D3, D4, "V MAT" V1, N3, N4, "G MAT" G1, G3, G4
01.24 A "DT" DT
01.25 S DN=V1*N4-N3*2; S S1=M3*N3/DN; S S2=M4*N1/DN; S S3=M3*N3/DN
01.26 S S4=M4*N3/DN; S S5=M3*N4/DN; S S6=M4*N4/DN
01.28 S DG=G1*G4-G3*2; S S7=(G1*M3-M1*G3)/DG; S S8=(G1*M4-M3*G3)/DG
01.40 S R=1; S F1=188/P; S D=FDIS(); F T=0, DT, P; D 2
01.45 S V(0)=V2+V3; S V4=G; S VI=VI+V4
01.50 S ET(1)=1-V1/V(0); S ET(2)=V1/V(0); S ET(3)=FSQT(ET(1)+2+ET(2)+2)
01.60 T !, "FH1="H1, " FH0="H0, !, "FG1="G1, " FG0="G0, !, "INT VD="V1, !
01.90 T "VIM="V2, !, "V(0)="V(0), !, "ETA1="ET(1), " ETA2"ET(2), " ETA="ET(3)
01.99 0

02.01 S VD=D1*E1+2+D4*E2+2; S VI=VI+DT*VD
02.02 S V1=M1*E1+2+2*M3*E1+E2+M4*E2+2; I (V1-V2) 2.1; S V2=V1; S V3=VI
02.10 S D=FDIS(P1*T-94, Z1); S ZD(2)=-121*Z1-22*Z2+187*R; S Z2=Z2+DT*ZD(2)
02.20 S Z1=Z1+DT*Z2; S XD(2)=X0*E1+K1*E2-H0*Z1-H1*Z2+G0*R
02.40 S X2=X2+DT*XD(2); S X1=X1+DT*X2; S E1=Z1-X1; S E2=Z2-X2
02.50 S HD(G)=-S5*E1*Z1-S6*E2*Z1+S3*E1*Z2+S4*E2*Z2
02.60 S HD(1)=-S1*E1*Z2-S2*E2*Z2+S3*E1*Z1+S4*E2*Z2
02.70 S GD(G)=R*S7*E1+R*S8*E2; S H0=H0+HD(G)*DT; S H1=H1+HD(1)*DT
02.80 S G0=G0+GD(G)*DT; S D=FDIS(P1*T-94, Z2)
*
```

Example 3

```

01.10 E
01.20 A "TIME" P, "STAR PAR H1-H0, G1-G0" H1, H0, G1, G0, "M MAT" M1, M3, M4
01.23 A "K MAT" K1, K0, "D MAT" D1, D3, D4, "V MAT" V1, V3, V4, "G MAT" G1, G3, G4
01.25 S DN=N1*N4-N3*2; S S1=(N4*M1-N3*M3)/DN; S S2=(N4*M3-M4*V3)/DN
01.26 S S3=(N1*M3-M1*V3)/DN; S S4=(N1*M4-M3*V3)/DN
01.27 S DQ=Q1*Q4-Q3*2; S S5=(Q4*M1-Q3*M3)/DQ; S S6=(Q4*M3-M4*Q3)/DQ
01.28 S S7=(Q1*M3-M1*Q3)/DQ; S S8=(Q1*M4-M3*Q3)/DQ
01.40 S R=1; S P1=198/P; S D=FDIS(); A "DT"="DT; F T=0, DT, P; D 2
01.45 S V(0)=V2+V3; S V4=0
01.50 S ET(1)=1-(V1+V4)/V(0); S ET(2)=V1/V(0)
01.55 S ET(3)=FSOT(ET(1)+2+ET(2)+2)
01.60 T "FH1="H1," FH0="H0,!, "FG1="G1," FG0="G0,!, "INT VD="V1, !
01.90 T "VIM="V2,!, "V(0)="V(0),!, "ETA1="ET(1), " ETA2"ET(2), " ETA="ET(3)
01.99 Q

02.01 S VD=D1*E1+2+D4*E2+2; S VI=VI+DT*VD
02.02 S V1=M1*E1+2+2*M3*E1*E2+M4*E2+2; I (V1-V2) 2.1; S V2=V1; S V3=VI
02.10 S D=FDIS(P1*T-94, H1); S Z3=-22*Z1+Z2+102; S Z4=-121*Z1+187
02.20 S Z1=Z1+DT*Z3; S Z2=Z2+DT*Z4; S XD(1)=-H1*Z1+K1*E1+X2+G1*R
02.40 S XD(2)=-H0*Z1+K0*E1+G0*R; S X1=X1+XD(1)*DT; S X2=X2+DT*XD(2)
02.50 S E1=Z1-X1; S E2=Z2-X2; S HD(1)=-Z1*S1*E1-Z1*S2*E2
02.60 S HD(0)=-Z1*S3*E1-S4*Z1*E2; S H1=H1+DT*HD(1); S H0=H0+DT*HD(0)
02.70 S GD(1)=R*S5*E1+R*S6*E2; S GD(0)=R*S7*E1+R*S8*E2
02.80 S G1=G1+GD(1)*DT; S G0=G0+GD(0)*DT

```

BIBLIOGRAPHY

1. Aschoff, J. C. and B. Cohen, "Changes in Saccadic Eye Movements Produced by Cerebellar Cortical Lesions," *Exp. Neur.*, v. 32, pp. 123-233, 1971.
2. Barnes, G. R. and A. J. Benson, "A Model for the Prediction of the Nystagmic Response to Angular and Linear Acceleration Stimuli," *AGARD Conference Proceedings on the Use of Nystagmography in Aviation Medicine*, May, 1973.
3. Becker, W. and A. F. Fuchs, "Further Properties of the Human Saccadic System: Eye Movements and Correction Saccades with and without Visual Fixation Points," *Vision Research*, v. 9, pp. 12470-12580, 1969.
4. Bender, M. B. and S. Shanzer, "Oculomotor Pathways Defined by Electric Stimulation and Lesions in the Brainstem of the Monkey," in *The Oculomotor System*, ed. M. B. Bender, New York: Harper and Row, 1964, pp. 81-140.
5. Brandt, Th. Dichgans and E. Koenig, "Differential Effects of Central Versus Peripheral Vision on Egocentric and Exocentric Motion Perception," *Exp. Brain Res.*, v. 16, pp. 476-491, 1973.
6. Cheng, M. and J. S. Outerbridge, "Inter-Saccadic Interval Analysis of Optokinetic Nystagmus," *Vision Res.*, v. 14, pp. 1053-1058, 1974.
7. Cohen, B. and J. Suzuki, "Eye Movements Induced by Ampullary Nerve Stimulation," *Amer. J. Physiol.*, v. 204, pp. 347-351, 1963.
8. Cohen, B. J. Suzuki and M. B. Bender, "Nystagmus Induced by Electric Stimulation of Ampullary Nerves," *Acta Oto-laryngol.* v. 60, pp. 422-436, 1965.
9. Cohen, B. A. Komatsuzaki, and M. B. Bender, "Electrooculographic Syndrome in Monkeys After Pontine Reticular Lesions," *Archives of Neurology*, v. 18, Jan. 1968.
10. Cohen, B. and M. Feldman, "Relationship of Electrical Activity in Pontine Reticular Formation and Lateral Geniculate Body to Rapid Eye Movements," *J. Neurophysiol.*, v. 31, pp. 806-817, 1968.
11. Cohen, B., "Vestibulo-Ocular Relations," in *The Control of Eye Movements*, ed. P. Bach-y-Rita, C. C. Collins, and J. E. Hyde, New York: Academic Press, 1971.
12. Cohen, B. and A. Komatsuzaki, "Eye Movements Induced by Stimulation of the Pontine Reticular Formation: Evidence for Integration in Oculomotor Pathways," *Exp. Neurol.*, v. 36, July, 1972.

13. Cohen, B. and V. Henn, "The Origin of Quick Phases of Nystagmus in the Horizontal Plane," *Bibliotheca Ophthalmologica*, v. 82, pp. 36-55.
14. Cohen, B. and V. Henn, "Unit Activity in the Pontine Reticular Formation associated with Eye Movements," *Brain Research*, v. 46, pp. 403-410, 1972.
15. Cohen, B. T. Uemura and S. Takemori, "Effects of Labyrinthectomy on Optokinetic Nystagmus (OKN) and Optokinetic After-nystagmus," *Equil. Res.*, v. 3, pp. 80-93, 1973.
16. Cohen, B. "The Vestibulo-Ocular Reflex Arc," *Vestibular Systems part I, Basic Mechanisms, Chapter 4 in Handbook of Sensory Physiology*, ed. Kornhuber, H. H. Springer, 1974.
17. Cohen, B. and V. Henn, "Coding of Information about Rapid Eye Movements in the Pontine Reticular Formation of Alert Monkeys," *Brain Research* (in press.)
18. Collewijn, H., "Optokinetic Eye movements in the Rabbit: Input Output Relations," *Vision Res.*, v. 9, pp. 117-132, 1969.
19. Collewijn, H. and F. Van der Mark, "Ocular Stability in Variable Visual Feedback Conditions in the Rabbit." *Brain Research*, v. 36, pp. 47-57, 1971.
20. Collewijn, H., "Latency and Gain of the Rabbit's Optokinetic Reactions to small Movements." *Brain Research*, v. 36, pp. 59-72, 1972.
21. Collewijn, H., "An Analog Model of the Rabbit's Optokinetic System," *Brain Research*, v. 36, pp. 71-88, 1972.
22. Collins, C. C. "Orbital Mechanics, in The Control of Eye Movements ed. P. Bach-y-Rita, C. C. Collins and J. E. Hyde. New York: Academic Press, 1971.
23. Cook, G. and L. Stark, "The Human Eye Movement Mechanism," *Arch. Ophthal.*, v. 79, April 1968.
24. Crosby, E. C. and J. W. Henderson, "The Mamalian Midbrain and Isthmus Region, Part II. The Fiber Connections of the Superior Colliculus B. Pathways Concerned in Automatic Eye Movements," *J. Comp. Neurol.*, v. 88, pp. 53-91, 1948.
25. Desoer, C. A. Notes for a Second Course on Linear Systems. New York: Van Nostrand Reinhart, 1970.

26. Dichgans, J. and Th. Brandt, "Visual-Vestibular Interaction and Motion Perception," in Cerebral Control of Eye Movements and Motion Perception, Bibl. Opthal., v. 82, pp. 327-338, Basel, Karger, 1972.
27. Dichgans, J. C. L. Schmidt, and W. Graf, "Visual Input Improves the Speedometer Functions of the Vestibular Nuclei in the Goldfish," Exp. Brain Res., v. 18, pp. 319-322, 1973.
28. Dix, M. R. and J. D. Hood, "Further Observation Upon the Neurological Mechanism of Optokinetic Nystagmus," Acta Otolaryng., v. 71, pp. 217-226, 1971.
29. Dodge, R. and T. S. Cline, "The Angular Velocity of Eye Movements," Psychol. Rev., v. 8, pp. 145-157, 1901.
30. Ewald, J. R., "Physiologische Untersuchungen über das Endorgan des Nervus Octavus," Wiesbaden, Bergmann, 1892.
31. Fender, D. H. and P. W. Nye, "An Investigation of the Mechanism of Eye Movement Control," Kybernetik, v. 1, pp. 81-88, 1961.
32. Fernandez, C., and J. M. Goldberg, "Physiology of Peripheral Neurons Innervating the Semicircular Canals of the Squirrel Monkey Response to Sinusoidal stimulation and Dynamics of the Peripheral Vestibular System," J. Neurophysiol., v. 34, pp. 661-675, 1971.
33. Freeman, W., "Paralysis of Associated Lateral Movements of the Eyes," Archives Neur. and Psychiat. v. 7, pp. 454-487, 1922.
34. Fuchs, A. F., "Periodic Eye Tracking in the Monkey," J. Physiol. (London), v. 193, pp. 161-171, 1967.
35. Fuchs, A. F., and Luschei, E. S., "Firing Patterns of Abducens Neurons of Alert Monkeys in Relationship to Horizontal Eye Movements," J. Neurophysiol., v. 33, pp. 382-392, 1970.
36. Fuchs, A., "The Saccadic System," in The Control of Eye Movements, ed. P. Bach-y-Rita, C. C. Collins and J. E. Hyde, Academic Press, New York, 1971.
37. General Electric, "A Survey of Adaptive Control Technology," General Electric, Electronics Laboratory, Syracuse, New York, 1964.
38. Goebel, Hans and A. Komatsuzaki, M. B. Bender and B. Cohen, "Lesions of the Pontine Tegmentum and Conjugate Gaze Paralysis," Archives of Neurology, v. 24, May 1971.

39. Goldberg, J. R. and C. Fernandez, "Physiology of Peripheral Neurons Innervating Semicircular Canals of the Squirrel Monkey. I. Resting Discharge and Response to Constant Angular Accelerations," *J. Neurophysiol.*, v. 34, pp. 635-657, 1971.
40. Goldberg, J. M. and C. Fernandez, "Physiology of Peripheral Neurons Innervating Semicircular Canals of the Squirrel Monkey. III. Variations Among Units in their Discharge Properties," *J. Neurophysiology*, v. 34, pp. 676-683, 1971.
41. Goto, K. and K. Tokumasu and B. Cohen, "Return Eye Movements, Saccadic Movements, and the Quick Phase of Nystagmus," *Acta Oto-Laryngologica*, v. 65, pp. 426-440, 1968.
42. Grayson, L. P., "The Design of Intentionally Non-linear controllers by the Second Method of Liapunov, Research Report PIB-MRI 884-60 Polytechnic Institute of Brooklyn, Dec. 1960.
43. Grayson, L. P., "The Status of Synthesis Using Liapunov's Method," *Automatica*, v. 3, pp. 91-121, 1965.
44. Hahn, W., Theory and Applications of Liapunov's Direct Method. Englewood Cliffs: Prentice Hall, 1963.
45. Hamming, R. W., Numerical Methods for Scientists and Engineers, Second Edition. New York: McGraw Hill, 1973.
46. Helmholtz, H. Von, Handbuch der physiologischen Optik. Leipzig: Voss, 1866.
47. Henn, V. and B. Cohen, "Quantative Analysis of Activity in Eye Muscle Motoneurons During Saccadic Eye Movements and Positions of Fixation.," *Journal of Neurophysiology*, v. 36, no. 1, Jan. 1973.
48. Henn, V., L. R. Young, and C. Finley, "Vestibular Nucleus Units in Alert Monkeys are Also Influenced by Moving Visual Fields," *Brain Research*, v. 71, pp. 144-149, 1974.
49. Highstien, S. M, M. Ito and T. Tsuchiya, "Synaptic Linkage in the Vestibulo-Ocular Reflex Pathway of Rabbit," *Exp. Brain Res.*, v. 13, pp. 306-326, 1971.
50. Highstien, S. M., B. Cohen, and K. Matsunami, "Monosynaptic Projections from the Pontine Reticular Formation to the IIIrd Nucleus in the Cat," *Brain Research*, v. 75, pp. 340-344, 1974.

51. Hood, J. D., "Observations Upon the Neurological Mechanism of Optokinetic Nystagmus with Especial Reference to the Contribution of Peripheral Vision," *Acta Oto-Laryng.*, v. 63, pp. 208-215, 1967.
52. Horridge, G. A., "Position of Onset of Fast Phase in Optokinetic Nystagmus," *Nature*, v. 216, no. 5119, pp. 1004-1005, Dec. 9, 1967.
53. Horrocks, T., "Investigations into Model Reference Adaptive Control Systems," *Proc. IEEE*, v. III (11), p. 1894-1906, Nov., 1964.
54. Kalman, R. E. and J. E. Bertram, "Control System Analysis and Design Via "Second Method" of Liapunov, Part 1, Continuous Time System," *Journal of Basic Engineering*, Trans. of the ASME v. 82-D, p. 371-393, June, 1960.
55. Keller, E. L and D. A. Robinson, "Abducens Unit Behavior in the Monkey During Vergence Movements," *Vision Res.*, V. 12, pp. 369-382, Pergamon Press, 1972. Printed in Great Britain.
56. Keller, E. L. and D. A. Robinson, "Absence of Stretch Reflex in the Extraocular Muscles of the Monkey," *J. Neurophysiol.*, v. 34, pp. 908-919, 1971.
57. Keller, E. L., "Participation of Medial Pontine Reticular Formation in Eye Movement Generation in Monkey," *J. of Neurophysiol.*, v. 37, pp. 316-332, 1974.
58. Komatsuzaki, A. H. E. Harvis, J. Alpert, and B. Cohen, "Horizontal Nystagmus of Rhesus Monkeys," *Acta Oto-laryng.*, v. 67, pp. 535-551, 1969.
59. Lasalle, J. and S. Lefschetz, Stability by Liapunov's Direct Method with Applications, New York: Academic Press, 1961.
60. Lorente de No, R., "Vestibular Ocular Reflex Arc," *Arch. Neur. and Psychiat.*, v. 30, pp. 245-291, 1933.
61. Lowenstien, O. and A. Sand, "The Mechanism of the Semicircular Canal," *Proc. R. Soc. B.*, v. 129, pp. 256-275, 1940.
62. Luschei, E. S. and A. F. Fuchs, "Activity of Brainstem Neurons During Eye Movements of Alert Monkeys," *J. of Neurophysiol.*, v. 35, pp. 455-461, 1972.
63. Margolis, M., "On the Theory of Process Adaptive Control Systems, the Learning-Model Approach," Doctoral Dissertation, Dept. of Engineering, University of California in Los Angeles, 1959.

64. Mekel, R., "A Class of Liapunov Functions for High Order Non-linear Control Systems," Asilomar Conference on Circuits and Systems, Monterey, Calif., Nov. 1-3, 1967.
65. Mekel, R., "Synthesis of Corrective Dynamics for Human Operator Models in Closed Loop Control Systems," NASA Working Paper, No. LWP-816, Oct. 1969.
66. Mekel, R., "An Adaptive Modeling Technique Using a Class of Liapunov Functions," Proceedings of 1972 Int. Conf. on Cybernetics and Society, Oct. 9-12, 1972.
67. Mekel, R., "Nonlinear and Digital Machine Control Systems Modeling," NASA Technical Report, No. 72-447-01, Nov., 1972.
68. Mekel, R. and P. Peru, "Design of Controllers for a Class of Non-linear Control Systems," IEEE Trans. on Automatic Control, vol. AC-17 (2), pp. 206-213, April, 1972.
69. Narendra, K. S. and P. Kudva, "Stable Adaptive Schemes for System Identification and Control: Part I," IEEE Trans. on Systems, Man, and Cybernetics, v. SMC-4, Nov. 1974.
70. Narendra, K. S. and P. Kudva, "Stable Adaptive Schemes for System Identification and Control: Part II," IEEE Trans. on Systems, Man, and Cybernetics, v. SMC-4, Nov., 1974.
71. Noback, C. R. and R. J. Demarest, The Nervous System: Introduction and Review, New York: McGraw Hill Book Co., 1972.
72. Osborn, P. V., H. P. Whitaker, and A. Kezer, "New Developments in the Design of Adaptive Control Systems," Institute of Aeronautical Sciences, 1961 International Automation Symp., Paper No. 61-39, 1961.
73. Parks, P. C., "Liapunov Redesign of Model-Reference Adaptive Control Systems," IEEE Trans. on Aut. Control, v. AC-11, pp. 362-367, July, 1966.
74. Pasik, P. and T. Pasik, "Oculomotor Functions in Monkeys with Lesions of the Cerebrum and the Superior Colliculi," in The Oculomotor System, ed. M. B. Bender. New York: Harper and Row, 1964, pp. 40-80.
75. Pasik, T. and P. Pasik, and J. A. Valciukas, "Nystagmus Induced by Stationary Repetitive Light Flashes in Monkeys," Brain Research, v. 19, pp. 313-317, 1970.
76. Pasik, T. and P. Pasik, "Experimental Models of Oculomotor Dysfunction in the Rhesus Monkey," in Advances in Neurology, v. 10, ed. B. S. Meldrum and C. D. Marsden. New York: Raven Press, 1975.

77. Precht, W., J. Grippo, and A. Richter, "Effect of Horizontal Angular Acceleration on Neurons in the Abducens Nucleus." *Brain Research*, v. 5, pp. 527-531, 1967.
78. Precht, W. "The Physiology of Vestibular Nuclei," in The Vestibular System v. Handbook of Sensory Physiology, ed. Kornhuber, and H. H. Springer, 1970.
79. Rashbass, C., "The Relationship between Saccadic and Smooth Tracking Eye Movements," *Journ. Physiology*, v. 159, pp. 326-338, 1961.
80. Rang, E. R. and C. R. Stone, "Adaptive State Vector Control Adaptive Controllers Derived by Stability Considerations," Minneapolis-Honeywell Regulator Company, Military Products Group, Report 1529-TR 9 March, 1962.
81. Reggiani, M. G. and F. E. Marchetti, "On Assessing Model Adequacy," *IEEE Transactions on Systems, Man, and Cybernetics*, v. SMC-5, May 1975.
82. Robinson, D. A., "The Mechanics of Human Saccadic Eye Movement," *Journ. Physiol.*, v. 174, pp. 245-264, 1964.
83. Robinson, D. A., "The Mechanics of Human Smooth Pursuit Eye Movements," *Journ. Physiol.*, v. 180, pp. 569-591, 1965.
84. Robinson, D. A., "The Oculomotor Control System: A Review," *Proc. of IEEE*, v. 56, No. 6, June, 1968.
85. Robinson, D. A., "Oculomotor Unit Behavior in the Monkey," *J. Neurophysiol.*, v. 23, pp. 393-404, 1970.
86. Robinson, D. A., "Models of Oculomotor Neural Organization," in The Control of Eye Movements, ed. P. Bach-y-Rita, C. C. Collins, and J. E. Hyde, New York: Academic Press, 1971.
87. Robinson, D. A. and E. L. Keller, "The Behavior of Eye Movement Motoneurons in the Alert Monkey," *Bibliotheca Ophthalmologica*, v. 82, pp. 7-16, 1972.
88. Robinson, D. A., "Models of the Saccadic Eye Movement Control System," *Kybernetik*, v. 14, pp. 71-83 (1973), Oby Springer Verlag, 1973.
89. Robinson, D. A., "Cerebellectomy and the Vestibulo-Ocular Reflex," *Brain Research*, v. 71, pp. 215-224, 1974.
90. Ron, S., D. A. Robinson and A. Skavenski, "Saccades and the Quick Phases of Nystagmus," *Vision Research*, v. 12, p. 2105, 1972.

91. Rosen, M. J., "A Theoretical Neural Integrator," *IEEE Transactions on Biomedical Engineering*, v. BME-19, No. 5, Sept. 1972.
92. Skavenski, A. A. and D. A. Robinson, "Role of Abducens Neurons in Vestibulo-Ocular Reflex," *J. Neurophysiol.*, v. 36, No. 4, July, 1973.
93. Sobotkin, F., "Controller Design for Modelling Problems with Application to a Class of Physiological Systems," *Doctoral Dissertation, CUNY, 1973.*
94. Shahein, H. I. H., M. A. R. Ghonaimy, and D. W. C. Shen, "Accelerated Model-Reference Adaptation via Liapunov and Steepest Descent Design Techniques," *IEEE Trans. On Automatic Control*, v. AC-17, Feb., 1972.
95. Sparks, David and Joseph P. Sides, "Brain Stem Unit Activity Related to Horizontal Eye Movements Occurring During Visual Tracking," *Brain Research*, v. 77, pp. 320-325, 1974.
96. Staffanson, Forrest L., "Determining Parameter Corrections According to System Performance- A Method and its Application to Real-Time Missile Testing," *Army Missile Test Center, White Sands Missile Range, Lab. Res. Rpt. 20, July 1960.*
97. Stark, L., G. Vossius, and L. R. Young, "Predictive Control of Eye Movements," *IRE Transactions on Human Factors in Electronics*, v. HFE-3, pp. 52-57, Sept. 1962.
98. Stark, L., "The Control System for Versional Eye Movements," in *The Control of Eye Movements*, ed. P. Bach-y-Rita, C. C. Collins, and J. E. Hyde, New York: Academic Press, 1971.
99. Steinhausen, W., "Über die Beobachtung der Cupula in den Bogen-gang-sampullen des Labyrinthes des Lebenden Hechts," *Pflügers Arch. ges. Physiol.*, v. 232, pp. 500-512, 1933.
100. Stern, T. E., Theory of Nonlinear Networks and Systems. Addison Wesley, 1965.
101. Sugie, N. and M. G. Jones, "A Model of Eye Movements Induced by Head Rotation," *IEEE Trans. SMC*, v. SMC-1, pp. 251-260, 1971.
102. Sugie, N. and M. G. Jones, "A Model of Eye Movements Induced by Head Rotation," *DRB Aviation Medical Research Unit of Reports*, v. 2, pp. 1968-1971, August, 1972.
103. Szentágothai, J., "The Elementary Vestibulo-Ocular Reflex Arc," *J. Neurophysiol.*, v. 13, pp. 395-407, 1950.

104. Uemura, T. and B. Cohen, "Vestibulo-Ocular Reflexes: Effects of Vestibular Nucleus Lesions," In Basic Aspects of Central Vestibular Mechanisms, Progr. Brain Res., v. 37, pp. 515-528, Amsterdam: Elsevier, 1972.
105. Uemura, T. and B. Cohen, "Effects of Vestibular Nuclei Lesions on Vestibulo-Ocular Reflexes and Posture in Monkeys," Acta Oto-laryng, Suppl. v. 315, pp. 1-71, 1973.
106. Westheimer, G., "Discussion of the Control of Eye Vergence Movements," in The Control of Eye Movements, ed. P. Bach-y-Rita, C. C. Collins, J. E. Hyde. New York: Academic Press, 1971.
107. Westheimer, G., "Mechanism of Saccadic Eye Movement," AMA Arch. Ophthal., v. 52, pp. 710-724, 1954.
108. Westheimer, G., "Eye Movement Responses to a Horizontally Moving Visual Stimulus," AMA Arch. Ophthal., v. 52, pp. 932-941, 1954.
109. Wheelles, L., R. Boynton, and G. Cohen, "Eye Movement Responses to Step and Pulse-Step Stimuli," J. Opt. Soc. Amer., v. 56, pp. 956-960, 1966.
110. Whitaker, H. P., J. Yarmon, and A. Kezer, "Design of Model Reference Adaptive Control Systems for Aircraft," MIT Instrumentation Lab, Report R-164, Sept. 1958.
111. White, A. J., "Analysis and Design of Model-Reference Adaptive Control Systems," Proc. IEEE, vol. 113(1), pp. 175-184, Jan. 1966.
112. Yasui, Syozo, "Nystagmus Generation, Oculomotor Tracking and Visual Motion Perception," PhD Thesis, Dept. of Aeronautics and Astronautics, MIT, 1974
113. Young, Lawrence R., "Measuring Eye Movements," American Journal of Med. Electronics, 1963, pp. 300-307.
114. Young, L. R., and L. Stark, "A Discrete Model for Eye Tracking Movements," IEEE Transactions on Military Electronics, v. MIL-7, numbers 2 and 3, April-July, 1963.
115. Young, L. R. and L. Stark, "Variable Feedback Experiments Testing a Sampled Data Model for Eye Tracking Movements," IEEE Transactions of the Professional Technical group on Human Factors in Electronics, v. HFE-4, no. 1, Sept. 1963.
116. Young, L. R. J. D. Forster and N. Van Houtte, "A Revised Stochastic Sampled Data Model for Eye Tracking Movements," Fourth Annual NASA-University Conf. on Man Control, Univ. of Michigan, Ann Arbor, 1968.

117. Young, L., "The Current Status of Vestibular System Models," *Automatica*, v. 1615, p. 369, 1969.
118. Young, L. and C. M. Oman, "Model for Vestibular Adaptation to Horizontal Rotation," *Aerospace Med.*, v. 40 (10), pp. 1076-1080, Oct. 1969.
119. Young, L., "Pursuit Eye Tracking Movement," in The Control of Eye Movements, ed. P. Bach-y-Rita, C. C. Collins, J. E. Hyde, New York: Academic Press, 1971.
120. Zadeh, L. and C. A. Desoer, *Linear System Theory: The State Space Approach*, New York: McGraw Hill, 1963.
121. Zuber, B. L., "Control of Vergence Eye Movements," in The Control of Eye Movements. ed. P. Bach-y-Rita, C. C. Collins, and J. E. Hyde. New York: Academic Press, 1971.

AUTOBIOGRAPHICAL STATEMENT

Theodore Raphan was born in Ainring, Germany on April 9, 1947. He received a B.E.(E.E) (1969) from The City College of New York and an M.E.(E.E) (1970) from The City University of New York.

During the period 1969 to the present, Mr. Raphan has taught in the Electrical Engineering department at the City College and has done research at The Mount Sinai School of Medicine.

Mr. Raphan is a member of Tau Beta Pi and Eta Kappa Nu, engineering honor societies.

He is married to the former Deborah Dichter. They currently live in Brooklyn, New York.